Excess volumes and isentropic compressibilities of binary mixtures of di-*n*-butylamine with iso-alkanols at 303·15 K

G S SASTRY, M RAMAMURTHY and P R NAIDU*
College of Engineering, Sri Venkateswara University, Tirupati 517 502, India

MS received 17 February 1983; revised 7 May 1983

Abstract. Volumes of mixing and deviations in isentropic compressibility for binary mixtures of di-*n*-butylamine with iso-propanol, iso-butanol and iso-pentanol were measured at 303·15 K. The excess volumes and deviations in isentropic compressibility are negative over the entire range of mole fractions in all the systems. The results point out that there is a strong H-bond interaction between unlike molecules.

Keywords. Mole fraction; dilatometer; isentropic compressibility; interferometer; volume fraction; sound velocity.

1. Introduction

New experimental data for excess volume and isentropic compressibility for mixtures of di-*n*-butylamine with iso-propanol, iso-butanol and iso-pentanol, determined at 303·15 K, are reported in this paper.

2. Experimental

Di-*n*-butylamine was dried over potassium hydroxide for three days, refluxed for 2 hr and fractionally distilled. Iso-propanol, iso-butanol and iso-pentanol were purified by the methods described in the literature (Riddick and Bunger 1970). The purity of the samples was checked by comparing the experimental densities with those reported in the literature (Timmermans 1950). The values were accurate to $\pm 5 \times 10^{-5}$ g cm^3.

Excess volumes were measured directly using a single composition per loading type dilatometer described earlier (Rao and Naidu 1974) at 303·15 K. Excess volumes were reproducible to $\pm 0{\cdot}003$ cm^{3}mol^{-1}.

Isentropic compressibilities were computed from densities and sound velocities determined at 303·15 K. Densities of the mixture were obtained from experimental excess volumes using the relation

$$\rho = (x_1 M_1 + x_2 M_2)/(V + V^E), \tag{1}$$

where x_1, x_2 and M_1, M_2 stand for the mole fractions and molecular weights of amine and alcohols respectively. V and V^E denote molar volume and excess volume respectively. Sound speed was measured as discussed earlier (Ramamurthy *et al* 1983).

The experimental densities of pure components at 303·15 K were compared with those reported below.

di-*n*-butylamine 0·75519 (−), iso-propanol 0·77692 (0·77690), iso-butanol 0·79439 (0·79437), iso-pentanol 0·80177 (0·80179)

Isentropic compressibilities were calculated from the relation

$$K_s = u^{-2}\rho^{-1} \tag{2}$$

where u and ρ denote sound velocity and density respectively. The deviation in isentropic compressibility (ΔK_s) was computed employing the equation

$$\Delta K_s = K_s - \phi_1 K_{s,1} - \phi_2 K_{s,2} \tag{3}$$

where K_s, $K_{s,1}$, $K_{s,2}$ are the isentropic compressibilities of the mixture and the pure components. ϕ_1 and ϕ_2 are the volume fractions of amine and alcohols. The deviation in isentropic compressibility (ΔK_s) for an ideal mixture is assumed to be additive with respect to volume fraction.

3. Results and discussion

Experimental V^E data for the three binary mixtures are included in table 1. The values of V^E may be expressed by an empirical equation of the form

$$V^E/\text{cm}^3\text{mol}^{-1} = x_1 x_2[a_0 + a_1(x_1 - x_2) + a_2(x_1 - x_2)^2], \tag{4}$$

where a_0, a_1 and a_2 are adjustable parameters, x_1 and x_2 are the molefractions of amines and alcohols respectively.

The values of the parameters obtained by least squares procedure are shown in table 1 along with the standard deviation (V^E).

Experimental ΔK_s values for the three binary mixtures are included in Table 2. The ΔK_s values for the binary mixtures at 303·15 K fit an empirical equation of the form

$$\Delta K_s/Tpa^{-1} = \phi_1\phi_2[b_0 + b_1(\phi_1 - \phi_2) + b_2(\phi_1 - \phi_2)^2], \tag{5}$$

Table 1. Experimental excess volumes for three binary mixtures at 303·15 K.

di-*n*-butylamine + iso-propanol		di-*n*-butylamine + iso-butanol		di-*n*-butylamine + iso-pentanol	
x	V^E (cm^{3}mol^{-1})	x	V^E (cm^{3}mol^{-1})	x	V^E (cm^{3}mol^{-1})
0·0651	−0·184	0·0578	−0·357	0·0809	−0·419
0·1912	−0·508	0·1841	−0·875	0·1552	−0·735
0·3100	−0·718	0·1923	−0·892	0·2360	−0·989

303·15 K.

ϕ	ρ (g cm^{-3})	u (msec^{-1})	K_s (Tpa^{-1})	ΔK_s (Tpa^{-1})
di-n-butylamine + iso-propanol				
0·00000	0·77692	1132	1004	0
0·12662	0·77589	1146	981	−7
0·34341	0·77358	1172	941	−19
0·49850	0·77129	1190	915	−26
0·59716	0·76941	1194	911	−29
0·68181	0·76740	1210	890	−28
0·76786	0·76490	1218	881	−26
0·80826	0·76347	1222	877	−25
0·89613	0·76005	1226	875	−16
0·94256	0·75796	1228	874	−11
1·00000	0·75519	1228	878	0
di-n-butylamine + iso-pentanol				
0·00000	0·80177	1218	840	0
0·12096	0·80018	1228	828	−16
0·22236	0·79631	1236	822	26
0·32472	0·79294	1240	820	−32
0·49355	0·78608	1242	824	−34
0·65219	0·77805	1242	833	−31
0·71853	0·77422	1238	842	−25
0·79186	0·78969	1228	839	−21
0·83611	0·76677	1234	856	−15
0·88780	0·76324	1234	860	−13
0·93765	0·75974	1232	860	−8
1·00000	0·75519	1228	878	0
di-n-butylamine + iso-butanol				
0·00000	0·79439	1176	910	0
0·10115	0·79332	1184	899	−7
0·29273	0·78933	1196	885	−15
0·30397	0·78897	1198	883	−17
0·40470	0·78577	1204	877	−20
0·47970	0·78298	1210	872	−22
0·59155	0·76948	1222	870	−21
0·69171	0·76683	1226	867	−20
0·75945	0·76239	1228	869	−16
0·81760	0·76287	1228	869	−14
0·89486	0·75993	1228	872	−9
1·00000	0·75519	1228	878	0

Table 3. Values of constants b_0, b_1, b_2 and $\sigma(K_s)$ in (Tpa^{-1}).

	di-*n*-butylamine plus		
	iso-propanol	iso-butanol	iso-pentanol
T(K)	303·15	303·15	303·15
b_0	−101·6302	−84·8580	−135·1384

where b_0, b_1 and b_2 are adjustable parameters obtained by the method of least-squares and are given in table 3.

References

Riddick J A and Bunger W B 1970 *Organic solvents* (New York: Wiley Interscience)
Timmermans J 1950 *Physico-chemical constants of pure organic compounds* (Amsterdam: Elsevier)
Rao M V P and Naidu P R 1974 *Can. J. Chem.* **52** 788
Ramamurthy M, Sastry G S and Naidu P R 1983 *Indian J. Pure Appl. Phys.* (in press)

ctron impact study of $C_6H_5^+$ fragment ion obtained from three lecules

EZZAT T M SELIM*, A I HELAL and N F ZAHRAN

Nuclear Physics Department, Atomic Energy Establishment, Cairo, Egypt.

MS received 19 February 1983; revised 31 May 1983

Abstract. $C_6H_5^+$ fragment ion produced from toluene, *n*-propylbenzene and acetophenone have been studied using an electron impact technique. The ionization efficiency data have been treated by the inverse convolution first differential technique. First and higher appearance energies for ions produced from the three precursors are reported. The heats of formation for the ions obtained at threshold from the three molecules are calculated.

Keywords. Electron impact study; differential technique; heat of formation; threshold; $C_6H_5^+$ fragment ion.

Introduction

tive ion $C_6H_5^+$ ($m/z = 77$) is a significant contributor to the spectra of nearly all natic and related compounds. Although studies (Grubb and Meyerson 1963; nigny *et al* 1962; Franklin and Carrol 1969) have been performed to establish its cture by determining heats of formation from different precursors, the structure heat of formation of the ion are not well established. The conclusions regarding the cture of the ions appear to oscillate between phenyl ions having ΔH_f around kJ mol^{-1} and linear ions having ΔH_f around 1255 kJ mol^{-1}. On the other hand er *et al* (1964) succeeded in measuring ionization energy of the phenyl radical and ulated ΔH_f to be 1180 kJ mol^{-1}. However, Momigny *et al* (1962) determined the of formation of $C_6H_5^+$ fragment ions from several linear C_6H_6 isomers and his indicated that $C_6H_5^+$ fragment formed from linear compounds is always acyclic $\Delta H_f = 1255$ kJ mol^{-1}. Franklin and Carrol (1969) had concluded that the ious measurements of the appearance energy (AE) of $C_6H_5^+$ ion from aromatic pounds could have involved excess energy which may or may not have resulted in opening.

ne main purpose of the present study is the careful investigation of AE at threshold $_6H_5^+$ fragment ion produced from toluene, *n*-propylbenzene and acetophenone in r to determine ΔH_f values for the ions and to try to identify the ionic structures. detection of the structure in the ionization efficiency (IE) curves of $C_6H_5^+$ ion ined from the three molecules for 3–4 eV above threshold (obtained from the ron impact technique) is also of interest. By combining the inverse convolution edure of Vogt and Pascual (1972) with the first derivative method we have been to measure the appearance energy at threshold for $C_6H_5^+$ produced from the three

molecules and determine the structure in IE curves. This combined technique was developed and examined previously by Selim (1982a) and applied by Selim and Helal (1982) for studying molecular ions of toluene, ethylbenzene and *n*-propylbenzene and to study $C_7H_7^+$ fragment ion obtained from these molecules.

2. Experimental technique

Ionization efficiency data are obtained using an Atlas CH-4 mass spectrometer with a normal electron impact ion source (AN4). The conditions of measurements and the method of calibration of the energy scale are the same as previously reported (Selim 1976). A sensitive electron multiplier is used for detecting the positive ions. The directly measured IE curves are smoothed by a 5-point smoothing technique (Savitzky and Golay 1964). The smoothed data are treated to obtain the first derivative (Savitzky and Golay 1964) IE curves, and then the inverse convolution procedure of Vogt and Pascual (1972) is applied to obtain the deconvoluted first differential IE curves. The complete details of the application of the combined technique have been reported elsewhere (Selim 1982a) together with the merits and limitations of the technique.

3. Results and discussion

The decovoluted first differential IE curves for $C_6H_5^+$ fragment ions produced from toluene, *n*-propylbenzene and acetophenone studied for 3–4 eV above threshold are given in figures 1–3. The AE threshold and higher energy values are compiled in table 1, together with previously available reported values for AE at threshold only. ΔH_f values for $C_6H_5^+$ ion calculated from our AE values are also introduced in table 1 together with previously reported ΔH_f values for the same ion from different sources. The AE values reported in table 1 are the average of four determinations and the errors quoted are the standard deviations. Only reproducible values are reported in table 1.

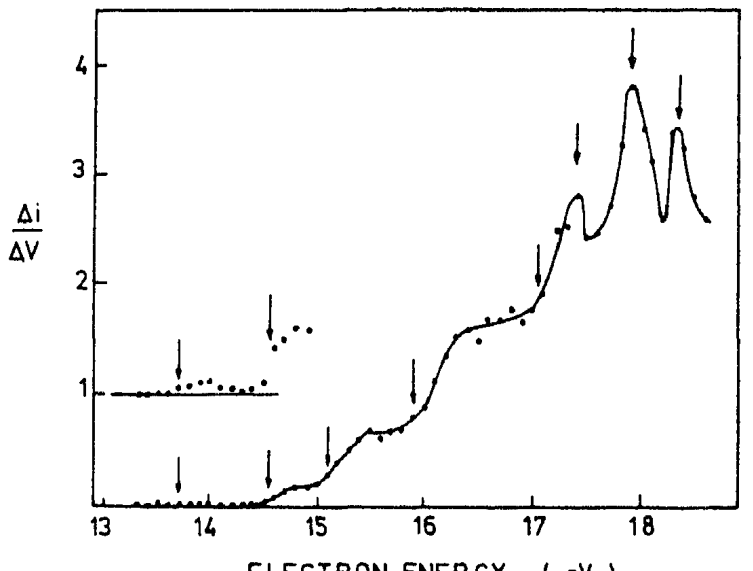

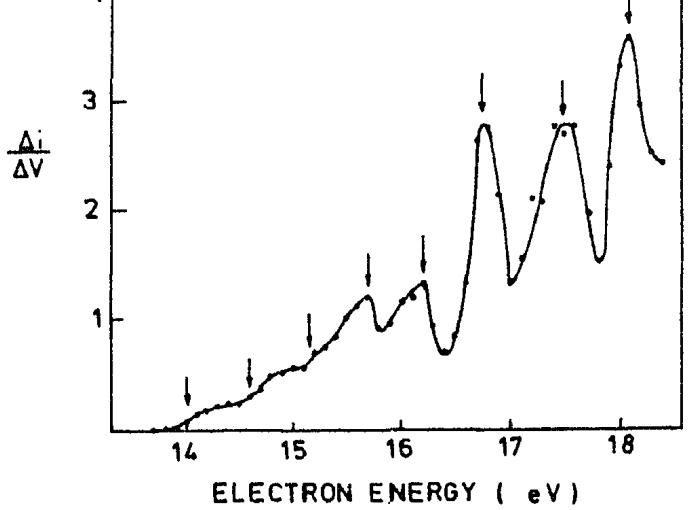

Figure 2. The deconvoluted first differential IE curve for $C_6H_5^+$ ($m/z = 77$) fragment ion obtained from *n*-propylbenzene.

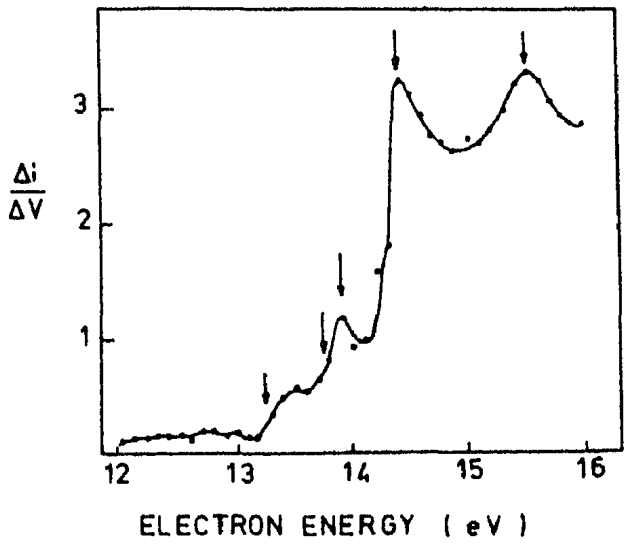

Figure 3. The deconvoluted first differential IE curve for $C_6H_5^+$ ($m/z = 77$) fragment ion obtained from acetophenone.

3.1 $C_6H_5^+$ *fragment ion from toluene*

The IE curve for $C_6H_5^+$ ion ($m/z = 77$) produced from toluene exhibits a relatively long tail (more than 1 eV) at threshold leading to a very low cross-section for the process forming the AE at threshold which is measured at 13·75 eV and is in good agreement with the value (13·70 eV) reported by Majer and Patrick (1962) and Kandel (1954). A wealth of structure have been detected in the deconvoluted first differential IE curve of the ion from toluene but in the absence of theoretical and experimental data one finds it difficult to interpret this structure.

The calculated ΔH_f value for $C_6H_5^+$ ion at threshold is equal to 1238 kJ mol^{-1} and is corresponding to acyclic structure which probably rules out the formation of $C_6H_5^+$ from toluene with phenyl structure. It is worth noting that the results reported

Table 1. AE's and heats of formation for $C_6H_5^+$ fragment ion ($m/z = 77$) obtained from toluene, *n*-propylbenzene and acetophenone.

Source	AE's (eV)		Heat of formation (kJ mol^{-1})	
	This work	Previous determination	This work	Previous determination
Toluene	13·75 ± 0·12	13·70 ± 0·1[a] 13·70 ± 0·05[b]	1238	1234[a]
	14·56 ± 0·09			
	15·02 ± 0·10			
	16·00 ± 0·11			
	17·21 ± 0·09			
	17·38 ± 0·12			
	17·81 ± 0·12			
	18·25 ± 0·13			
	14·10 ± 0·06		1276	—
	14·59 ± 0·06			
	15·14 ± 0·08			
	15·68 ± 0·07			
n-propylbenzene	16·12 ± 0·09			
	16·80 ± 0·10			
	17·53 ± 0·11			
	18·12 ± 0·09			
Acetophenone	13·21 ± 0·09			
	13·47 ± 0·07	13·50[c], 13·42[d]	1150	1180[c], 1171[d]
	13·62 ± 0·13			
	14·36 ± 0·10	14·23 ± 0·05[e]	1261	1251[e]
	14·50 ± 0·20			

(*a*) Majer and Patrick 1962; (*b*) Kandel 1954; (*c*) Majer and Patrick 1963; (*d*) Foffani *et al* 1963; (*e*) Natalis and Franklin 1965.

$C_6H_5^+$ fragment ion from toluene molecular ion by abstraction of CH_3 radical is either by simple cleavage of phenyl-methyl bond or by some sort of rearrangement in the molecular ion before forming $C_6H_5^+$ and CH_3. The ΔH_f value obtained presently for $C_6H_5^+$ at threshold rules out the formation of the ion by simple cleavage. This finding agrees completely with the opinion of Grubb and Meyerson (1963) who reported that the interpretation of the available data in terms of simple cleavage of phenyl-methyl bond proved to be based on erroneous assumptions.

3.2 $C_6H_5^+$ *fragment ion from n-propylbenzene*

The AE at threshold for $C_6H_5^+$ fragment ion ($m/z = 77$) obtained from *n*-propylbenzene is measured at 14·10 eV. No available similar value was previously reported in the literature to compare with. Higher AE have been detected in the IE curve of the ion at 14·59, 15·14, 16·12, 17·53 and 18·12 eV and can be correlated, within experimental errors, with similar higher AE values measured in the IE curve of $C_6H_5^+$ ion produced from toluene at 14·56, 15·02, 16·00, 17·38 and 18·25 eV, respectively. The similarity

(linear) structure for the fragment ion. If one compares the ΔH_f value for $C_6H_5^+$ obtained from *n*-propylbenzene (1276 kJ mol^{-1}) to that obtained from toluene (1238 kJ mol^{-1}) one may suggest that the process of formation of $C_6H_5^+$ from *n*-propylbenzene is associated with about 0·4 eV of excess energy. Similar to the case of toluene one may suggest that the $C_6H_5^+$ fragment ion is obtained from *n*-propylbenzene by some sort of rearrangement of the molecular ion and not by simple cleavage of C_3H_7 radical.

3.3 $C_6H_5^+$ *Fragment Ion from acetophenone*

The deconvoluted first differential IE curve for $C_6H_5^+$ ion produced from acetophenone exhibits a relatively long tail at threshold and a very sharp rise at about 14·20 eV. The previously reported AE values for the ion at threshold measured by Majer and Patrick (1963) at 13·50 eV and Foffani *et al* (1963) at 13·42 eV probably do not correspond to the first AE for the ion but to the second one. These AE can be correlated to the presently measured second AE at 13·59 eV. Also the high AE value at threshold for the ion reported by Natalis and Franklin (1965) at 14·23 eV probably corresponds to a higher AE since it can be correlated with our fourth detected AE at 14·36 eV.

The ΔH_f value calculated for the ion at threshold is equal to 1150 kJ mol^{-1}. This value is in good agreement with ΔH_f value reported previously for the phenyl ion (calculated from ionization energy of C_6H_5 radical) by Lossing *et al* (1964) suggesting that $C_6H_5^+$ produced from acetophenone at threshold has a phenyl ion structure. The path of formation of $C_6H_5^+$ fragment ion from acetophenone was established by Grubb and Meyerson (1963) based on the detection of two metastable peaks at masses 91·9 and 56·7. These two metastable peaks confirm the following two reactions which indicate that $C_6H_5^+$ fragment ion is obtained from $C_7H_5O^+$ fragment ion and not from acetophenone molecular ion by elimination of CO:

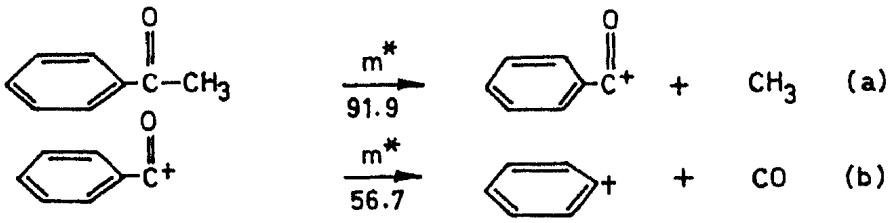

These dissociation paths agree with our results concerning the formation of $C_6H_5^+$ at threshold with phenyl structure since according to reaction (b) CO is eliminated from $C_7H_5O^+$ by simple cleavage to form $C_6H_5^+$ fragment as phenyl ion.

It is possible that at energy higher than the threshold, $C_6H_5^+$ fragment ion can be formed from acetophenone with the less stable acyclic structure. There is supporting evidence for this from the higher AE for this ion. The calculated ΔH_f value corresponding to the fourth AE, for $C_6H_5^+$ fragment ion obtained from acetophenone, at 14·36 eV is equal to 1261 kJ mol^{-1}. The latter value is in agreement with ΔH_f value for the linear ion obtained at 1255 kJ mol^{-1} by Momigny *et al* (1962). The formation of

Fisher I P, Palmer T F and Lossing F D 1964 *J. Am. Chem. Soc.* **86** 2741
Foffani A, Pignataro S, Cantone B and Grasso F 1963 *Nuovo Cimento* **29** 918
Franklin J L and Carrol S R 1969 *J. Am. Chem. Soc.* **91** 5940
Grubb H M and Meyerson S 1963 *Mass spectrometry of organic ions* (ed.) F W McLafferty (New Academic Press)
Kandel R J 1954 *J. Chem. Phys.* (USA) **22** 1426
Majer J R and Patrick C R 1963 *Trans. Faraday Soc.* **59** 1274
Majer J R and Patrick C R 1962 *Trans. Faraday Soc.* **58** 17
Momigny J, Brakier L and D'Or L 1962 *Bull. Cl. Sci. Acad. R. Belg.* **48** 1002
Natalis P and Franklin J L 1965 *J. Phys. Chem.* **69** 2943
Savitzky A and Golay M J E 1964 *Anal. Chem.* **36** 1627
Selim E T M 1976 *Indian J. Pure Appl. Phys.* **14** 547
Selim E T M 1982a *Can. J. Phys.* (communicated)
Selim E T M 1982b (unpublished work)
Selim E T M and Helal A I 1982 *Org. Mass Spectrom.* **17** 539
Vogt J and Pascual C 1972 *Int. J. Mass Spectrom. Ion Phys.* **9** 441

Thermal decomposition studies of catalysed double base propellants

HARIDWAR SINGH* and K R K RAO

Explosives Research and Development Laboratory, Pashan, Pune 411 021, India

MS received 31 January 1983; revised 19 August 1983

Abstract. To understand the role of lead salts of organic acids in the combustion of double base rocket propellants, thermal decomposition behaviour of propellants was studied by DTA and TG methods. Catalysed propellants decomposed at lower temperatures than the control. Percent thermal decomposition of propellants containing lead salts was also higher. Rate constants were higher and energy of activation was lower for catalysed propellants. Results obtained suggest that condensed phase reactions may be the site for the action of lead salts in the combustion of double base propellants.

Keywords. Thermal decomposition; propellants; kinetic study.

1. Introduction

Lead salts of organic acids are reported to produce enhanced burning rates of double base propellants, followed by plateau burning in certain pressure region (Preckel 1961, 1962; Camp 1963; Henry *et al* 1966; Kubota *et al* 1973). Platonized propellants offer many advantages over conventional propellants and therefore, platonization and its mechanism are the subject matter of regular research (Camp *et al* 1954; Sinha and Patwardhan 1968; Kubota *et al* 1974; Lee *et al* 1978). Any catalyst or ballistic modifier to be effective should participate in, influence or modify the reactions taking place in various reaction zones. Many research workers hypothesised that surface and fizz zones are the likely site for the action of lead salts and reactions of luminous flame zone are less important. While studying the thermal decomposition products of organic lead and copper salts by mass spectrometer, Farber and Srivastava (1978) found that metallic salts of organic acids decompose to metallic elements, whereas organo-metallic compounds like tetraphenyl lead merely vapourise. They found that lead acetate, lead salicylate and lead-β-rescorcylate decompose to form H_2, H_2O, CO_2 and OH between 200–500°C. With lead acetate at 550°C, CO peak was more pronounced but was smaller than CO_2 intensity. At around 500–600°C, lead atoms were seen at fairly high intensity. The residue in the cell left after decomposition contained lead droplets and solid carbon. Eisenreich and Pfeil (1978) observed that propellants containing lead salts produce lower activation energy (E) and higher heats of reaction. Lead salts can influence the kinetics and/or energetics of the reactions of various zones. Hence, it appeared of interest to study the role of thermal decomposition of lead salts on the combustion of double base propellants.

prepared in the laboratory by precipitation method (Klare and Markley 1961). Propellant strands were prepared by solventless extrusion technique (Warren 1960).

Differential thermal analysis (DTA) of propellants and lead salts was carried out with an indigenously fabricated instrument having stanton Redcroft (UK) temperature programmer. Platinum/platinum-13% rhodium thermocouples were used. Platinum crucibles were used as a container for samples. Alumina was used as a reference sample. Thermogravimetric analysis (TG) of propellants was carried out with the help of TG apparatus of Stanton Redcroft (UK) make. All experiments were carried out under atmospheric condition.

3. Results and discussions

During steady state burning of double base propellant, four distinct reaction zones, namely, foam, fizz, dark and luminous zones have been identified (Kubota *et al* 1974). Lead salts are expected to affect the reactions taking place in one or more of these zones. We have reported earlier that lead salts of aliphatic acids like lead acetate, lead palmitate, lead stearate, lead oxalate, lead succinate etc decompose in an exothermic mode in the temperature range 300–500°C (Singh *et al* 1982a). Lead sebacate decomposes between 204–500°C with peak temperature (*Tm*) at 483°C. Among lead salts of aromatic acids, lead salicylate decomposed between 344–462°C with peak temperature at 446°C, whereas lead phthalate decomposed between 353–563°C with peak temperature at 474°C. Lead methylene di-salicylate (LMDS) is reported to decompose between 230–325°C with peak temperature at 305°C (Singh *et al* 1982b). These results suggest that, in general, lead salts of organic acids decompose exothermally in the temperature range of 300–500°C, which is very close to the temperatures of surface and fizz zones. Hence, exothermic decomposition of lead salts is likely to affect the reactions of these zones.

The DTA results of propellants are presented in table 1. The control propellant decomposed between 150–179°C with *Tm* at 174°C, whereas propellants containing lead salts decomposed between 145–165°C, with peak temperatures varying between 155–158°C. We have reported earlier that propellants containing lead acetate, lead palmitate and lead oleate plus carbon black (0.5 part) decomposed exothermally in the temperature range 147–166°C (Singh *et al* 1982a). Thus, at very low rate of heating (3°C/min) propellants containing lead salts decomposed at lower temperatures than the control. In view of these observations, further experiments were carried out at higher rate of heating (5°C/min). Even at the heating rate of 5°C/min, catalysed propellants decomposed at lower temperatures than the control. When the experiments were carried out under nitrogen atmosphere (flow rate of 10 l/hr), the nature of thermogram was the same as under atmospheric condition. Thus, lower decomposition temperatures and higher heats of reaction of catalysed propellants (area under thermogram for catalysed propellant was higher than the control for the same weight of propellant) may be the probable reasons behind the catalytic effect produced by lead salts. Though these data were generated at lower temperatures and at lower heating rate than the

Additives (2 parts per 100 parts)	Weight (mg)	Decomposition Temperature (°C) Inception (T_i)	Final Temp. (T_f)	Peak Temp. (T_m)
	(i) Heating rate – 3°C/min			
nil	17·6	150	179	174
Lead sebacate	18·3	145	162	157
Lead oleate	17·8	147	164	156
Lead-β-resorcylate	18·2	145	162	155
Lead phthalate	17·5	146	165	158
	(ii) Heating rate – 5°C/min			
nil	16·0	157	181	180
Lead sebacate	15·6	153	168	166
Lead oleate	16·0	149	168	164
Lead-β-resorcylate	16·8	152	175	173
Lead phthalate	16·0	154	173	170

(Composition: NC-51·0, NG-37·0, Carbamite-3·0, DNT-3·5, DBP-5·5)
Maximum temperature – 500°C

Table 2. Percent thermal decomposition of propellants (TG).

Temperature (°C)	Control	Lead palmitate (2 parts)	Lead sebacate (2 parts)	Lead stearate (2 parts)	Lead oleate (2 parts)
		Rate of Heating – 5°C/min			
110	5·0	4·5	4·5	4·5	4·5
120	8·5	8·0	8·0	10·5	10·5
130	15·0	14·0	11·0	22·5	16·8
140	22·5	22·0	13·5	37·5	41·0
150	30·0	30·0	16·0	47·0	48·0
160	33·5	36·0	18·5	54·0	60·0
170	36·5	40·5	22·5	69·0	70·0
180	40·0	43·0	27·5	—	—

(Composition: NC-51·0, NG-37·0, Carbamite – 3·0, DNT-3·5, DBP-5·5)

conditions of actual propellant combustion, still the results show the trend on the pattern of reactions occurring during combustion.

TG analysis of propellants containing a few selected lead salts was carried out to find out the effect of lead salts on the percent decomposition of propellants. The

140–170°C (near the ignition temperature of propellant) than the control. Lower percent decomposition in lead sebacate containing composition is an odd case and needs further investigation. This may be due to enhanced thermal stability of propellant, probably due to stabilization effect of lead sebacate on the propellant decomposition products.

From the results of weight loss of propellants at different temperatures for a fixed duration of 3 hr, two kinetic parameters namely, rate constants and energy of activation (using Arrhenius equation $E = 2{\cdot}3033\, RT_1T_2 \log K_2/K_1/(T_2 - T_1)$, where K_1 and K_2 are rate constants at temperatures T_1 and T_2, R is gas constant) for the thermal degradation of propellants were calculated for temperature ranges 130–150°C and 140–160°C. These two temperature ranges were chosen based on the consideration that double base propellants decompose/ignite between 140–160°C. Results are given in table 3. Rate constants were higher and energy of activation was lower for catalysed propellants than those for the control propellant.

Considering the results obtained from a semi-quantitative angle, the heat balance equation at the propellant surface can be given by (Rastogi *et al* 1977);

$$\dot{m} C_s(T_s - T_0) = \frac{\lambda_g (T_f - T_s)}{L} + \dot{m} Q_s \tag{1}$$

Where, $\dot{m}$ = mass burning rate, C_s = specific heat of solid propellant, T_s = surface temperature, T_0 = ambient temperature, T_f = flame temperature, Q_s = net heat release for gasification of propellant, λ_g = average thermal conductivity of gas, L = thickness of the reaction zone.

Table 3. Kinetic parameters for the thermal degradation of propellants.

Additives	Temperature (°C)	Rate constant (K) (hr^{-1})	Energy of activation (E) (K. cal/mole)
Control	130	0·036	16·9
	150	0·097	
Lead stearate	130	0·049	14·6
(2 parts)	150	0·115	
Lead oleate	130	0·076	13·5
(2 parts)	150	0·171	
Lead sebacate	130	0·054	11·4
(2 parts)	150	0·107	
Control	140	0·063	53·5
	160	1·305	
Lead stearate	140	0·063	51·2
(2 parts)	160	1·146	
Lead sebacate	140	0·075	51·0
(2 parts)	160	1·328	
Lead oleate	140	0·065	51·7

To understand the role of the thickness of the reaction zone, the reaction zone may be considered as a continuous chemical reactor [volume (V) = $L \times$ area], where reactant gases are fed with certain velocity depending on the rate of thermal decomposition of propellant from the surface. The thickness of reaction zone represents the distance, which the reactants have to travel for the completion of gas phase reactions and hence smaller the reaction zone, faster will be the reaction. Therefore, if solid or gas phase reactions are catalysed, L would be smaller, implying increased burning rate. Higher rate constants and lower energy of activation for catalysed propellants (table 3) suggest that lead salts can reduce the thickness of reaction zone considerably, accounting for higher burning rates.

4. Conclusion

Lead salts of organic acids decompose exothermally in the temperature range 300–500°C, which is very close to surface temperature of double base propellants. Propellants containing lead salts decompose at lower temperatures than the control. The per cent thermal decomposition and rate constants were higher for modified propellants. Energy of activation (E) was lower for catalysed propellants.

References

Camp A T 1963 *U.S. Patent* **3** 088 858

Camp A T, Cartan C H and Hansman H K 1954 *Bull. 10th meeting of JANAF Solid propellant group* p. 81

Eisenreich N and Pfeil A 1978 *Thermo-chimica Acta* **27** p. 339

Farber M and Srivastava R D 1978 *Combust. flame* **31** p. 309

Henry R A and Mcewan W S 1966 *U.S. Patent* **3** 228 815

Kubota N, Ohlemiller T J, Caveny L H and Summerfield M 1973 *Tenth Int. Symp. Space Technol. Sci.* Tokyo

Kubota N, Ohlemiller T J, Caveny L H and Summerfield M 1974 *AIAA* 12 p. 1709

Klare S Markley 1961 *Salts of fatty acids*, Fatty acids their chemistry, properties, production and uses, Part II (New York: Interscience Publishers)

Lee L A, Austin T D and Camp A T 1978 *A photo chemical combustion mechanism for mesa and plateau burning of double base propellants.* (Private communication)

Preckel R F 1961 *ARS* **31** p. 1286

Preckel R F 1962 *U.S. Patent* **3** 009 796

Rastogi R P, Singh G and Singh R R 1977 *Combust. Flame* **30** p. 117

Sinha S K and Patwardhan W D 1968 *Explosivstoffe* **10** p. 223

Singh H and Rao K R K 1982a *J. Spacecraft rocket* **19** p. 478

Singh H and Rao K R K 1982b *Propellant, Explosives, Pyrotechnics* **7** p. 61

Warren F A 1960 *Rocket propellants*, (New York: Reinhold Publishers)

Compensation effect in the electrical conduction process in a series of pyrenyl polyenes

A SIRCAR, B MALLIK and T N MISRA*

Optics Department, Indian Association for the Cultivation of Science, Jadavpur, Calcutta 700032, India

MS received 26 April 1983; revised 1 August 1983

Abstract. The semiconductive properties of a series of pyrenyl polyenes of the type R–$(CH{=}CH)_n$–R, are studied as a function of the adsorption of different amount of a vapour. With regard to the compensation temperature (T_0) the compounds are divided into two groups. For compounds which have odd number of double bonds, T_0 is infinite and in compounds having even number double bonds, T_0 is finite. T_0 for II_2 is higher while that of II_4 is lower than the experimental temperature. Different T_0 for the compounds having odd or even number of double bonds suggests a physical basis for the compensation rule, which we believe, is related to the molecular and crystalline structure of the compounds.

Keywords. Pyrenyl polyenes; electrical conduction; compensation effect.

1. Introduction

Earlier investigations (Mallik *et al* 1979, 1980a) in some linear conjugated polyenes revealed that the compensation temperature (T_0) of an organic semiconductor plays an important role in the dark conduction process. The decrease or increase in activation energy (E) with concomitant increase in conductivity (σ) as a result of adsorption of vapours on the polyene crystallites depends on whether T_0 is higher or lower than the experimental temperatures. As for example in vitamin A (alcohol and acetate) (Mallik *et al* 1979) a decrease in activation energy (E) with increase in σ on adsorption of vapours were observed and the compensation temperature for these compounds were at much higher value than the experimental temperatures. On the other hand the compensation temperatures of polyenes (Mallik *et al* 1980a) β-apo-8′-carotenal, astacene and methyl bixin being lower than the experimental temperatures, an increase in activation energy with a simultaneous increase in σ were observed on adsorption of vapours. It has been pointed out (Rosenberg *et al* 1968; Waclawck and Zabcowska 1980) that T_0 depends on the molecular property of the semiconductors. But it is still not clear which factors control the T_0 value. Recently it has been shown (Sircar *et al* 1982) that the observed compensation behaviour as well as the kinetics of adsorption and desorption for a series of naphthyl polyene compounds with odd number of double bonds are distinctly different from those having even number of double bonds. We have extended such investigations on a series of pyrenyl polyenes, with increasing number of double bonds to study the effect of the polyene end group and also the number of double bonds on the compensation temperature. In this paper we present the results of our investigations.

* To whom all correspondence should be addressed.

Highly pure samples of α,ω-di-2-pyrenyl polyenes of the type R–(CH=CH)$_n$–R, where R stands for the pyrenyl group and $n = 1$ to 4, were used for study. The samples were gifted to us by Prof. Nakagawa of Osaka University, Japan, who synthesised these chemicals and performed spectral studies (Nakasuji *et al* 1972). We have followed their convention of denoting the samples II_n. Sandwitch cell technique (Mallik *et al* 1979) was employed with a conducting glass and a stainless steel electrode. Organic solvents of spectrograde quality (E Merck, BDH) were used for adsorption studies. Dry nitrogen gas was used as carrier to pass the reagent vapour in the chamber. Repeated heating and cooling of the sample initially in vacuum and finally in dry nitrogen atmosphere ensured desorption of water vapour or any other adsorbed gases. The currents were measured with an electrometer amplifier EA 815 of the Electronic Corporation of India Ltd. The details of the experimental arrangement are as described earlier (Mallik *et al* 1979).

3. Results and discussions

As in other polyenes (Mallik *et al* 1979, 1980a), in pyrenyl polyenes also, the current starts increasing on adsorption of vapours and finally attains a saturation value. The maximum value of the current reached at equilibrium, under a particular experimental condition, depends on the vapour pressure of the reagent chemical and the temperature of the sample cell. The time required to attain this maximum equilibrium value at a fixed vapour pressure depends on the rate of flow. With increase in semiconduction current, the activation energy also changed significantly. The $\log \sigma\ (T)$ vs $1/T$ plot for any sample studied gives two distinct straight lines: One in the low temperature region after complete adsorption and the other in the high temperature region after complete desorption. The slope of the line in the low temperature region gives the activation energy in the adsorbed stage and that in the high temperature region reproduces the activation energy of the original sample. Such a plot of $\log \sigma$ and $1/T$ for II_1 on adsorption of ethyl acetate vapour is shown in figure 1.

4. Semiconductive properties

We have studied the effect of adsorption of different amount of a particular vapour on the activation energy of these polyene semiconductors in the usual manner (Mallik *et al* 1979, 1980b). The change in E is different for different amount of the same vapour adsorbed. In figures 2 and 3 change in E for II_1 and II_2 compounds on adsorption of different amount of ethyl acetate vapours are shown. For II_1 compound almost parallel extrapolated lines for different amount of adsorption are obtained. In II_2 compound the change in E is appreciable and the extrapolated lines all pass through a single point corresponding to a temperature T_0. At this point the $\sigma\ (T_0)$ value is called σ_0' which is a constant. Excellent plot of $\log \sigma_0$ vs E was obtained for II_2 compound and is shown in figure 4. σ_0' and T_0 values as obtained from figures 3 and 4 are $2{\cdot}4 \times 10^{-7}$ ohm^{-1} cm^{-1} and 310·5 K. Agreement between the set of values obtained from figures 3 and 4 confirm

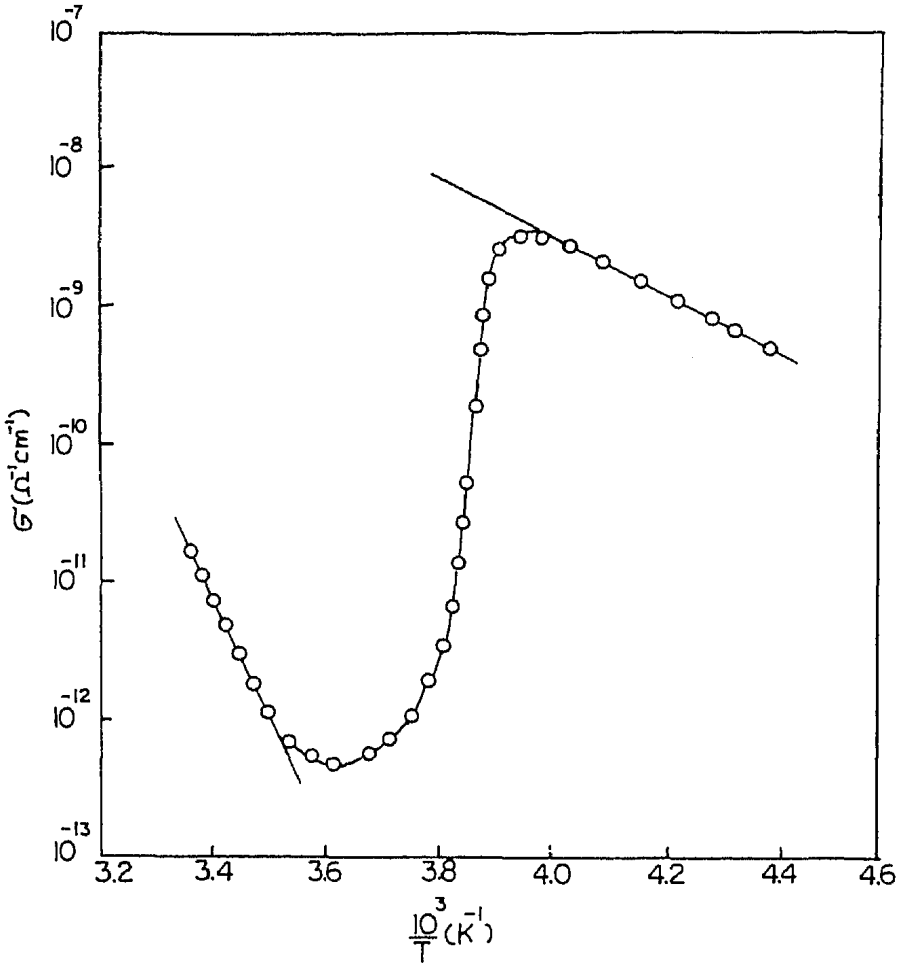

Figure 1. Semiconductivity data in an ethyl acetate adsorbed powder cell of II_1 compound as a function of temperature. Ambient vapour pressure at 60 torr; sample temperature 250 K.

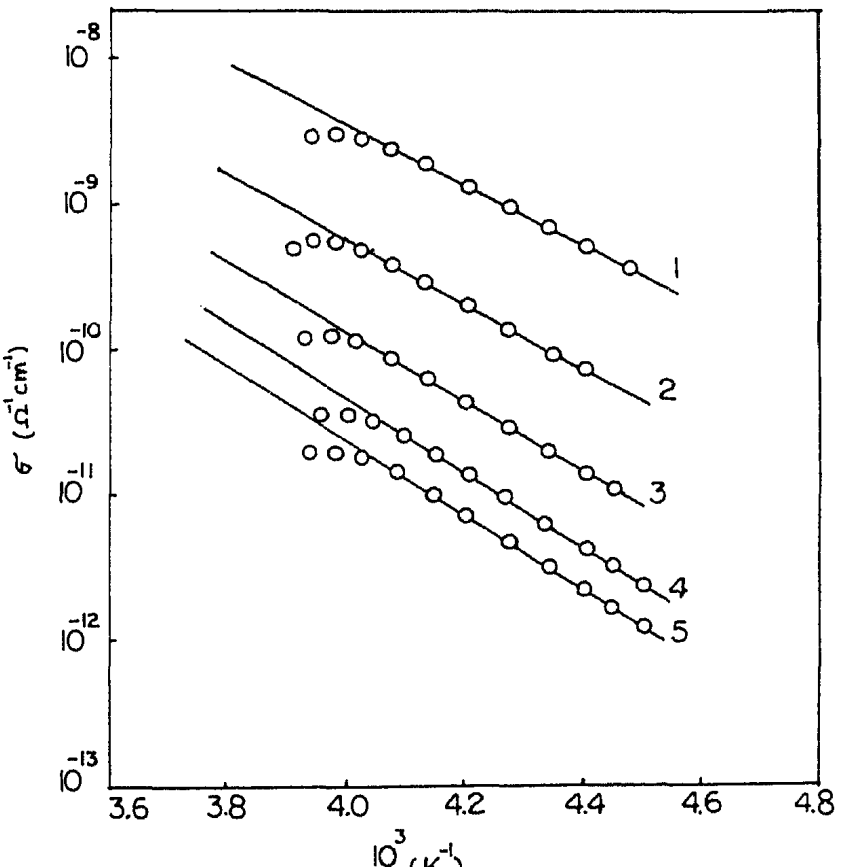

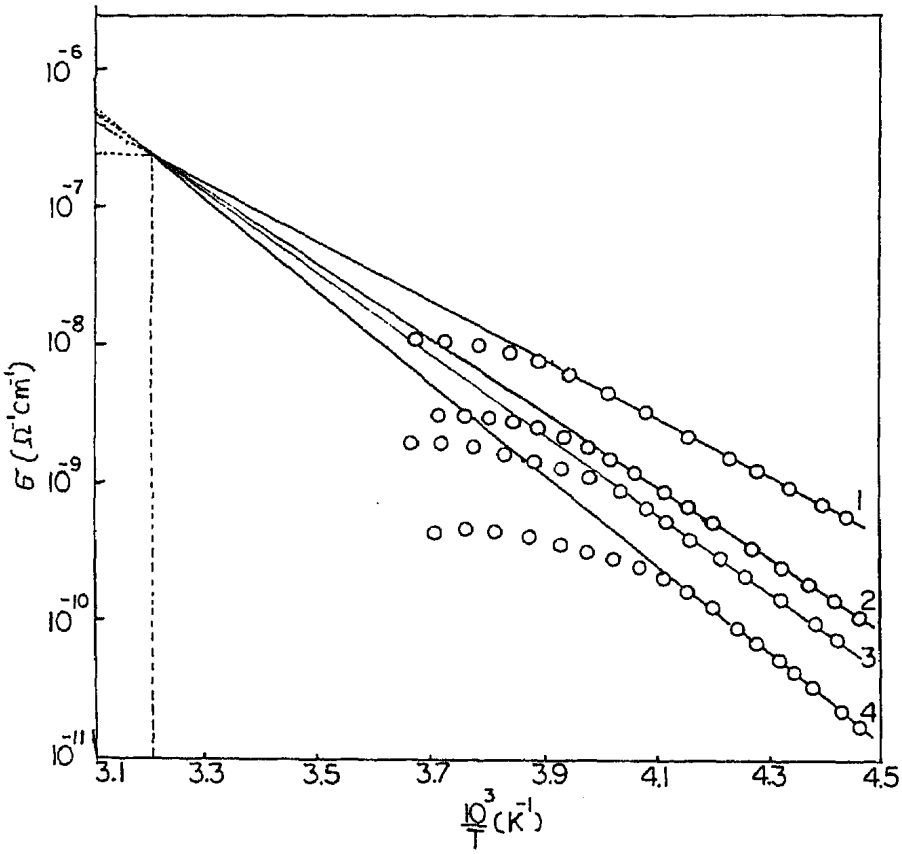

Figure 3. Semiconductivity data for II_2 compound with the adsorption of different amount of ethyl acetate vapour at 60 torr pressure and at sample temperature of 263·5 K. The curves (1) to (4) refer to the states with decreasing amount of adsorbed vapour.

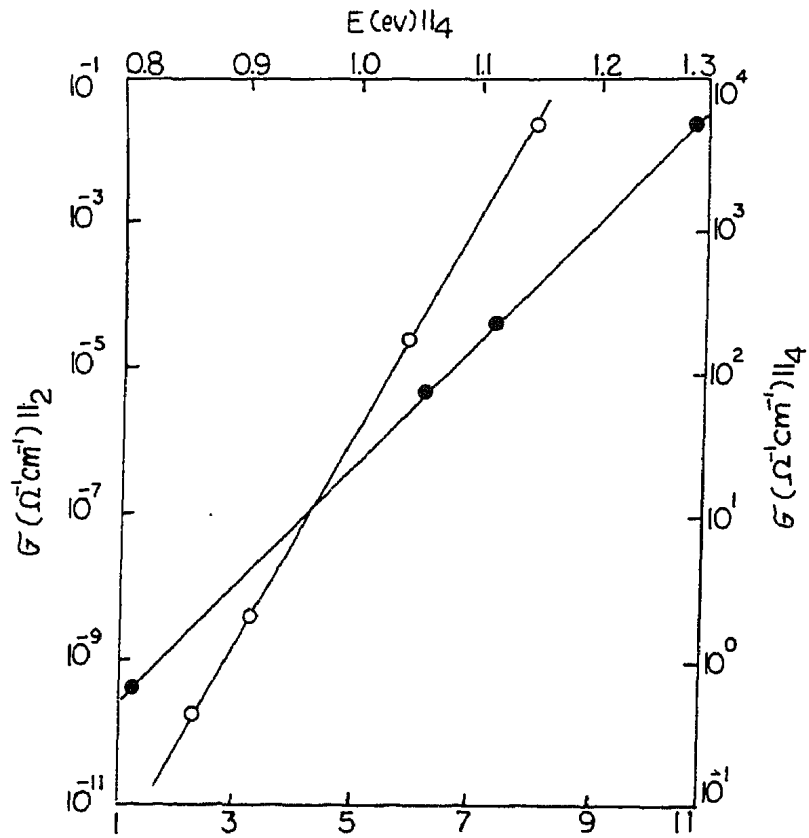

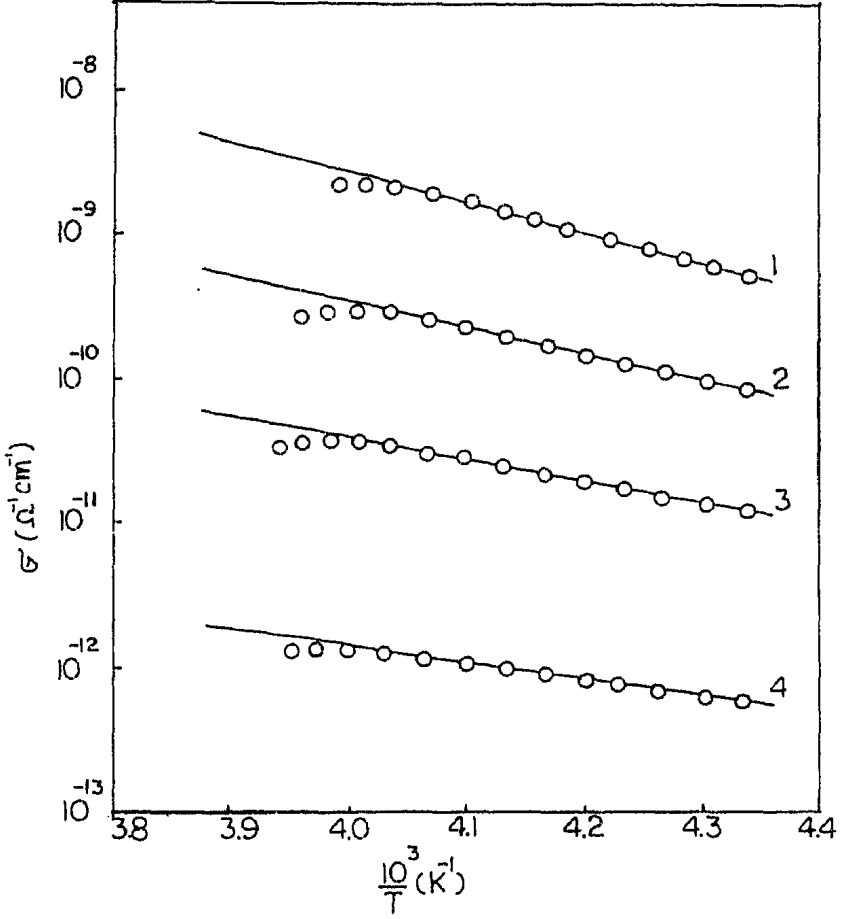

Figure 5. Semiconductivity data for II_3 compound with the adsorption of different amount of ethyl acetate vapour at 60 torr pressure and at a sample temperature of 250 K. The curves (1) to (4) refer to the decreasing amount of adsorbed vapour.

ll and the extrapolated lines are almost parallel whereas for II_4 the extrapolated s meet at a fixed point. Contrary to that in II_2, in II_4 compound the slope of log σ vs plot increases as the amount of adsorbed vapour increases. The plot of log σ_0 vs E II_4 is shown in figure 4; T_0 and σ'_0 values as obtained from figures 4 and 6 for II_4 = 172·7 K; $\sigma'_0 = 4{\cdot}7 \times 10^{-14}$ ohm^{-1} cm^{-1}) are also in good agreement. Thus the luctivity equation for II_2 and II_4 takes the form $\sigma(T) = \sigma'_0 \exp E/2k(1/T_0 - 1/T)$ ompensation rule is also valid in these cases. It is obvious from the equation that if T (or $T_0 \ll T$) a small change in E compared to (T) is expected as is observed for II_1 II_3 respectively in our limited experimental range. Experimentally observed set of llel lines in ln σ vs $1/T$ plots in figures 2 and 5 suggests T_0 of the above equation is er ∞ or 0. However, T_0 cannot be zero, for in that case, $\sigma(T)$ becomes infinite. On other hand, $T_0 = \infty$, gives $\sigma(T) = \sigma_0 \exp(-E/2kT)$ which is the operational nition of semiconductor. These results indicate that in these polyene semiconduc- compensation temperature T_0 is finite only for compounds with even number of ble bonds. For compounds with odd number of double bonds T_0 becomes infinite.

nowledgements

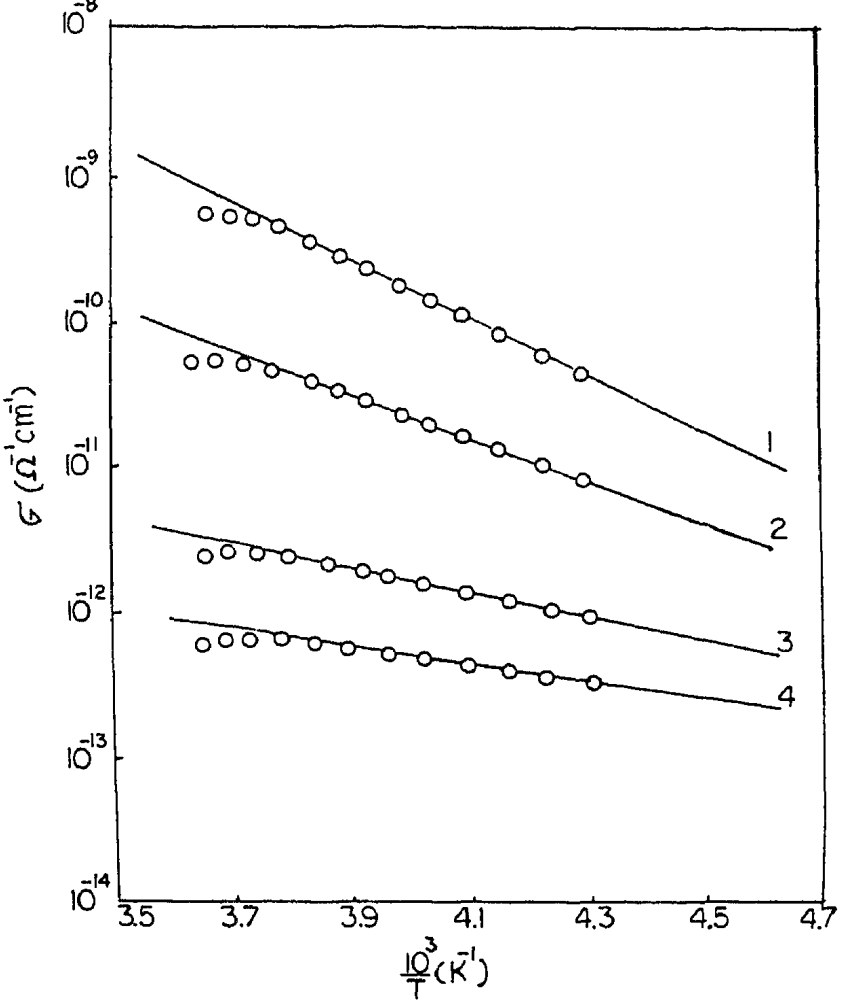

Figure 6. Semiconductivity data for II_4 compound with the adsorption of differen of ethyl acetate vapour at 60 torr pressure and at sample temperature 263·5 K. The c to (4) refer to the states with decreasing amount of adsorbed vapour.

References

Mallik B, Ghosh A and Misra T N 1979 *Bull. Chem. Soc. Jpn.* **52** 2091
Mallik B, Ghosh A and Misra T N 1980a *Phys. Status Solidi* **62** 267
Mallik B, Ghosh A and Misra T N 1980b *Jpn. J. Appl. Phys.* **19** 207
Nakasuji K, Akiyama S and Nakagawa M 1972 *Bull. Chem. Soc. Jpn.* **45** 875
Rosenberg B, Bhowmick B, Harder H C and Postow E 1968 *J. Chem. Phys.* **49** 4108
Sircar A, Mallik B and Misra T N 1982 *Phys. Status Solidi* **69** 767
Waclawck W and Zabkowska M 1980 *Phys. Status Solidi* **K60** 17

benzaldehydes

P VENKOJI

Molecular Spectroscopy Laboratories, Department of Physics, Andhra University, Waltair 530 003, India

MS received 15 January 1983; revised 8 July 1983

Abstract. The vibrational frequencies of 2,4- and 2,5-dimethylbenzaldehydes have been reported from the study of IR absorption and Raman spectra of these molecules recorded in liquid phase. The probable assignments for all the frequencies are presented in terms of the fundamentals, overtones or combinations.

Keywords. Infrared spectrum; Raman spectrum; vibrational frequencies; dimethylbenzaldehydes.

1. Introduction

As a part of the general programme to obtain the vibrational frequencies pertaining to the (a) ground electronic state from the IR absorption, Raman and emission spectra and (b) excited electronic state from the near UV absorption spectra of polysubstituted benzenes and also with a view to apply them to the study of molecular force fields, mean square amplitudes of vibration, centrifugal distortion constants etc., the present paper deals with the recording of the IR and Raman spectra of 2,4- and 2,5-dimethylbenzaldehydes and the identification of the observed frequencies, in the ground electronic state, which have not been investigated so far.

2. Experimental

The IR absorption spectra of both the molecules are recorded in the liquid phase on a UR 10 spectrophotometer in the region 400–4000 cm^{-1}. The Raman spectra are recorded on a Cary 82 spectrophotometer with Argon-Ion laser source. The traces of these spectra are shown in figures 1 to 4.

3. Analysis

Both the molecules belong to 1,2,4-trilight substituted benzene class on the basis of Varsányi's classification of the molecules (Varsányi 1974).

These molecules are expected to give rise to 30 fundamental vibrations characteristic of the phenyl ring and 24 fundamental vibrations characteristic of the internal vibrations of the substituent groups.

The identification of the 30 phenyl ring vibrations is based on (i) the procedure adopted by Varsányi (1974) in classifying the molecules and the identification of the

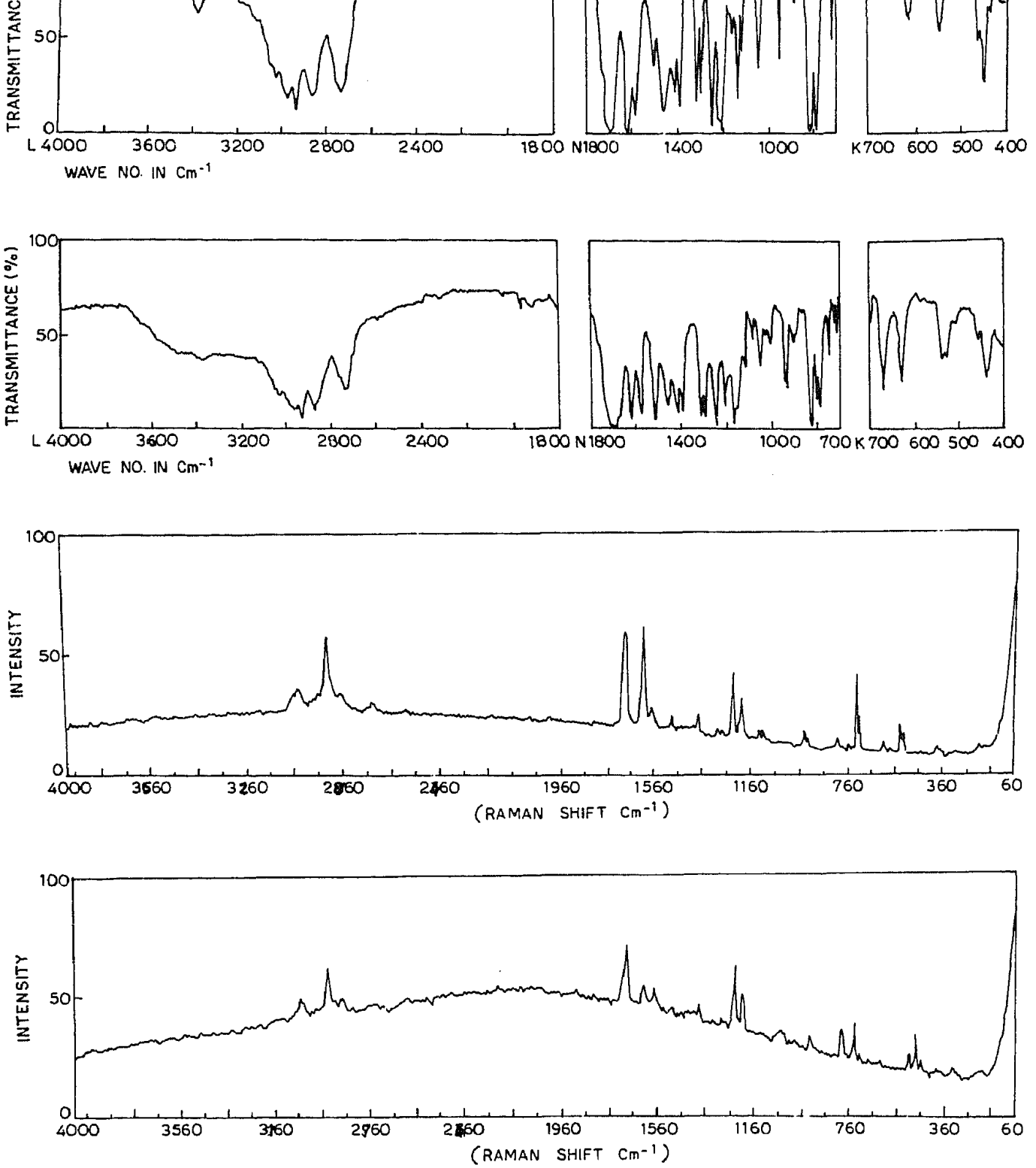

Figures 1–4. **1, 2.** IR spectrum of **1.** 2,4-dimethyl benzaldehyde **2.** 2,5-dimethyl benzaldehyde **3, 4.** Raman spectrum of **3.** 2,4-dimethyl benzaldehyde **4.** 2,5-dimethyl benzaldehyde.

fundamental modes of vibrations in such substituted benzenes together with the expected ranges for the modes of vibrations, (ii) a comparison of the spectra of benzaldehyde, isomers of methyl benzaldehyde, and other related molecules in-

Table 1. Observed frequencies and their proposed assignments.

2,4-dimethyl bzh		2,5-dimethyl bzh			
IR Freq. (cm^{-1}) (1)	Raman Freq. (cm^{-1}) (2)	IR Freq. (cm^{-1}) (3)	Raman Freq. (cm^{-1}) (4)	Wilson's mode (5)	Proposed assignments (6)
3376 w					441 + 2930
3116 vw					1500 + 1615
3043 sh	3057 w	3050 sh	3056 vw	2	C–H stretching
3028 w	3038 w, p	3030 vw	3041 vw	20 b	C–H stretching
2968 sh		2969 m			C–H asym. stretching in CH_3 gro
2954 sh					C–H asym. stretching in CH_3 gro
2930 ms	2919 vs, p	2935 s	2937 s		C–H sym. stretching in CH_3 grou
2869 br	2865 w	2874 m	2875 m		2 × C–H asym. def.
2738 s	2738 w	2735 br			C–H stretching in CHO group
		2183 vw			939 + 1248
		2115 vw			826 + 1291
1961 vw					717 + 1246
1913 vw					791 + 1117
		1913 vw			826 + 1083
		1800 vw			905 × 2
1700 vs	1693 vs	1700 vs	1695 s		C=O stretching
		1687 sh			783 + 905
1615 vs	1609 vs, dp	1617 vs	1625 m	8 b	C–C stretching
1577 vs	1571 w, p	1574 vs	1579 m	8 a	C–C stretching
1500 ms	1489 w, p	1508 vs	1506 vw	19 b	C–C stretching
1465 s		1461 s			CH_3 asym. def.
1409 ms	1400 vw	1417 s		19 a	C–C stretching
1390 vs	1377 w	1391 vs	1391 vw		CH_3 sym. def.
1310 s	1300 s	1308 vs	1302 w		C–H i.p. bending (CHO group)
1291 s	1281 vw	1291 s		14	C–C stretching
1246 vs	1235 s, p	1248 vs	1248 vs	7 a	C–CH_3 stretching
1209 vs	1197 m	1209 s	1217 s	13	C–CHO stretching
1175 vw					456 + 717
		1165 vw	1145 vw	18 a	C–H i.p. bending
1161 vw					441 + 717
1138 vs	1127 w, p			18 a	C–H i.p. bending
1117 m	1110 w, p	1117 mw	1118 vw	18 b	C–H i.p. bending
1083 vw					545 × 2
		1083 vw			535 × 2
1045 s		1048 m	1050 vw		CH_3 rocking
1008 vw		1005 w	1002 vw		CH_3 rocking
950 ms	943 w, p			7 b	C–CH_3 stretching
938 vw	931 vs, dp	939 s	941 w	17 b	C–H o.p. bending
		905 w		7 b	C–CH_3 stretching
888 w		869 vw		5	C–H o.p. bending
817 s		826 vs		11	C–H o.p. bending
800 sh	802 w, p	800 ms	802 w		C=O i.p. bending
791 vs	785 vs	783 vs		12	C–C–C i.p. bending
717 m	722 ms	743 m	745 s	1	ring breathing
		718 vw	715 vw		333 + 393

Table 1. (*Continued*)

2,4-dimethyl bzh		2,5-dimethyl bzh			
IR Freq. (cm^{-1}) (1)	Raman Freq. (cm^{-1}) (2)	IR Freq. (cm^{-1}) (3)	Raman Freq. (cm^{-1}) (4)	Wilson's mode (5)	Proposed assignments (6)
545 m	537 w	535 w	517 w	6 a	C–C–C i.p. bending
456 m	452 vw	508 vw	491 m	6 b	C–C–C i.p. bending
441 s		458 w	468 w	16 b	C–C–C o.p. bending
425 vw	425 vw	437 ms		9 b	C–CHO i.p. bending
	383 vw		393 vw	10 a	C–CH_3 o.p. bending
			333 w	9 a	C–CH_3 i.p. bending
	210 vw		210 vw	10 b	C–CHO o.p. bending

bzh = benzaldehyde, v = very, s = strong, m = medium, w = weak, sh = shoulder, br = broad, p = polarized, dp = depolarized, sym = symmetric, asym = asymmetric, def = deformation, i.p = in-plane, o.p = out-of-plane.

general comparison of the frequencies identified by Green *et al* (1971) in the 1,2,4-trisubstituted benzenes, and also (iv) taking care to see that overlaps of the regions expected of different modes of vibrations are properly explained. The frequencies together with their visual intensities and modes thus identified are shown in table 1.

Regarding the 24 vibrational frequencies characteristic of the substituents, one expects 9 vibrations for a methyl group and 6 vibrations for the aldehyde group. As these internal frequencies are not expected to show any marked variations, in the substituted benzenes having these substituents, these internal frequencies could be identified with less ambiguity. In the present investigation seven internal frequencies—two asymmetric stretching, one symmetric stretching, one asymmetric deformation, one symmetric deformation and two rocking modes—due to methyl group, and five internal frequencies—C=O stretching, C=O in-plane-bending, C=O out-of-plane bending, C–H stretching and C–H in-plane bending—due to the aldehyde group could be identified.

The assignments, are well in agreement with those made in substituted toluenes (Singh and Singh 1968), xylenes (Varsányi 1974) and benzaldehydes (Padhye and Viladkar 1960; Varsányi 1974) and are shown in table 1.

Acknowledgements

The author is deeply indebted for the invaluable help rendered by the CISL, Bangalore for recording the IR spectra and also to Prof. Surjit Singh, Head, RSIC, Madras for recording the Laser Raman spectra. He is grateful to the UGC, New Delhi for the award

edi C P D 1968 *Indian J. Pure Appl. Phys.* **6** 440
n J H S, Harrison D J and Kynaston W 1971 *Spectrochim. Acta.* **A27** 807
n J H S and Harrison D J 1976 *Spectrochim. Acta.* **A32** 1265
B, Srivastava M P and Singh I S 1973 *Indian J. Pure Appl. Phys.* **11** 615
ye M R and Viladkar B G 1960 *J. Sci. Ind. Res.* **B19** 45
l N K, Goel R K and Agarwal M L 1981 *Indian J. Pure Appl. Phys.* **19** 480
V B and Singh I S 1968 *Indian J. Pure Appl. Phys.* **6** 682
S J and Ranjeet Singh 1978 *Indian J. Pure Appl. Phys.* **16** 939
stava M P, Singh O N and Singh I S 1968 *Curr. Sci.* **37** 100
stava M P, Lal B B and Singh I S 1972 *Indian J. Pure Appl. Phys.* **10** 50
inyi G 1974 *Assignments for vibrational spectra of seven hundred benzene derivatives*, Vols I & II England: Adam Hilger)
inyi G, Molnár-Paal E, Kósa K and Keresztury G 1979 *Acta Chimica Academiae, Scientiarum ungaricae*, Tomus 100 (1–4) 481

Preparation and characterization of vanillin thiosemicarbazone complexes with Co(II), Ni(II), Cu(II), Zn(II), Cd(II) and Hg(II)

K K ARAVINDAKSHAN* and C G R NAIR

Department of Chemistry, University of Kerala, Trivandrum 695 034, India
* Department of Chemistry, Government College, Kasaragod P.O. Vidyanagar 670 123, India

MS received 7 March 1983; revised 5 October 1983

Abstract. Complexes of vanillin thiosemicarbazone (3-methoxy-4-hydroxybenzaldehyde thiosemicarbazone), (VTSCH) with several divalent metal ions have been isolated. Structures have been assigned to these complexes based on electrical conductivity, magnetic susceptibility and spectroscopic measurements.

Keywords. Vanillin thiosemicarbazone complexes; electrical conductance; magnetic susceptibility; spectral studies.

1. Introduction

The thiosemicarbazones of substituted benzaldehydes show marked differences in their donor properties and biological activities compared to that of unsubstituted benzaldehyde. Vanillin thiosemicarbazone has long been studied for its fungicidal and antitubercular activities (Paulo da Silva Lacaz *et al* 1958). It has also been tested as a reagent for metal ions. Apart from these, structural studies on the metal derivatives of this thiosemicarbazone, however, have not been carried out so far.

2. Experimental

2.1 *Reagents*

Vanillin thiosemicarbazone was prepared by refluxing recrystallised thiosemicarbazide with vanillin (1 : 1 ratio) in ethanol for 2 hr.

2.2 *Preparation of the complexes*

The complexes of Co(II), Ni(II) and Cu(II) were prepared by adding a hot aqueous solution of the respective metal acetate or chloride, dropwise, to a refluxing methanolic solution of the ligand containing sodium acetate (1 g) until the metal-to-ligand ratio reached 1 : 2 (in copper complex the ratio was 1 : 1). The solid separated was filtered out, washed with water and then with methanol and dried over P_4O_{10}.

The halide complexes of Zn(II), Cd(II) and Hg(II) were prepared by adding methanolic solutions of the respective metal halide to refluxing methanolic solution of the ligand. The reaction mixture was maintained at the refluxing temperature for 3 hr.

---

* To whom all correspondence should be addressed.

The chloride and bromide complexes of Cd(II) and Hg(II) separated as yellow solids. The other complexes were obtained by concentrating the resulting solutions and by subsequent cooling of the viscous mass obtained. The complexes were filtered, washed with small quantities of methanol and dried over P_4O_{10}.

2.3 *Physical methods and analysis*

Molar conductances of the complexes in methanol and nitrobenzene (*ca* 10^{-3} M) were determined at $28 \pm 2°C$ using an Elicos conductance bridge. The magnetic susceptibilities were determined by Gouy method at room temperature. The electronic spectra were recorded in methanol on a Schimadzu recording spectrophotometer SP200. IR spectra (KBr disc) were recorded on a Perkin-Elmer 397 spectrophotometer.

The metal, sulphur and halogens in the complexes were determined by standard procedures (Vogel 1978). Carbon, hydrogen and nitrogen were determined by microanalysis.

3. Results and discussion

The analytical data (table 1) show that the complexes have the formulae: $M(\text{VTSC})_2$, where M = Co or Ni; $[\text{Cu(VTSC)Cl}] \cdot H_2O$; Zn(VTSCH)_2X_2, where X = Cl or Br; Zn(VTSCH)_4I_2; Cd(VTSCH)_2X_2, where X = Cl, Br or I and $\text{Hg(VTSCH)}X_2$, where X = Cl, Br or I.

3.1 *Electrical conductance*

The cobalt, nickel and copper complexes are non-electrolytes in methanol as well as in nitrobenzene. The Zn(II), Cd(II) and Hg(II) complexes dissociate in methanol, in the concentration range 10^{-3} M. However, these values are much lower than the value expected for 1:2 electrolyte in methanol (Deacon *et al* 1965). Their non-electrolytic nature is confirmed by the molar conductance values in nitrobenzene.

3.2 *Magnetic properties*

The Co(II) complex gives a magnetic moment of 2·13 BM. This suggests a square planar configuaration (Figgis and Lewis 1964). The magnetic susceptibility values obtained for Ni(VTSC)_2 indicates that it is diamagnetic and has a square planar configuration. The Cu(II) complex shows a low value (1·09 BM) compared to the spin-only value (1·73 BM). This suggests a polynuclear configuration, i.e. $[\text{Cu(VTSC)Cl}]_x \cdot X\ H_2O$ facilitating antiferromagnetic exchange (Figgis and Lewis 1964). As expected, all the Zn(II), Cd(II) and Hg(II) complexes are diamagnetic.

3.3 *Electronic spectra*

The weak broad band at 1050 nm in the absorption spectrum of Co(II) complex is characteristic of square planar geometry (Nishikawa and Yamada 1964). It also presents a charge-transfer band at 440 nm. The green nickel complex Ni(VTSC)_2 has

Table 1. Analytical data of vanillin thiosemicarbazone complexes*

Complex	%Metal	%Carbon	%Hydrogen	%Nitrogen	%Sulphur	%Halogen
$Co(VTSC)_2$	11·68 (11·61)	43·01 (42·61)	4·17 (3·94)	16·59 (16·57)	12·21 (12·64)	—
$Ni(VTSC)_2$	11·56 (11·59)	43·09 (42·63)	4·16 (3·94)	16·77 (16·58)	12·43 (12·64)	—
$[Cu(VTSC)Cl]\cdot H_2O$	18·54 (18·62)	31·70 (31·68)	3·18 (3·52)	12·56 (12·32)	9·40 (9·40)	10·27 (10·39)
$Zn(VTSCH)_2Cl_2$	11·10 (11·14)	36·90 (36·85)	3·80 (3·75)	14·55 (14·33)	10·90 (10·93)	12·00 (12·09)
$Zn(VTSCH)_2Br_2$	9·72 (9·68)	31·85 (32·00)	3·25 (3·26)	12·40 (12·44)	9·38 (9·49)	23·80 (23·65)
$Zn(VTSCH)_4I_2$	5·41 (5·36)	35·40 (35·44)	3·64 (3·61)	13·90 (13·78)	10·22 (10·51)	20·40 (20·80)
$Cd(VTSCH)_2Cl_2$	17·70 (17·74)	34·52 (34·12)	3·50 (3·47)	13·38 (13·27)	10·10 (10·12)	11·30 (11·19)
$Cd(VTSCH)_2Br_2$	15·52 (15·56)	29·83 (29·93)	3·08 (3·04)	11·60 (11·64)	8·49 (8·88)	22·02 (22·12)
$Cd(VTSCH)_2I_2$	13·22 (13·77)	26·50 (26·48)	2·65 (2·69)	10·25 (10·30)	7·80 (7·85)	31·00 (31·09)
$Hg(VTSCH)Cl_2$	40·00 (40·39)	21·72 (21·76)	2·14 (2·21)	8·40 (8·46)	6·18 (6·45)	14·16 (14·27)
$Hg(VTSCH)Br_2$	34·12 (34·25)	18·40 (18·46)	1·80 (1·88)	7·09 (7·18)	5·20 (5·47)	27·32 (27·29)
$Hg(VTSCH)I_2$	29·22 (29·52)	15·91 (15·90)	1·65 (1·62)	6·20 (6·18)	4·75 (4·72)	37·30 (37·35)

* Calculated values in parenthesis

(Jorgensen 1962). This is in accordance with the magnetic data. The Cu(II) complex exhibits a broad absorption band at 460 nm which may be attributed to $L \rightarrow M$ charge-transfer transition. Another broad band observed with an absorption maximum at 690 nm is assigned to $d \rightarrow d$ transition. This suggests a square planar geometry for the complex (Campbell 1975; Ajayi and Goddard 1971).

3.4 *IR spectra*

The IR spectra of the ligand and the complexes were examined in detail. The characteristic IR bands are given in table 2. The strong bands in the spectra between 3520 and 3270 cm^{-1} may be assigned to ν_{NH_2} and ν_{NH} (Haines and Sun 1968; Campbell and Grzeskowiak 1967; Burns 1968). The strong band at 3150 cm^{-1} in the spectrum of the ligand may be due to ν_{OH}. The low frequency shift of this band compared to normal OH vibration band (at 3480 cm^{-1}) (Nakamoto 1963) may be due to hydrogen bonding. The corresponding δOH band appears at 1610 cm^{-1} in the ligand spectrum. The fact that these two bands are retained almost at the same positions excludes any possible participation of the oxygen atom of the phenolic group in coordination. The shifting of the band at 1600 cm^{-1} ($\nu_{C=N^3}$) to lower wave number in the complexes indicates the participation of N^3 in coordination (Podder and Saha Nityananda 1975). However, in $Zn(VTSCH)_4I_2$ this band does not show any appreciable shift and hence there may not be nitrogen coordination. The absence of bands in the region 2650–2500 cm^{-1} in the free ligand indicates the absence of S-H grouping in the free ligand (Bellamy 1978).

After eliminating numerous well-defined bands in the region 940 to 700 cm^{-1} in the spectrum of the ligand, a band of strong intensity at 775 cm^{-1} can be assigned to pure $\nu_{C=S}$ (Bellamy 1978). In a set of complexes, $Co(VTSC)_2$, $Ni(VTSC)_2$ and $[Cu(VTSC)Cl]\cdot H_2O$ this band disappears and a new band appears around 660 cm^{-1} (in ν_{C-S} region). These facts are compatible with the enolisation of the $-NH-\underset{|}{C}=S$ group, in the ligand, to $-N=\underset{|}{C}-SH$ in the presence of the metal ion and the coordination of the metal ion through the S atom after the elimination of H. In another set of complexes (complexes of Zn(II), Cd(II) and Hg(II) halides) the $\nu_{C=S}$ band shifted to lower

Table 2. Characteristic IR bands (cm^{-1}) of vanillin thiosemicarbazone and its complexes

	δ OH	ν OH	ν C=N^3	ν C=S	ν C–S	ν M–N
VTSCH	3150 s	1610 s	1600 vs	775 s	—	—
$Co(VTSC)_2$	3150 s	1620 s	1580 s	—	660 m	550 m
$Ni(VTSC)_2$	3150 m	1610 m	1585 s	—	660 m	550 m
$[Cu(VTSC)Cl]\cdot H_2O$	3150 s	1620 s	1590 vs	—	650 m	540 m
$Zn(VTSCH)_2Cl_2$	3170 s	1615 s	1590 vs	742 m	—	545 m
$Zn(VTSCH)_2BR_2$	3180 s	1620 s	1590 vs	745 m	—	535 m
$Zn(VTSCH)_4I_2$	3180 s	1620 s	1600 vs	745 s	—	—
$Cd(VTSCH)_2Cl_2$	3160 s	1620 s	1590 s	745 m	—	540 m
$Cd(VTSCH)_2Br_2$	3180 s	1620 s	1590 vs	745 m	—	540 m
$Cd(VTSCH)_2I_2$	3200 s	1615 m	1580 vs	745 m	—	540 m
$Hg(VTSCH)Cl_2$	3160 s	1625 s	1590 vs	745 m	—	540 m

frequency region (~745 cm^{-1}). However, there are situations where the $\nu_{C=S}$ band of the ligand is shifted only by ~ 40 cm^{-1} in the complexes (Sujuki 1962). Hence, in the present case, the shift of $\nu_{C=S}$ band in the complexes, eventhough small, indicates coordination through sulphur of –NH–C(=S)– group in the ligand (without enolisation). The bands appearing around 550 cm^{-1} in the spectra of the complexes may be assigned to M–N stretching frequencies.

Acknowledgement

The authors thank Drs C P Prabhakaran and P Indrasenan for helpful discussions.

References

Ajayi S O and Goddard D R 1971 *J. Chem. Soc.* (*A*) p. 2673

Bellamy L J 1978 *The infrared spectra of complex molecules* (London; Chapman and Hall)

Burns G R 1968 *Inorg. Chem.* 7 277

Campbell M J M 1975 *Coord. Chem. Rev.* **15** 311

Campbell M J M and Grzeskowiak R 1967 *J. Chem. Soc.* (*A*) p. 396

Deacon G B, Green J M S and Nyholm R S 1965 *J. Chem. Soc.* p. 3411

Figgis B N and Lewis J 1964 *Progress in inorganic chemistry* (ed) F A Cotton (New York; Interscience) Vol. **6**

Haines R A and Sun K K W 1968 *Can. J. Chem.* **46** 3241

Jorgensen C K 1962 *J. Inorg. Nucl. Chem.* **24** 1571

Nakamoto K 1963 *Infrared spectra of inorganic and coordination compounds* (New York; John Wiley)

Nishikawa H and Yamada S 1964 *Bull. Chem. Soc. Jpn.* **37** 8

Paulo da Silva Lacaz, Maria Lucia Bittencourt Salac, Laerte Manchaes de Andrade and Ivone Rocco Suassuna 1958 *Rev. Brasil trberc* **26** 783

Poddar S N and Saha Nityananda 1975 *J. Indian Chem. Soc.* **52** 57

Sujuki I 1962 *Bull. Chem. Soc. Jpn.* **35** 1286

Vogel A I 1978 *A text book of quantitative inorganic analysis* (London; The English Language Book Society and Longman)

efficient method of preparation of pheophytin *a*—Divalent metal ophytinates

P R DROUPADI and V KRISHNAN*

Department of Inorganic and Physical Chemistry, Indian Institute of Science, Bangalore 560012, India

MS received 9 July 1983; revised 5 October 1983

Abstract. An efficient and rapid method of preparation of pheophytin *a* from leaves using silica gel as column material is described. The different divalent metallo, Co, Ni, Cu and Zn derivatives of pheophytin have been prepared and characterised. The optical absorption and emission, and ^{1}H NMR spectral data of pheophytin *a* and its metal derivatives are presented.

Keywords. Pheophytin *a*; metal pheophytinates; ^{1}H NMR spectra.

Introduction

rophyll *a* (Chl *a*) and its metal-free derivative pheophytin *a* (Phe *a*) have been gnized as the electron donor-acceptor system in the primary photosynthetic ess. In the development of artificial photosynthetic devices employing different l derivatives of the cell-free pigments to investigate their electron donor-acceptor ties and their relative stabilities, it became necessary to isolate spectrally pure Phe *a*. riety of procedures are available in literature for the extraction, isolation and fication of the plant pigments from chloroplast (Omata and Murata 1980; Svec ; Hynninen 1977; Hynninen and Assandri 1973; Strain and Sherma 1972; Strain Svec 1966, 1969). A necessity for several methods arose since a large number of ients are intimately associated with chlorophyll (Chl) in the chloroplast. Moreover, is been observed that during the extraction and separation procedures using rent solvents, column materials and employing a variety of experimental con- ns lead to alteration products of the *in vivo* pigment molecules which are either erized, demetallated or oxidized. A few such identified products are demetallated (Phe) (besides the Phe which is intrinsically present) chlorophyllide, pyrochloro- l, isomer of Chl (Chl′) (figure 1), oxidized components of auxillary pigments tenoids and xanthophylls.

is customary to employ mild adsorbents such as sugar, cellulose, sepharose and h to reduce the number of alteration products during chromatographic pro- res. Usage of strong adsorbents like silica gel, alumina, kieselguhr are known to e alteration of the *in vivo* pigments (Sherma 1971; Strain and Svec 1969; Bacon and len 1967; Strain *et al* 1967). The difficulties encountered in the prescribed edures are that they are often laborious and time consuming calling for repeated matographic runs resulting in the larger extent of formation of altered products.

---

whom all correspondence should be addressed.

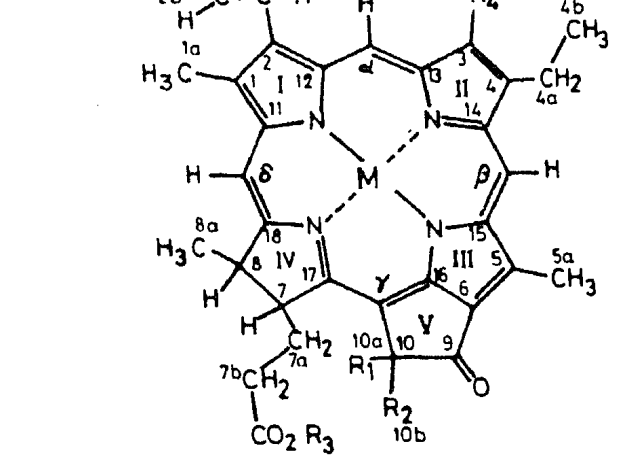

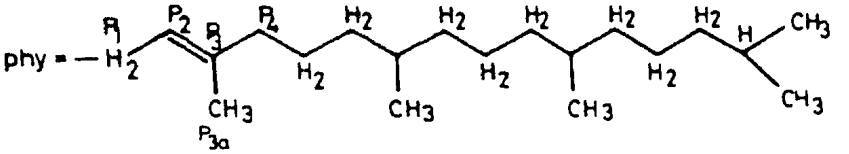

1. R_1= H , R_2= $COOCH_3$, R_3= Phy , R_4= CH_3 (a) M = Mg : Chlorophyll a
   (b) M = H_2 : Pheophytin a
2. R_1 = $COOCH_3$, R_2 = H , R_3= Phy, R_4=CH_3 (a) M = Mg : Chlorophyll a'
   (b) M = H_2 : Pheophytin a'
3. R_1 = H , R_2= $COOCH_3$, R_3 = H , R_4=CH_3 (a) M = Mg : Chlorophyllide a
   (b) M = H_2 : Pheophorbide a
4. R_1 = H , R_2 = H , R_3 = Phy , R_4 = CH_3 (a) M = Mg : Pyrochlorophyll a
   (b) M = H_2 : Pyropheophytin a
5. R_1 = H , R_2 = $COOCH_3$, R_3= Phy, R_4=CHO (a) M = Mg : Chlorophyll b
   (b) M = H_2 : Pheophytin b

Figure 1. Structure of chlorophyll *a* and its major altered products.

Thin layer chromatography on cellulose plate is recommended; however it is a microtechnique. Separation on a column of sepharose is a good method but is costly for the preparation of pigments in large quantities. Despite a great deal of experimentation in the direction of extraction, separation and purification of Chl, no one method combines simplicity, wide applicability and high sensitivity. Further, many efforts that have been made are towards the isolation of pure chlorophylls. Our interest lies in the preparation of metalloderivatives which requires the isolation of Phe *a* in fairly large quantities (> 250 mg).

Here we report an efficient method for the separation of Phe *a* directly from the plant material using silica gel as the column material. This method avoids the preparation of Chl *a* and its subsequent acidification to yield Phe *a* which is time consuming and leads to possible photobleaching. The metallo derivatives prepared from the purified Phe *a*

Experimental

Materials

ves of *Amaranthus caudatus*, a plant that is richly grown around all seasons was loyed for the extraction of plant pigments. Silica gel-G was procured from Achme thetic Chemicals (Bombay). GR grade methylene chloride (BDH, India), commercial one and benzene were purified according to standard procedures (Vogel 1968). The ates of Co(II), Cu(II) and Zn(II) were employed to prepare their respective ophytinates. 2,4-pentananedionato nickel(II) was prepared according to known cedures (Fackler 1966) and it was used to prepare Ni(II) pheophytinate. All other gents were of GR grade.

Methods

sh green leaves devoid of mid ribs (500 g), were cut into small pieces and treated with f boiling water for 2 min to remove the water soluble pigments and oily material. s treatment also helps to coagulate the proteins present in the leaves. The leaves were dried using a towel. The dried leaves (300 g) were then suspended in 4 l of acetone stirred with a mechanical stirrer at full speed for 5 min to hasten the extraction of pigments into the solvent. The suspension was allowed to settle for 5 min. The dark n supernatant liquid was filtered through a plug of cotton to remove the suspended y materials. A second extraction was carried out with 1 l of acetone to completely ove the greenness of the leaves. The solvent was removed from the extract batch- (employing not more than 500 ml of extract) by distillation under reduced pressure 0–50°C. After the removal of acetone, the pigments were transferred to 20 ml iethyl ether. A total of 200 ml of ether extract was collected in this fashion. Sodium ride solution (100 ml of 20% aqueous) was employed to enhance the transfer of nents to ether layer. The ether extract was shaken well with 20 ml of 1 N rochloric acid in a separating funnel for 1 min and the blue acid layer was removed nediately. The brown ether layer was washed repeatedly with 200 ml water each time emove the traces of acid. Emulsion formation at this stage was overcome with the ition of 200 ml of 20% aqueous sodium chloride solution. The ether extract taining crude Phe was dried over anhydrous sodium sulphate. Ether was porated under reduced pressure. Traces of water remaining in the brown coloured erial sticking to the glass were removed by repeated codistillation with dry ontetrachloride under reduced pressure. The crude Phe (2 g) thus obtained was l for chromatographic separation.

he Phe (2 g) was dissolved in minimum amount of benzene (10–15 ml) and loaded o a column of silica gel packed in benzene (height of the column = 42 cm, diameter ·5 cm, height of silica gel packed = 30 cm). Initially the flow rate of benzene was ntained at 1 ml/min till the brown extract was completely adsorbed on the silica bed the eluent on the top of the column bed was colourless. Increasing the flow rate to l/min results in the fast separation of yellow carotenoids while the brown coloured d of Phe moves slowly. Polarity of the eluent was gradually increased by adding erent amounts of acetone/alcohols (the proportion of the solvents is shown in

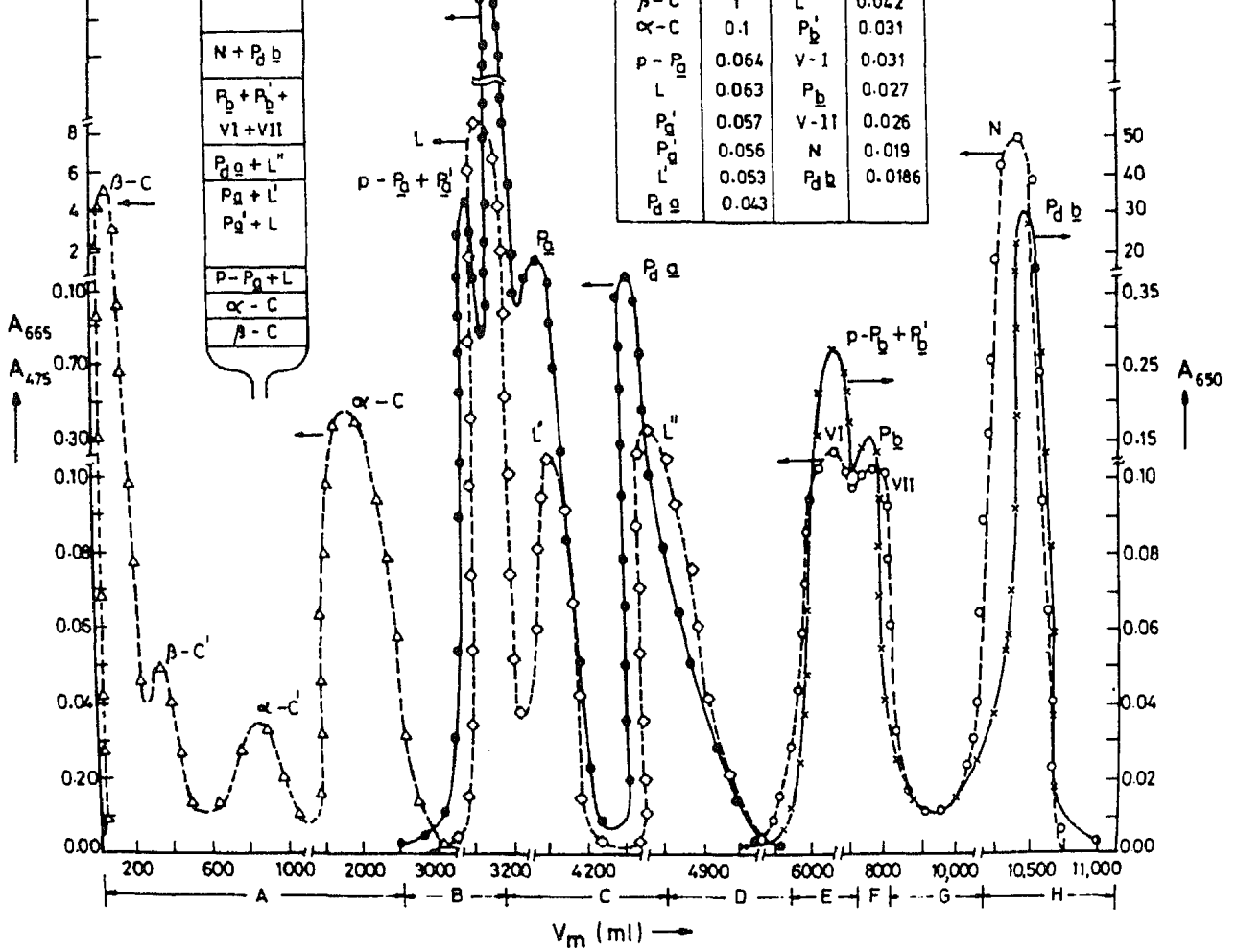

β-C	1	L	0.042
α-C	0.1	Pb'	0.031
p - Pa	0.064	V-I	0.031
L	0.063	Pb	0.027
Pa'	0.057	V-II	0.026
Pa	0.056	N	0.019
L'	0.053	Pd b	0.0186
Pd a	0.043		

Figure 2. Separation of acidified leaf extract on a silica gel column. V_m = eluent volume. The different solvents used are marked as A = benzene; B = 1% acetone in benzene; C = 2% acetone in benzene; D = 2% *n*-propanol in benzene; E = 4% *n*-propanol in benzene; F = 10% *n*-propanol in benzene; G = 25% ethanol in benzene and H = methanol. R_c value is defined in the text. The upper left hand part of the figure shows the separation of various pigments and the R_c values are given in the upper right hand part. β-C = β-carotene; α-C = α-carotene; p-p*a* = pyropheophytin *a*; P*a'* = pheophytin *a'*; P*a* = Pheophytin *a*; L = Lutein; Pd*a* = pheophorbide *a*; p-P*b* = pyropheophytin *b*; P*b'* = pheophytin *b'*; P*b* = pheophytin *b*; VI = violoxanthin fraction I; VII = violoxanthin fraction II; Pd*b* = pheophorbide *b*; N = neoxanthin. β-C' and α-C' are altered products.

conveniently be stored after the removal of the solvent under N_2 in a sealed tube. The material should be protected from light and kept in a refrigerator.

2.3 *Preparation of divalent metallo (Co, Ni, Zn and Cu) pheophytinates*

A solution of 50 mg of Phe *a* in 100 ml of chloroform was refluxed with excess of metal acetate/acetylacetonate (200 mg) dissolved in acetic acid for about 30 min under N_2. The bluish-green solution was cooled and washed repeatedly with water and then dried over anhydrous sodium sulphate. The solution was concentrated to 5 ml and loaded on to a silica gel column packed in benzene and eluted with benzene containing 0–6% of acetone. The brown material was left behind in the column and the metallopheophytin coloured blue was collected. This solution was again chromatographed to obtain pure

ation of extraction and separation of the pigments was carried out under dim light in an atmosphere of N_2.

ne optical absorption spectra of Phe *a* and its divalent metal derivatives were rded using CH_2Cl_2 as solvent on a Beckman model 25 spectrometer. Fluorescence tra of the solutions were recorded on a Perkin-Elmer MPF-44A spectrofluorimeter. concentration of solutions employed for optical absorption and emission surements was 10^{-5} M and 10^{-6} M respectively. The ^{1}H NMR spectra of Phe *a* and valent metal derivatives in $CDCl_3$ (0·05 M) were recorded on a Brucker WH 270 z FT NMR spectrometer using TMS as an internal standard.

Results

different pigments in the eluent were identified by making use of their characteristic rption spectra and their R_F values. The maxima at 475 nm were used to represent carotenes, xanthophylls and lutein (Nelson and Livingston 1967). The isomeric s of these pigments, however, have not been collected individually in the eluent. presence of Phe *a* and Phe *b* in the eluent was monitored at the absorption maxima and 650 nm respectively. Owing to the closeness of these absorptions, the spectra he eluents containing these components often appear as a band with an mpanying shoulder. It was found necessary to dilute the eluent to an appropriate me for the absorbance measurements. The absorbance values corrected for the

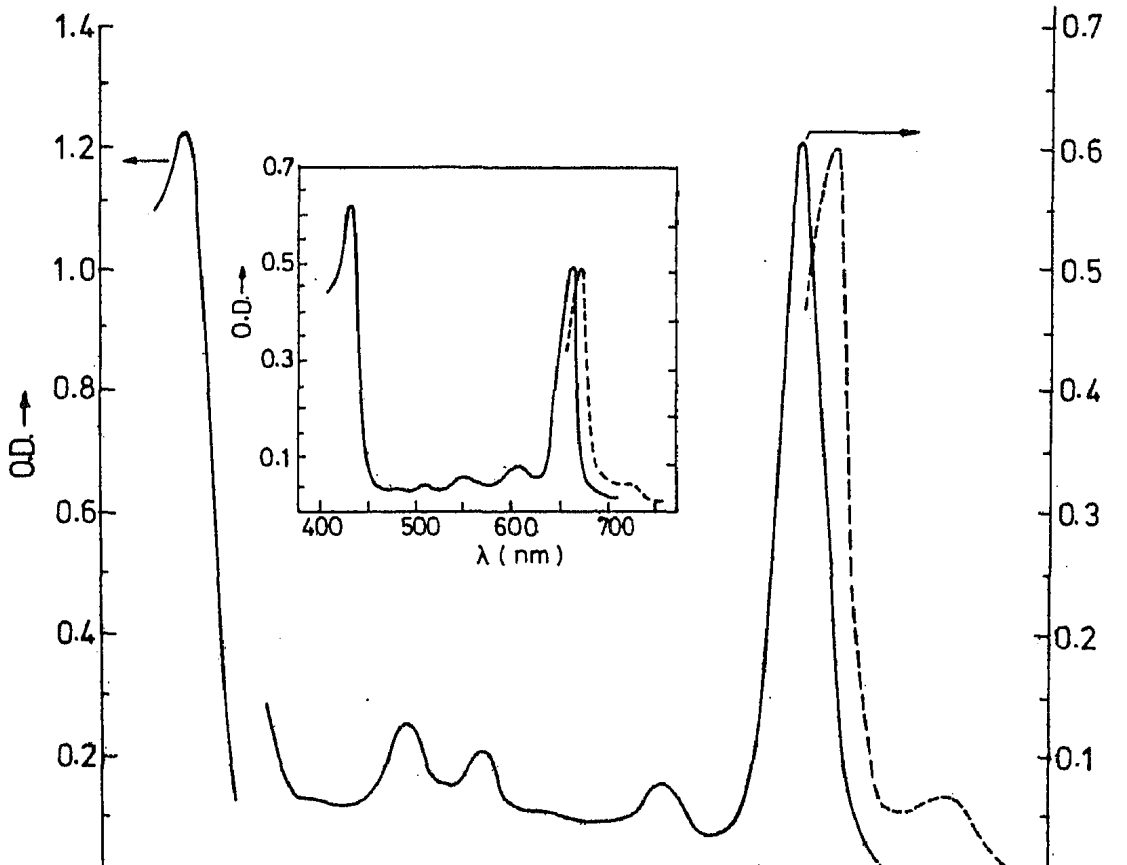

Compound	λ_{max} nm (red)	λ_{max} nm (blue)	$\frac{I_{max}\text{ (blue)}}{I_{max}\text{ (red)}}$	I_{max} (red)
Phe *a*	665	412	2·05	56,666
	(667)	(409)	(2·09)	(61,000)
Zn Phe *a*	654	421·5	1·32	45,424
	(658)	(426)	1·30	
Cu Phe *a*	650·5	421·5	1·29	40,196
	(654)	(425)	(1·18)	
Ni Phe *a*	649	421·5	1·34	33,856
	(652)	(423)	0·95	
Co Phe *a*	650·5	422	1·36	37,903

[a] The values in parenthesis are those reported in literature: Pennington *et al* (1964); Boucher and Katz (1967).

dilution are shown in figure 2. The relative order of elution of the pigments with increasing polarity of the eluent, is the same as that observed in the sugar column (Pennington *et al* 1964). The R_c values of different pigments were calculated as the ratio of the eluent volumes with respect to the first eluted component β-carotene. The results of the absorption spectral measurements at different volumes of the eluent and the R_c values of the various components are depicted in figure 2. The volume of the eluent just before the elution of the first component β-carotene corresponds to zero in figure 2. The appearance of shoulders in the elution curve (figure 2) signifies the trailing of major zones with increasing polarity of the solvent. Also, minor zones like pyropheophorbides *a*/*b* and pyropheophytin *b* are not seen clearly due to overloading of the column as well as due to the sudden increase in polarity of the eluent before their elution. Owing to the closeness of the R_c values and similar absorption spectral features, the isomers *a* and *a'* of Phe were collected in the same eluent volume.

The visible absorption spectrum of Phe *a* prepared in this fashion is given in figure 3 along with its emission spectrum. The inset in figure 3 shows the absorption and emission spectrum of Zn(II) Phe *a*. The absorption spectral data of Phe *a* and its divalent metal derivatives are given in table 1. The ratio of intensities of the blue to red band has often been used to check the purity of the products. The present values agree with those reported in literature (Boucher and Katz 1967; Pennington *et al* 1964). Excitation of Phe *a* and Zn Phe *a* at their red absorption maxima leads to emissions at 676 nm followed by a shoulder at 726 nm and 665 nm with a shoulder at 713 nm respectively. The ^{1}H NMR spectrum of Phe *a* in $CDCl_3$ is shown in figure 4. The appearance of well-resolved spectrum indicates the purity of the sample and the assignments of the proton resonances are analogous to the reported values (Katz 1973). Presence of *a'* in the sample is clearly seen from the satellite peaks near the meso proton resonances. It has not been possible to estimate the relative amount of *a'* component in the purified sample. The vinyl proton resonances appear as an ABX multiplet with 2*a* proton resonating at 7·98 δ while 2*b* and 2*b'* proton resonances occur at 6·23 δ and 6·27 δ respectively ($J_{AB} \approx 2H_z$, $J_{AX} \approx 18\ H_z$, $J_{BX} \approx 12\ H_z$). The 5*a*, 3*a* and 1*a* proton resonances are clearly seen at 3·69, 3·23 and 3·34 δ respectively. The 10*a* and 10*b* proton resonances are observed at 6·26 δ and 3·88 δ respectively. Exhibition of these resonances

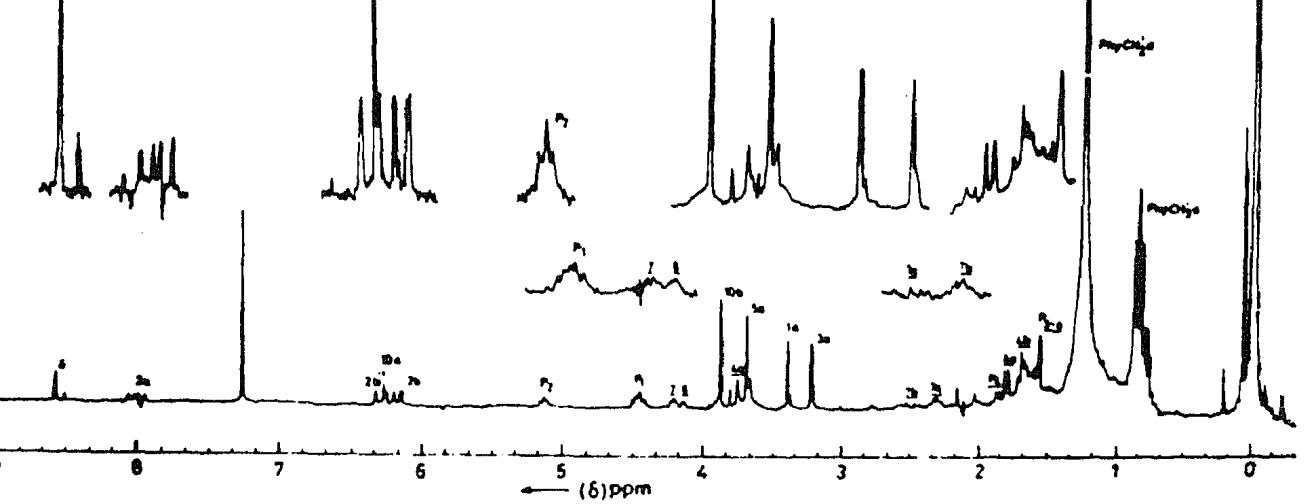

Figure 4. 270 MHz ^{1}H NMR spectrum of pheophytin *a*. The numbering is the same as in figure 1. Numbers underlined indicate tentative assignments. The expanded spectrum is designated above the corresponding proton resonances.

lear indication that the Phe *a* sample prepared by the method described is not an zed product.

oreover the appearance phythyl resonances, P_1, P_2, P_3, P_4, P-CH_2 and P-CH_3 ring at 4·45, 5·14, 1·57, 1·86, 1·25 δ and 0·89 to 0·77 δ respectively provides ional check on the purity of the Phe *a*.

Discussion

known that carotenoids and xanthophylls undergo isomerization and oxidation silica gel is used as the adsorbent (Strain *et al* 1967). Thus the elution curve e 2) represents the altered products of the pigments besides the major pigments. It rthy to note that the usage of pure benzene as the eluent separates the major on of carotenes. The order of sorbability of the different pigments in silica gel x is found to be β-carotene < α-carotene < pyropheophytin *a* ⩽ pheophytin *a'* tein ⩽ pheophytin *a* ⩽ lutein' < pheophorbide *a* ⩽ lutein'' < pheophytin *b'* + *b* oloxanxthin I & II < neoxanthin < pheophorbide *b*. L' is regarded to be an altered uct of lutein. It is not known with certainty whether L'' is the altered product of or the altered product of violoxanthin. The strongly adsorbed pigments anthin, pheophorbide *b* and other oxidized products of Phe are eluted using pure anol. Owing to the closeness of the band separation of these pigments, the eluent nes containing a given major pigment are always contaminated with the ding component. However, repeated chromatography of the eluent fraction tially yields the desired pigment.

e misgivings of the usage of silica gel as a column material for the separation of ophyll *a* from the plant pigments have been cited in literature (Bacon 1966; Bacon Holden 1967). These essentially point out to the formation of a variety of alteration ucts of Chl with Phe as one of the components. The identification of the altered ucts has been based on phase test and the absorption spectra. Despite the

ambiguities involved in the phase tests and similar absorption spectral features, components *viz* 'unknown' or Chl *a*, 'unknown', Chl *a*-1, Chl *a*-2 and Chl *a*-3 have been proposed after a thin layer chromatographic separation of Chl *a* on silica gel. The R_F values and the ratio of the intensities of blue to red bands in the absorption spectra of the different components observed by Bacon seem to suggest that the proposed components can possibly be pyro Chl *a*, Phe *a*, Chl *a*, Chl *a'* and chlorophyllide *a* (and/or pyrochlorophyllide *a*) respectively. The present method of separation starts with the acidified plant extract with the explicit intention of obtaining Phe *a* for the preparation of metalloderivatives. Thus, the caution expressed in literature against the usage of silica gel as an adsorbent is of little significance in the efforts described here. No attempts were made to separate the *a* and *a'* isomers of Phe. The relative amounts of *a'* in a sample of *a* seem to depend on the nature of solvent and temperature. The cooccurrence of *a'* component does not seem to alter the absorption and emission spectral features of Phe *a*. However, it is shown that the CD spectra can be used with advantage to distinguish the presence of *a'*.

The optical absorption and emission spectra of Phe *a* and its Zn(II) derivative (figure 3) assure the purity of Phe *a* obtained in the present study. Moreover, the appearance of resonances of 10a and 10b protons show the absence of oxidized products (*a*-1, *a*-2 and *a*-3). Interestingly the 13-carbon resonance spectra of the Phe *a* and its divalent metal derivatives show a large down field shifts of meso carbons and carbonyl carbon in the Co(II) complex relative to the spin-free Zn(II) complex. Further work is in progress to relate these carbon shifts with their ability to function as π-donors.

Acknowledgements

One of the authors (PRD) is thankful to the Department of Science and Technology, New Delhi for the award of a fellowship.

References

Bacon M F 1966 *Biochem. J.* **101** 340
Bacon M F and Holden M 1967 *Phytochem.* **6** 193
Boucher L J and Katz J J 1967 *J. Am. Chem. Soc.* **39** 1703
Fackler Jr J P 1966 in *Progress in inorganic chemistry* (ed.) F A Cotton (New York: Interscience, John Wiley) Vol. 7, p. 361
Hynninen P H 1977 *Acta Chem. Scand.* **B31** 829
Hynninen P H 1981 *Z. Naturforsch.* **36b** 1000
Hynninen P H and Assandri S 1973 *Acta Chem. Scand.* **27** 1478
Katz J J 1973 in *Inorganic biochemistry* (ed.) Eichhorn (Amsterdam: Elsevier) p. 1022
Nelson J W and Livingston A L 1967 *J. Chromatogr.* **28** 465
Omata T and Murata N 1980 *Photochem. Photobiol.* **31** 183
Pennington F C, Strain H H, Svec W A and Katz J J 1964 *J. Am. Chem. Soc.* **86** 1418
Sherma J 1971 *J. Chromatogr.* **61** 202
Strain H H and Sherma J 1972 *J. Chromatogr.* **70** 87
Strain H H and Svec W A 1966 in *The chlorophylls* (ed.) L P Vernon and G R Seely (New York, London: Academic Press) p. 21
Strain H H and Svec W A 1969 *Adv. Chromatogr.* p. 119

nsition metal derivatives of 3-4-diphenyl-5-mercapto-1,2,4-zole

J SINGH* and N K SINGH

Department of Chemistry, U P College, Varanasi 221 005, India
* Department of Chemistry, Banaras Hindu University, Varanasi 221 005, India

MS received 29 October 1982; revised 7 April 1983

Abstract. Neutral chelates of 3,4-diphenyl-5-mercapto-1,2,4-triazole (DPMTH) with Fe(II), Co(II), Ni(II), Cu(II), Zn(II), Cd(II) and Hg(II) have been prepared and characterized by analytical and physicochemical techniques such as magnetic susceptibility measurements, TGA, electronic ESR and IR spectral studies. The IR data suggest that DPMTH behaves as a uninegative bidentate ligand in all the complexes except Fe(II) and Ni(II) where it is tridentate. The complexes have been found to display significant antifugal activity against *A. alternata* and *A. flavus*.

Keywords. Metal complexes; analytical techniques; physicochemical techniques; neutral chelates; mercapto triazole.

Introduction

liphenyl-5-mercapto 1,2,4-triazole (DPMTH) containing a mercapto group can form ıte with transition metal ions in the *thiol* form utilizing the ring nitrogen (N^1) as ın below.

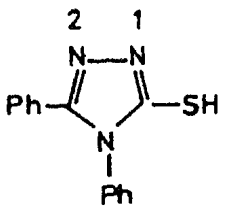

Thiol form

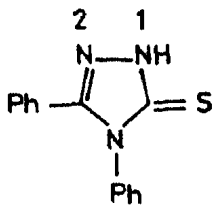

Thione form

o work has so far been done on the metal complexes of the title ligand. It was efore thought worthwhile to prepare and characterise its metal complexes and y their fungicidal activity.

Experimental

ligand DPMTH was prepared by the method described earlier (Ram and Pandey 3) and was crystallized from ethanol (m.p. 295–297°C).

Preparation and characterization of metal complexes

Table 1. Analytical data and magnetic moment of the metal complexes

Complex	Colour	Observed (%)			Calculated (%)			
		M	*N*	*S*	*M*	*N*	*S*	μ_{eff}
$Cu(DPMT)_2$	Dark green	11·24	14·24	11·38	11·18	14·80	11·27	1·8(
$Ni(DPMT)_2$	Light yellow	10·82	14·64	11·42	10·43	14·92	11·37	2·9{
$Co(DPMT)_2$	Blue	10·28	14·52	11·38	10·46	14·92	11·36	4·4:
$Fe(DPMT)_2$	Brown	9·54	14·98	11·28	9·96	15·00	11·43	4·9:
$Zn(DPMT)_2$	White	11·48	14·62	10·98	11·12	14·75	11·24	Diam
$Cd(DPMT)_2$	White	17·98	13·58	10·62	18·23	13·62	10·38	Diam
$Hg(DPMT)_2$	White	28·82	12·06	9·26	28·47	11·92	9·08	Diam

a 1:2 molar ratio in ethanol and then adding an aqueous solution of sodium aceta except in the Cu(II) complex. The complexes thus precipitated were digested f ~30 min, filtered, washed with hot ethanol and dried *in vacuo*.

The analyses of the metal and sulphur contents were carried out by standa methods (Vogel 1978; Treadwell and Hall 1958). Nitrogen was analysed by micr analysis. The analytical data are given in table 1.

3. Physical measurements

The magnetic susceptibilities of the complexes were determined by the Faraday meth using $Hg[Co(NCS)_4]$ as calibrant and experimental magnetic susceptibilities we corrected (Figgis and Lewis 1960) for diamagnetism. Magnetic moments of t complexes are included in table 1.

The electronic spectra of the complexes were recorded on a Cary-14 spectrophot meter in Nujol. The various absorption bands and their assignments are given in table The ESR spectra were recorded at room temperature as well as at liquid nitrog temperature in DMF on a Varian X-band spectrometer model E-4 and the spectr parameters calculated using DPPH as the internal standard.

The IR spectra of the ligand and the complexes were recorded with a Perkin Elm 621 grating infrared spectrophotometer in Nujol mull in the range 4000–200 cm^{-1}. Th important IR bands and their assignments are given in table 3.

The antifungal activity was evaluated by agar-plate technique (Horsfall 1945) Czapek's medium using acetone solutions of the compounds. The percentage inhibitic is given in table 4.

4. Results and discussion

The complexes are insoluble in non-polar and polar organic solvents such a chloroform, carbon tetrachloride, ethanol, methanol etc., but soluble in high coordinating organic solvents such as DMF and DMSO.

4.1 *Magnetic moments*

Table 2. Electronic spectral bands, their assignments and ligand field parameters.

Compounds	Bands (cm^{-1})	Assignments	10 Dq (cm^{-1})	B' (cm^{-1})	β	$\beta°$(%)	LESE (kJ/mole)
$Fe(DPMT)_2$	10000, 16600	$^5T_{2g} \rightarrow {}^5Eg(D)$, $t_{2g} \rightarrow \pi^*$	10000	—	—	—	47·71
$Co(DPMT)_2$	7020, 8160	$^4A_2 \rightarrow {}^4T_1(F)$	4500	715	0·736	26·4	64·58
	15500, 18000	$^4A_2 \rightarrow {}^4T_1(P)$					
$Ni(DPMT)_2$	10000, 13700, 16240	$^3A_{2g}(F) \rightarrow {}^3T_{2g}(F)$, ^1Eg, $^3T_{1g}(F)$	10000	877	0·830	17·0	143·10
$Cu(DPMT)_2$	16600	$^2B_{1g} \rightarrow {}^2A_{1g}$, $^2B_{2g}$, ^2Eg	16600	—	—	—	118·8

Table 3. Infrared spectral bands and their assignments·

Compound	ν(NH)	ν(SH)	Thioamide I	Thioamide II	Thioamide III	ν(N–N)	ν(M–S)	ν(M–N)
DPMTH	3110	2750w	1475	1240	1020	995	—	—
$Fe(DPMT)_2$	—	—	1450	1260	1035	1060	310	340
$Co(DPMT)_2$	—	—	1445	1260	1030	1020	315	325
$Ni(DPMT)_2$	—	—	1445	1270	1040	1065	310	330
$Cu(DPMT)_2$	—	—	1440	1260	1025	1020	310	345
$Zn(DPMT)_2$	—	—	1445	1265	1025	1020	320	340
$Cd(DPMT)_2$	—	—	1440	1265	1025	1020	315	340
$Hg(DPMT)_2$	—	—	1440	1270	1035	1015	320	345

Table 4. Antifungal activity.

Compound Conc· (ppm)	Average percentage inhibition after three days: Organism *A. altarnate* 1:100	1:1000	1:10,000	Organism *A. flavus* 1:100	1:1000	1:10,000
$Cu(DPMT)_2$	60	40	20	57	29	07
$Ni(DPMT)_2$	65	44	27	46	28	11
$Zn(DPMT)_2$	67	36	26	60	33	07
$Cd(DPMT)_2$	63	40	33	63	33	17
$Hg(DPMT)_2$	73	57	43	66	46	23

Lewis 1964). The μ_{eff} value of copper(II) complex lies in the range reported for square planar Cu(II) complexes (Sacconi and Ciampolini 1964).

4.2 *Electronic and ESR spectra*

The spectrum of $Fe(DPMT)_2$ shows a broad *d–d* band at 10000 cm^{-1} and a more intense charge-transfer band at 16600 cm^{-1} which may be assigned to $^5T_{2g} \rightarrow {}^5Eg(D)$ and $t_{2g} \rightarrow \pi^*$ transitions respectively (Lever 1968).

The spectrum of $Co(DPMT)_2$ shows four bands at 7020, 8160, 15500 and 18000 cm^{-1}. The first two bands may be due to splitting of $\nu_2[^4A_2 \rightarrow {}^4T_1(F)]$ while the last two due to the components of $\nu_3[^4A_2 \rightarrow {}^4T_1(P)]$. The energies of ν_2 and ν_3 bands have been selected to be 7550 and 16670 cm^{-1} respectively by taking the centre of gravity of the total intensity by visual method (Cotton *et al* 1961) and from these values the various ligand-field parameters calculated by the method of Drago (1965) are given in table 2.

Of the three bands occurring in the spectrum of $Ni(DPMT)_2$ at 10000, 13700 and 16240 cm^{-1}, the first and third may be assigned to $^3A_{2g}(F) \rightarrow {}^3T_{2g}(F)\,(\nu_1)$ and $^3A_{2g}(F) \rightarrow {}^3T_{1g}(F)\,(\nu_2)$ transitions respectively while the second may be attributed to

ectively. Further, the ratio $\nu_2/\nu_1 = 1{\cdot}624$ and the values of β_{35} (0·830) and B_{33} 36) being very close to each other suggest an octahedral geometry for Ni(MPMT)$_2$ coni 1969; Lever 1968).

he spectrum of Cu(DPMT)$_2$ shows a broad band at 16600 cm^{-1} assigned to the lope of $^2B_{1g} \rightarrow {}^2A_{1g}$, $^2B_{2g}$, ^2E_g transitions in the square planar environment of II) (Proctor *et al* 1968).

hus the findings from the electronic spectral studies of the complexes regarding r stereochemistry are consistent with the magnetic susceptibility measurements ussed earlier.

the ESR spectrum of Cu(DPMT)$_2$ in DMF, the parallel and perpendicular features of u are clearly resolved and are characteristic of axial symmetry. The ESR magnetic ameters for the complex as calculated from the analysis of the spectra at 77°K and m temperature are: $g_{\|} = 2{\cdot}3132$, $g_{\perp} = 2{\cdot}0530$, $A_{\|} = 160G$, $g_{iso} = 2{\cdot}135$, which cate the trend $g_{\|} > g_{\perp}$ free-spin (2·0023) showing that the unpaired electron is in $_{y^2}$ orbital of Cu(II) ion (Goodman and Rayney 1970). The $g_{\|}$ and $g_{\perp}$ values depart siderably from the free-spin values indicating a strong axial distortion of the ecule (Lewis *et al* 1966; Van Landschoot *et al* 1976) probably due to the rdination of DMF in the axial positions.

IR spectra

IR spectrum of DPMTH shows bands at 3110 and 2750 cm^{-1} assigned to ν(NH) and H) groups respectively (Singh *et al* 1980; Gadag and Gajendragad 1980). These ds are absent in the spectra of the complexes indicating removal of the proton from ligand and subsequent bonding of the metal ion with the thiol sulphur on plexation. The disappearance of thioamide band IV [mainly due to ν(C=S)] urring at 960 cm^{-1} in DPMTH and appearance of a band in the 720–730 cm^{-1} region to ν(C–S) in the spectra of the complexes show bonding through the sulphur (Singh *l* 1980). The bonding through sulphur is further supported by a negative shift of 35 cm^{-1} in thioamide I band and positive shift of 20–30 cm^{-1} in thioamide II and amide III bands in the spectra of the complexes. A positive shift of $\sim$ 65 cm^{-1} in –N) in the spectra of Fe(II) and Ni(II) complexes and of $\sim$ 25 cm^{-1} in others cate that both the nitrogens of –C=N–N=C– moiety are involved in bonding in the case while only one nitrogen is taking part in the other case (Braibanti *et al* 1968). non-ligand bands occurring in 300–320 and 330–350 cm^{-1} regions may be atively assigned to ν(M–S) (Nigam and Pandey 1972; Browall and Interrante 1973) ν(M–N) (Speca *et al* 1974; Paoletti *et al* 1973) modes respectively. The IR spectral lies thus suggest that DPMTH act as mononegative tridentate in Fe(II) and Ni(II) plexes bonding through sulphur and the two hydrazidic nitrogens and as nonegative bidentate in all other complexes bonding through sulphur and one razidic nitrogen.

Fungicidal test

antifungal activity given in table 4 show that the complexes are fairly toxic to both

Acknowledgements

The authors are grateful to Dr N B Singh, for encouragement. Thanks are due to the Heads of Chemistry Department, BHU, RSIC and IIT, Madras for the spectra of the samples. Financial support received from CSIR, New Delhi is gratefully acknowledged.

References

Braibanti A, Dallvalle F, Pellinghell M A and Laporati E 1968 *Inorg. Chem.* 7 1930
Browall K W and Interrante L V 1973 *J. Coord. Chem.* **3** 27
Cotton F A, Goodgame D M L and Goodgame M 1961 *J. Am. Chem. Soc.* **83** 4691
Drago R S 1965 *Physical methods in inorganic chemistry* 412
Figgis B N and Lewis J 1960 *Modern coordination chemistry*, (eds) J Lewis and R J Wilkins, (New York: Interscience) 403
Figgis B N and Lewis J 1964 *Prog. Inorg. Chem.* **6** 197
Gadag R V and Gajendragad M R 1980 *J. Indian Chem. Soc.* **57** 270
Goodman B A and Rayney J B 1970 *Adv. Inorg. Chem. Radiochem.* **13** 135
Horsfall J G 1945 *Bot. Rev.* **5** 357
Lever A B P 1968 *Inorganic electronic spectroscopy* (Amsterdam: Elsevier) pp. 183, 215, 301, 333
Lewis W B, Alei M and Morgan L C 1966 *J. Chem. Phys.* **45** 4003
Nigam H L and Pandey K B 1972 *Curr. Sci.* **41** 449
Paoletti P, Fabbrizzi L and Barbucci R 1973 *Inorg. Chem. Acta Rev.* 7 43
Proctor I M, Hathaway B J and Nicholls P 1968 *J. Chem. Soc. A* 1678
Ram V and Pandey H N 1973 *Agric. Biol. Chem.* **37** 575
Sacconi L and Ciampolini M 1964 *J. Chem. Soc.* (*A*) 276
Sacconi L 1969 *Transition Metal Chem.* **4** 199
Singh P D, Jha N K and Misra L K 1980 *J. Inorg. Nucl. Chem.* **42** 282
Speca A N, Karayanis N M and Pytlewski L L 1974 *Inorg. Chim. Acta* **9** 87
Treadwell F P and Hall W T 1958 *Anal. Chem.* **2** 77, 199
Van Landschoot R C, Van Hest J A M and Reedijk 1976 *J. Inorg. Nucl. Chem.* **38** 185
Vogel A I 1978 *A textbook of quantitative inorganic analysis* (London: Longman-group) p. 440, 447, 457, 460, 462, 470, 489
Witkowski J J and Robins R K 1976 *Chem. Abstr.* **84** 4966

. Indian Acad. Sci. (Chem. Sci.), Vol. 93, No. 2, March 1984, pp. 131–138.
Printed in India.

aracterisation and antimicrobial activity studies of the mixed ligand nplexes of Cu(II) with 8-hydroxyquinoline and salicylic acids†

Y ANJANEYULU*, R Y SWAMY and R PRABHAKARA RAO
Department of Chemistry, Nagarjuna University, Nagarjunanagar 522 510, India

MS received 6 April 1983; revised 8 July 1983

Abstract. Mixed ligand complexes of copper(II) with 8-hydroxyquinoline and various salicylic acids were isolated. Elemental analysis, conductometric and IR data of these complexes were recorded. The ESR and electronic spectral data of these complexes indicate distorted square planar coordination for central copper ion. The σ bond and inplane π bond coefficients α^2 and β^2 respectively, of these complexes indicate partial covalency in the metal ligand bonding. The antimicrobial activity studies show that the mixed ligand complexes act as more effective toxic agents than *bis* (8-hydroxyquinolinato) copper(II) against certain bacteria and fungi. The lipophilic tendency of these complexes is determined and its influence on their antimicrobial activity is critically examined. A probable mechanism for the antimicrobial activity of these complexes is discussed.

Keywords. 8-hydroxyquinoline; salicylic acid; mixed complexes; characterisation; antimicrobial activity.

Introduction

copper chelate of 8-hydroxyquinoline is recognised as one of the most highly ctive fungicide and is used in preservation of textiles, cordage, paints and various ustrial products (Albert *et al* 1953). Though its utility as an agricultural fungicide well established, its applicability has been limited by its prohibitive cost. Powell 54) observed that its cost factor can be minimised by combining the copper chelate n low cost fungicides without losing its protective properties against certain plant ases. This may be due to the formation of mixed complexes. The mixed ligand nplexes play an important role in controlling the antimicrobial activity of the metal ates as their formation can greatly bring changes in their structure, stability, solubility etc., By suitably selecting combinations of hetero chelating agents, the ation can be exploited to attain the desired effect on the metal chelates.

axena and Mishra (1978) have prepared number of mixed ligand complexes of Cu, Zn, Co and Mn with 8-hydroxyquinoline and thiocyanate and studied their microbial activity against various bacteria and fungi. Saxena *et al* (1979) have orted the preparation of mixed ligand complexes of various metals like Cu, Ni, Co Fe with salicylic acid and oxine, pyridine, nicotinic acid, β-picoline as secondary nds and studied their antifungal activity. We have taken up a systematic study to

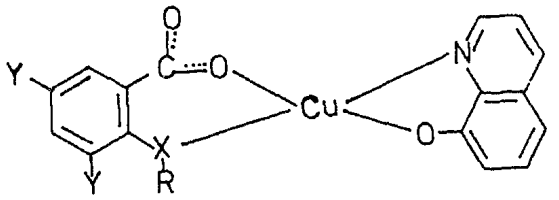

R = H or $COCH_3$, X = O or S, Y = Cl, Br, I, NO_2, H

ctivity of the mixed ligand complexes of Cu(II) with 8-hydroxyquinoline and various ubstituted salicylic acids as hetero ligands with the general formula (scheme I). The esults are presented in this paper.

Experimental

ll the chemicals used were of analytical grade (BDH) reagents.

.1 *Physical measurements*

r spectra were recorded on a Perkin Elmer model 577 spectrophotometer 4000–200 cm^{-1}) using the KBr disc technique. The electronic spectra were recorded as iffuse reflectance spectra on a Beckman DK-2A ratio recording spectrophotometer in ne 400–2500 nm region. ESR solution data (DMF) at room (RT) and liquid nitrogen emperature (LNT) were recorded on a Varian instrument at X-band. The conductivity of the complexes was measured at 27°C by Systronics conductivity bridge 305.

.2 *General method for the preparation of the complexes*

Equimolar solutions of salicylic acid or substituted salicylic acids (0·2 M), 8-hydroxy-quinoline (0·2 M) and copper(II) acetate monohydrate (0·2 M) in 80% aqueous methanol were mixed and stirred for 30 min. The solid product was removed by filtration, washed with several volumes of water and boiled in acetone to remove any free ligand. After filtration, the complex was dried at 70°C for 12 hr.

2.3 *Composition of the complexes*

The percentage composition of metal and nitrogen in these complexes were determined by the following procedures.

2.3a. % *metal*: 100 mg of the sample was decomposed by digestion with 1 ml of sulphuric acid, adding three to six drops of 100 vol. hydrogen peroxide to clear the digest. Afterwards the contents of the Kjeldahl flask were rinsed out into a 100 ml conical flask with distilled water and the solution was boiled for several minutes to destroy the excess of peroxide. The copper present in the peroxide free solution was then determined by idometric titration with sodium thiosulphate (Ingram 1962).

2.3b. % *nitrogen*: 25 mg of the sample was pyrolysed in a stream of hydrogen and the gases were passed over a nickel/magnesia catalyst heated to 350°C. The ammonia

Antimicrobial activity

e antimicrobial activity of the dimethyl formamide solutions of these compounds re examined *in vitro* by serial dilution method (Schaub *et al* 1958) against various teria and by paper disc method (Jasper *et al* 1958) against fungi. All the stock tures were supplied by the Department of Microbiology, All India Institute of dical Sciences, New Delhi, India. Peptone water and saline water were used for king the inoculum for bacteria (18 hr culture) and fungi respectively. Nutrient broth l Sabourand's dextrose agar (Hindustan Dehydrated Media, Bombay) were used as media for bacteria and fungi respectively. The minimum inhibitionary concen-tion (MIC) (μg/ml) of the compounds against bacteria and the average zone of ibition (mm) of the compounds at 1000 μg/ml against fungi are given in table 2. All tests were carried out in duplicate.

Results and discussion

e elemental analysis and other physical measurements (table 1) show that the copper ms a 1:1:1 mixed ligand complex with 8-hydroxy-quinoline and substituted cylic acids. The low conductance (2–4 mhos cm^2/g) of these complexes show that y are of non-electrolyte type.

IR data

e important peaks of the IR spectra of these complexes agree with the proposed uctures. In all the mixed ligand complexes, the symmetric and asymmetric stretching rations of the (O–C–O) group (Goyal and Khosla 1980) of salicylic acids are served at 1420 cm^{-1} and 1570 cm^{-1} respectively. Charles *et al* (1956) reported that

Table 1. Analytical data, physical measurements and distribution data of the complexes.

npound	Colour	Decomp. temp. (°C)	% of N		% of Cu		Percentage extraction of Cu(II) as mixed complex into chloroform from 7·4 pH phosphate buffer
			cal	obs	cal	obs	
OX) (SA)*	Green	266	4·06	4·19	18·43	18·51	55
OX) (Cl-SA)	Yellowish green	270	3·69	3·68	16·76	16·70	72
OX) (2Br-SA)	Yellowish green	253	2·79	2·72	12·64	12·69	79
OX) (2I-SA)	Green	252	2·35	2·33	10·66	10·72	90
OX) ($2NO_2$-SA)	Yellowish green	290	9·66	9·62	14·61	14·70	68
OX) (Thio-SA)	Green	260	3·88	3·68	17·61	17·50	48
OX) (Ace-SA)	Bluish green	227	3·62	3·64	16·43	16·49	76

Table 2. Antimicrobial activity of copper complexes with 8-hydroxyquinoline and substituted salicylic acids.

Compound	Anti bacterial activity MIC (μg/ml)**								Antifungal activity (mm)			
	Gram-Positive		Gram-negative						Average zone of inhibition at 1000 ppm			
	1	2	3	4	5	6	7	8	a	b	c	d
Oxine	12·5	12·5	100	100	100	100	100	100	8	8	7	8
$Cu(OX)_2$	6·2	12·5	25	25	50	100	50	50	11	18	12	12
Cu(OX) (SA)	10	25	50	50	50	12·5	25	25	8	12	14	10
Cu(OX) (Cl-SA)	10	25	50	25	50	50	50	50	9	12	14	10
Cu(OX) (2Br-SA)	10	25	50	6·2	100	1·5	12·5	6·2	9	12	14	10
Cu(OX) (2I-SA)	12	25	50	50	50	100	50	25	8	12	14	10
Cu(OX) ($2NO_2$-SA)	6·2	12·5	25	12·5	25	25	25	50	8	12	17	12
Cu(OX) (Thio-SA)	12·5	35	75	25	25	25	25	50	9	10	12	9
Cu(OX) (Ace-SA)	25	6·2	100	50	100	12·5	25	100	10	10	14	9

1. *Staphylococcus albus*; 2. *Staphylocous auresus*; 3. *Shigella schmitzi*; 4. *Shigella sonnei*; 5. *Proteus morganii*; 6. *Vibrio cholerae*; 7. *Escherichi coli*; 8. *Salmonella typhi.*

a. *Pencillium* spp; b. *Aspergillus niger*; c. *Trychophyton rubrum*; d. *Aspergillus fumigatus.*

incubation period: **24 hr at 37°C; *48 hr at 30°C.

in several 8-hydroxyquinoline complexes of divalent metals, the $\nu_{(C-O)}$ appeared at 1120 cm^{-1} region and the region position of the band slightly varies with the metal. The $\nu_{(C-O)}$, observed in the free oxine molecule at 1090 cm^{-1}, shifted to higher frequencies in all the mixed complexes giving a strong absorption band at 1110 cm^{-1}. This clearly indicates the coordination of 8-hydroxyquinoline in these complexes. The observed sharp peaks at 310–320 cm^{-1} and 260–280 cm^{-1} may be assigned to the M–O and M–N stretching frequencies respectively (Ohkaku and Nakamoto 1971).

3.2 *Ligand field and* ESR *spectra*

In all these complexes the crystal field symmetry of the copper ion may be taken as axial arising out of two oxygens of salicylic acids and nitrogen and oxygen atoms of 8-hydroxyquinoline, forming a distorted square planar coordination (distorted D_{4h} symmetry). Electronic and the ESR spectra of copper(II) compounds with square planar and octahedral coordination stoichiometry can be easily understood using figure 1 (Hathaway and Billing 1970; Reedijk 1981). Such a distortion will be smallest for strongly coordinating axial ligands and will increase when the coordinating power of the axial ligands decreases, resulting in the observation of only one overlapping band. Since only one broad maximum in between 15000 to 16000 cm^{-1} (ΔE) is observed in DMF of these compounds the nonexistence of axial coordination or at best weak axial coordination of the solvent may be taking place. Regular tetrahedral complexes of Cu(II) show no *d–d* absorption bands in the region 10000 to 20000 cm^{-1} (Gersman and Swalen 1962).

The spin Hamiltonian parameters ($g_{\|}$, $g_{\perp}$ and $A_{\|}$) derived from frozen solution (DMF) spectra at liquid nitrogen temperature are given in table 3. The molecular orbital parameters α^2 and β^2 which describe the fraction of the copper *d* orbitals used in σ bond and inplane π bond respectively are calculated by the standard procedure (Hathaway and Billing 1970; Reedijk 1981; Gersman and Swalen 1962; Nieman and Kivelson 1961) employing equations (a)–(c) and taking $K = 0{\cdot}43$ (Nieman and Kivelson 1961).

$$g_{\|} = g_e - 8\lambda\alpha^2\beta^2/\Delta E_{xy} \tag{a}$$

$$g_{\perp} = g_e - 2\lambda\alpha^2\beta^2/\Delta E_{xz} \tag{b}$$

$$A_{\|} = p[-\alpha^2(K + 4/7) + (g_{\|} - 2) + 3(g_{\perp} - 2)/7] \tag{c}$$

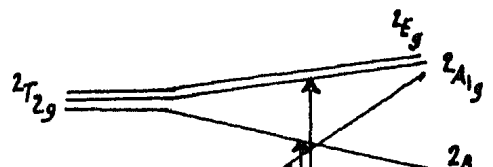

Table 3. ESR and electronic spectral data.

Compound	Solution data at LNT			*d-d* transition energy (cm^{-1})	α^2	β^2
	$g_\parallel$	$g_\perp$	$A_\parallel cm^{-1}$			
$Cu(OX)_2$	2·244	2·025	168×10^{-4}	16000	0·759	0·768
Cu(OX) (SA)	2·299	2·029	149×10^{-4}	16340	0·762	0·960
Cu(OX) (Cl-SA)	2·297	2·035	153×10^{-4}	14815	0·774	0·852
Cu(OX) (2Br-SA)	2·299	2·041	149×10^{-4}	16000	0·767	0·934
Cu(OX) (2I-SA)	2·305	2·044	151×10^{-4}	15385	0·739	0·951
Cu(OX) ($2NO_2$-SA)	2·302	2·052	149×10^{-4}	16000	0·775	0·934
Cu(OX) (Thio-SA)	2·298	2·069	168×10^{-4}	15385	0·751	0·901
Cu(OX) (Ace-SA)	2·291	2·026	158×10^{-4}	16340	0·779	0·914

The accuracies in the evaluated values of $g_\parallel$, $g_\perp$ and $A_\parallel$ are $\pm 0{\cdot}004$, $\pm 0{\cdot}006$ and $\pm 5 \times 10^{-4}$ respectively.

The σ bond coefficient α^2 describes the covalency between the central paramagnetic ion and its ligands. The α^2 values from table 3 indicate a partial covalency in σ bond, ranging in between the complete ionic bond ($\alpha^2 = 1$) and the complete covalency ($\alpha^2 = 0{\cdot}5$) for all these complexes. The α^2 values are comparable to those found for other ternary complexes which have shown to possess axial symmetry (Kuska *et al* 1967). The inplane π bonding coefficient β^2 is sensitive to back donations from the filled $d_{xz} \cdot d_{yz}$ orbitals from copper. From examination of β^2 values given in table 3 it appear that significant back donation occurs in $Cu(OX)_2$ and Cu(OX) (Thio-SA) complexes.

3.3 *Antimicrobial activity*

In general all the mixed complexes possess comparable activity against the bacteria and fungi studied with that of binary copper oxinate though in some cases the mixed complexes are more effective toxic agents. Simple salicylic acids and their binary chelates have very low activity against these organisms which may be due to their higher water solubility. The antimicrobial activity of (8-hydroxyquinolinato) copper(II) complexes were explained by several workers (Albert *et al* 1953; Block 1955; Zentmyer *et al* 1960; Esposito and Fletcher 1961; Gershon *et al* 1966) assuming that this complex first penetrates the cell and at the site of action it undergoes dissociation to a 1 : 1 copper(II) 8-hydroxyquinoline complex which will then become the toxic entity by combining with and blocking metal binding sites on enzymes as shown below (scheme II).

Thus the 1 : 2 chelate due to its liposolubility is necessary to take the toxic moiety. *i.e.* the 1 : 1 charged complex which is unable to penetrate the cell membrane due to its charge. According to Overtone's concept (Overtone 1901) of cell permeability, the lipoid membrane that surrounds the cell favours the passage of only lipid soluble materials due to which lipo solubility has been considered as one of the important factors which control the antimicrobial activity of any toxic agent. The partition of the toxic agent between oleyl alcohol or chloroform and 7.4 pH phosphate buffer (pH of the biological medium) system has been considered as a good model to understand the

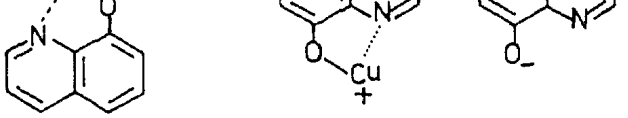

Dissociation of 1 : 2 copper oxine complex

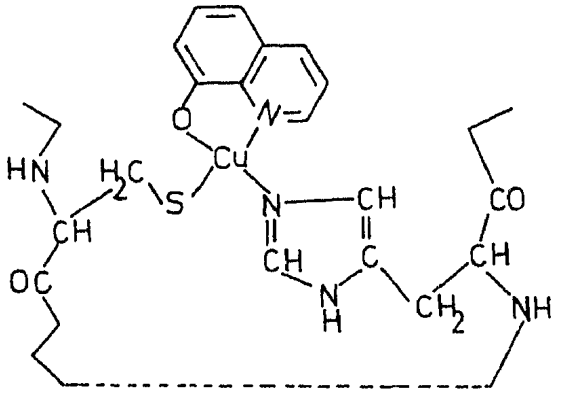

table 1. As expected the mixed complexes have lower partition coefficient in chloroform due to the presence to hydrophilic salicylate ion than compared to copper(II) 8-hydroxyquinoline complex which is quantitatively extractable under these conditions.

Thus the mixed complexes in many cases are better toxic agents though they have lower lipophilic character which indicates different mechanism may be working at the site of action. The probable mechanism at the site of action can be understood by considering the dissociation of the mixed complex into corresponding 1 : 1 binary complexes as shown below.

$$2\,Cu(OX)(SA) \longrightarrow Cu(OX)^{+} + Cu(SA)^{+} + OX^{-} + SA^{-}$$

Such a kind of dissociation of ternary complex to form binary complexes to an extent of 25 % each can be reasonably expected to be in equilibrium due to statistical reasons (Sigel 1975). Thus in the mixed complexes in addition to 1 : 1 copper oxinate, 1 : 1 copper salicylate may be also acting as a toxic agent which increases their activity. The 1 : 1 copper salicylate is better transported to the site of action as a mixed complex than the *bis*(salicylato)copper(II) complex which is found to possess very low activity most likely due to its higher hydrophilic character.

Acknowledgements

The authors are highly grateful to Prof. Jan Reedijk and Mr F B Hulsbergen, of Gorlaeus Laboratories, The Netherlands, for their help in getting the ESR and electronic spectra, and specially to Prof. Reedijk for his constant encouragement and valuable suggestions. They also wish to thank Prof. L N Mohapatra, of AIIM, New Delhi for the supply of stock culture of bacteria and fungi and Dr V G K M Pisipati of Nagarjuna University for helpful discussions. The financial support given by CSIR is gratefully acknowledged.

References

Albert A. Gibson M I and Rubbo S D 1953 *Brit. J. Exptl. Pathol.* **34** 119

Block S S 1955 *J. Agric. Food. Chem.* **3** 229

Charless R G, Freiser H, Friedel R, Hilliard L E and Johnston W D 1956 *Spectrochim. Acta.* **8** 1

Dixon J P 1968 *Modern method in organic microanalysis* (London: Nostrand Co. Ltd.)

Dwyer F D and Mellor D P 1964 *Chelating Agents and Metal Chelates* (New York: Academic Press

Esposito R G and Fletcher A M 1961 *Arch. Biochem. Biophys.* **93** 369

Gersman H R and Swalen J D 1962 *J. Chem. Phys.* **36** 3221

Gershon H, Parmegiani R, Weiner A and Ascoli R 1966 *Contributions from Boyce Thompson Institute* **23**

Goyal K C and Khosla B P 1980 *J. Indian Chem. Soc.* **57** 124

Hathaway B J and Billing D E 1970 *Coord. Chem. Rev.* **5** 143

Ingram G 1962 *Methods of Organic Elemental Microanalysis* (London: Chapman and Hall)

Jasper C, Maruzzella and Henry P A 1958 *J. Am. Pharm. Assoc.* **47** 471

Kuska H A, Max Rogers T and Brullinger R E 1967 *J. Phys. Chem.* **71** 109

Nakamato K 1970 *Infrared spectra of inorganic and coordination compounds* (New York: Wiley-Interscie

Nieman R and Kivelson D 1961 *J. Chem. Phys.* **35** 149

Ohkaku N and Nakamoto K 1971 *J. Inorg. Chem.* **10** 798

Overton E 1901 *Studien Uber div. Narkosen* (Jena: Gustav Fisher) p. 195

Powell D 1954 *Plant Disease Rept.* **38** 76

Reedijk J 1981 *Transition Met. Chem.* **6** 195

Saxena C P, Mishra S H and Khadikar P V 1979 *Curr. Sci.* **48** 20

Sexena M C and Mishra K 1978 *Chemicals and Petrochemicals J.* May 11

Schaub I G, Foley M K, Scott G E G and Bailey W R 1958 *Diagnostic Bacteriology* (St. Louis: The M
C. V. Company)

Sigel H 1975 *Angew Chenve* **14** 394

Zentmyer G A, Rich S and Horsfall J G 1960 *Phytopathology* **50** 421

Reactions of dichloro-bis(cyclopentadienyl)titanium(IV) with bidentate Schiff bases

B KHERA and N K KAUSHIK*

Department of Chemistry, University of Delhi, Delhi 110 007, India

MS received 12 September 1983; revised 28 November 1983

Abstract. A series of $Cp_2Ti(SB)Cl$ complexes, where *SB* is the anion of bidentate Schiff bases derived from salicylaldehyde and different primary amines *viz* *o*-anisidine, *m*-anisidine, *o*-phenetidine, *o*-chloroaniline, *m*-chloroaniline, *m*-nitroaniline, α-naphthylamine and benzylamine, have been synthesised by the reaction of dichloro-*bis*(cyclopentadienyl) titanium(IV), Cp_2TiCl_2, and bidentate Schiff base (SBH) in a 1 : 1 molar ratio in refluxing THF in the presence of triethylamine. The new derivatives have been characterised on the basis of their elemental analyses, conductance measurements and spectral (IR, ^1H NMR and electronic) studies.

Keywords. Cyclopentadienyl; titanium(IV); Schiff bases.

1. Introduction

Schiff bases derived from the reaction of salicylaldehyde with primary amines represent a versatile series of ligands, the metal complexes of which have been widely studied (Sacconi 1966; Yamada 1966; Holm *et al* 1966). Some organometallic complexes of titanium(IV) with bidentate, terdentate and quadridentate Schiff bases are known (Sharan *et al* 1978; Sharma *et al* 1980). Recently, we have reported (Sharma *et al* 1984) some reactions of dichloro-*bis*(cyclopentadienyl) zirconium(IV) with N-aryl salicylidimines. The present work describes the reactions of dichloro-*bis*(cyclopentadienyl) titanium(IV) with bidentate Schiff bases derived from salicylaldehyde and different primary amines.

2. Experimental

2.1 *Materials and methods*

All the reagents used were of analytical grade. Dichloro-*bis*(cyclopentadienyl) titanium(IV), Cp_2TiCl_2, was obtained from Fluka AG, Switzerland and was used without further purification. Schiff bases were prepared by the condensation of salicylaldehyde and an appropriate amine in ethanol as reported earlier (Sharma *et al* 1983). THF (Baker AR) was dried over sodium metal and then boiled under reflux until it gave a blue colouration with Ph_2CO. It was finally dried by distillation from $LiAlH_4$. *n*-Hexane (BDH) was dried by refluxing over sodium metal followed by distillation. Nitrobenzene for conductance measurements was purified as given in the literature

Titanium was determined gravimetrically as its oxide whereas chlorine was estimated as silver chloride. Nitrogen was estimated by Kjeldahl's method.

Conductance was measured in nitrobenzene at $20 \pm 0{\cdot}05°C$ using a Systronic digital direct reading conductivity meter type 304. Infrared spectra were recorded in KBr pellets in the 4000–200 cm^{-1} region on a Perkin–Elmer 621 grating spectrophotometer. The proton NMR spectra were recorded with a Perkin–Elmer R-32 spectrometer. Chemical shifts (δ) are expressed relative to an internal reference of TMS (1% by volume). Electronic spectra of the complexes in acetone were recorded on a Perkin–Elmer UV-visible spectrophotometer, model 554.

2.2 *Preparation of the complexes*

All operations were carried out under strictly anhydrous conditions. Special precautions were taken to exclude moisture from apparatus and chemicals. Quickfit apparatus of standard interchangeable glass joints lubricated with silicon grease was employed throughout the experimental work. The Schiff base (5 mmol) was added to a solution of dichloro-*bis*(cyclopentadienyl)titanium(IV), Cp_2TiCl_2, (5 mmol) in 40 ml of dry tetrahydrofuran. Triethylamine, Et_3N, (6 mmol) was added to the mixture and it was refluxed for 10–12 hr. Precipitated $Et_3N \cdot HCl$ was removed by filtration and the volume of the filtrate was reduced to *ca* 25 ml by evaporating the solvent under reduced pressure at room temperature. The crystals of the product were obtained by adding about 50 ml of dry *n*-hexane. All the complexes were prepared by a similar method.

3. Results and discussion

Dichloro-*bis*(cyclopentadienyl)titanium(IV), Cp_2TiCl_2, reacts with bidentate Schiff

Table 1. Analytical data and physical characteristics of the complexes.

Compound	Yield (%)	Dec. temp.[a] (°C)	Conductance $M \times 10^3 = 0{\cdot}5$ ($ohm^{-1} cm^2 mol^{-1}$)	% Found (Calc.) Ti	N	Cl
Cp_2Ti(sal-*o*-anisidine)Cl	62	130–132	0·26	10·80 (10·89)	3·10 (3·18)	7·97 (8·07)
Cp_2Ti(sal-*m*-anisidine)Cl	65	135–136	0·22	10·76 (10·89)	3·06 (3·18)	8·01 (8·07)
Cp_2Ti(sal-*o*-phenetidine)Cl	70	166–168	0·22	10·42 (10·56)	3·01 (3·09)	7·72 (7·82)
Cp_2Ti(sal-*o*-Claniline)Cl	68	176–179	0·24	10·73 (10·79)	3·23 (3·15)	16·12 (15·99)
Cp_2Ti(sal-*m*-Claniline)Cl	60	143–146	0·28	10·86 (10·79)	3·08 (3·15)	15·92 (15·99)
Cp_2Ti(sal-*m*-NO_2 aniline)Cl	62	147–149	0.24	10·60 (10·54)	6·24 (6·16)	7·96 (7·81)
Cp_2Ti(sal-α-naphthylamine)Cl	63	188–191	0·30	10·31 (10·43)	3·13 (3·04)	7·64 (7·72)
Cp_2Ti(sal-benzylamine)Cl	65	195–197	0·24	11·40	3·18	8·26

bases in a 1:1 molar ratio to yield complexes of the type $Cp_2Ti(SB)Cl$ according to the following equation:

$$Cp_2TiCl_2 + SBH + Et_3N \xrightarrow[68^\circ C]{THF} Cp_2Ti(SB)Cl + Et_3N \cdot HCl$$

where $(SB)^-$ represents the anion of the corresponding bidentate Schiff base SBH.

All the Schiff base complexes crystallise as yellow to yellowish brown crystals. They are highly soluble in common organic solvents, *viz* benzene, nitrobenzene, THF, acetone, dichloromethane and chloroform. Electrical conductance measurements in nitrobenzene show these complexes to be nonelectrolytes and susceptible to hydrolysis. The analytical and physical data of the complexes are given in table 1.

3.1 *IR spectra*

The assignment of characteristic infrared frequencies for $Cp_2Ti(SB)Cl$ complexes is listed in table 2.

A strong band is observed at *ca* 1630 cm^{-1} in the spectra of the Schiff bases, which may be assigned to the azomethine (–HC=N–) group. In the Schiff base complexes, this band is very slightly shifted to the lower wave number in our studies (*ca* 1600 cm^{-1}), suggesting coordination through the azomethine nitrogen (Sharan *et al* 1978; Sharma *et al* 1980; Uttamchandani and Kapoor 1978). A high intensity band at *ca* 1275 cm^{-1} in the Schiff bases can be assigned to the phenolic C–O stretching (Sharan *et al* 1978). In the complexes, the C–O stretching vibrations appear at $\sim$ 1320 cm^{-1}. This shift to higher frequency indicates bonding of the ligand to the metal through oxygen.

Bands in the region 570–540 and 525–425 cm^{-1} are attributed to the ν(Ti-O) and ν(Ti-N) vibrations, respectively (Sharan *et al* 1978). Besides, the band at *ca* 355 cm^{-1} may be assigned to ν(Ti-Cl) (Sharma and Kaushik 1981) vibration.

3.2 ^1H *NMR spectra*

Proton magnetic resonance spectra of the complexes were taken in deuterated chloroform. Chemical shifts for protons (δ scale) have been indicated in table 2. The azomethine and aromatic protons in the Schiff base complexes show a considerable downfield shift as compared to the corresponding Schiff base ligands ($\sim \delta 8{\cdot}45$ ppm and $\sim \delta 6{\cdot}6$–$7{\cdot}3$ ppm respectively) indicating the coordination of the azomethine nitrogen of the Schiff base to the metal.

3.3 *Electronic spectra*

The electronic spectra of the complexes were observed in chloroform. The bands appearing at *ca* 250, 325 and 385 nm are due to the $\pi \rightarrow \pi^*$ (benzoid), $\pi \rightarrow \pi^*$ (azomethine) and $n \rightarrow \pi^*$ (azomethine) electronic transitions, respectively. In the ligands (Schiff bases) the first two bands were observed at the same positions, whereas the third band was observed at *ca* 425 nm. A single band in the 402–412 nm region may be assigned to a charge transfer band in accordance with the electronic configuration

Table 2. Characteristic IR bands and ^{1}H NMR data.

Compound	IR (cm^{-1})		^{1}H NMR (δ, ppm)			
	ν (C=N)	ν (C–O)	C_5H_5	–CH=N–	Aromatic ring protons	$-OCH_3/OC_2H_5$
Cp_2Ti(sal-*o*-anisidine)Cl	1600	1310	6·42 (s)	8·60 (s)	6·78–7·60 (m)	3·62 (s)
Cp_2Ti(sal-*m*-anisidine)Cl	1610	1300	6·40 (s)	8·62 (s)	6·70–7·62 (m)	3·65 (s)
Cp_2Ti(sal-*o*-phenetidine)Cl	1600	1320	6·38 (s)	8·62 (s)	6·76–7·68 (m)	3·70 (q) 1·32 (t)
Cp_2Ti(sal-*o*-claniline)Cl	1600	1310	6·32 (s)	8·62 (s)	6·80–7·60 (m)	—
Cp_2Ti(sal-*m*-claniline)Cl	1605	1320	6·32 (s)	8·58 (s)	6·72–7·70 (m)	—
Cp_2Ti(sal-*m*-NO_2 aniline)Cl	1610	1305	6·40 (s)	8·60 (s)	6·70–7·68 (m)	—
Cp_2Ti(sal-α-naphthylamine)Cl	1600	1310	6·38 (s)	8·62 (s)	6·74–7·60 (m)	—
Cp_2Ti(sal-benzylamine)Cl	1605	1310	6·40 (s)	8·60 (s)	6·76–7·70 (m)	—

s = singlet, t = triplet, q = quartet, m = multiplet.

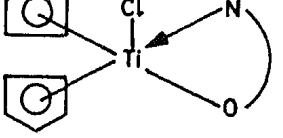

where, 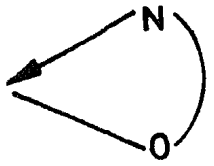 represents the anion of a bidentate Schiff base.

The structure shown is analogous to those already reported for Schiff base complexes of titanium (Sharan *et al* 1978; Sharma *et al* 1980).

Acknowledgement

The authors thank CSIR, New Delhi for awarding a fellowship to BK.

References

Fay R C and Lowry R N 1967 *Inorg. Chem.* **6** 1512
Holm R H, Everett G W and Chakravorty A 1966 *Progr. Inorg. Chem.* **7** 83
Kaushik N K, Bhushan B and Chhatwal G R 1980 *J. Inorg. Nucl. Chem.* **42** 457
Kaushik N K, Sharma A K and Sodhi G S 1981 *Indian J. Chem.* **20** 847
Sacconi L 1966 *Coord. Chem. Rev.* **1** 126
Sharan R, Gupta G and Kapoor R N 1978 *Transition Met. Chem.* **3** 282
Sharma R K, Singh R V and Tandon J P 1980 *J. Inorg. Nucl. Chem.* **42** 1382
Sharma A K and Kaushik N K 1981 *Synth. React. Inorg. Met.-Org. Chem.* **11** 685
Sharma A K, Khera B and Kaushik N K 1984 *Acta Chimi.* (in press)
Sharma A K, Khera B and Kaushik N K 1983 *Synth. React. Inorg. Met.-Org. Chem.* **13** 491
Uttamchandani J and Kapoor R N 1978 *Transition Met. Chem.* **3** 79
Yamada S 1966 *Coord. Chem. Rev.* **1** 415

Anomalous ^{1}H NMR spectra of 3,4-dihydroisoquinolines and related compounds

S NARAYANASWAMI[a], S RAJESWARI, B R PAI, K NAGARAJAN[b], W J RICHTER[c] and S J SHENOY[b]

Department of Chemistry, Presidency College, Madras 600005, India

Research and Development Laboratories, Amrutanjan Limited, Madras 600004, India
[a]Present address: Pfizer Corporation, Sandwich, England
[b]Hindustan CIBA-GEIGY Research Centre, Bombay 400063, India
[c]CIBA-GEIGY Limited, Basel, Switzerland

MS received 11 July 1983; revised 1 October 1983

Abstract. Solutions of 3,4-dihydro-6,7-methylenedioxyisoquinoline (1) and analogues 2–5 and 9 as well as isoquinolines 7 and 8 in certain samples of $CDCl_3$, CCl_4, DMSO-d_6 or acetone-d_6 gave rise to anomalous ^{1}H NMR spectra with extreme line broadening, signals due to protons at C-1 and C-3 most often not being seen. The spectra of 1 and 3 were most striking in this respect. ^{1}H NMR spectra of the quaternary salt 10 and the model schiff base 11 were normal. Several hypotheses for the observed line broadening have been considered and rejected, a slow equilibrium 1 ⇄ 13 being one of them. $NaBH_4$ reduction of 1 and 2 followed by mass spectrometric analysis of the crude tetrahydroisoquinolines 16 and 17 ruled out a slow equilibrium 1 ⇄ 14 and 2 ⇄ 15 as contributory cause for line broadening. The crude reduction products unexpectedly contained N-ethyl species 22 and 25. Their formation is rationalised.

Keywords. 3,4-dihydroisoquinolines; isoquinolines; anomalous NMR spectra; $NaBH_4$ reduction.

1. Introduction

In the course of our many exercises in aporphine (Suguna and Pai 1977) and protoberberine (Pai *et al* 1982) chemistry, we had occasion to run routinely the ^{1}H NMR

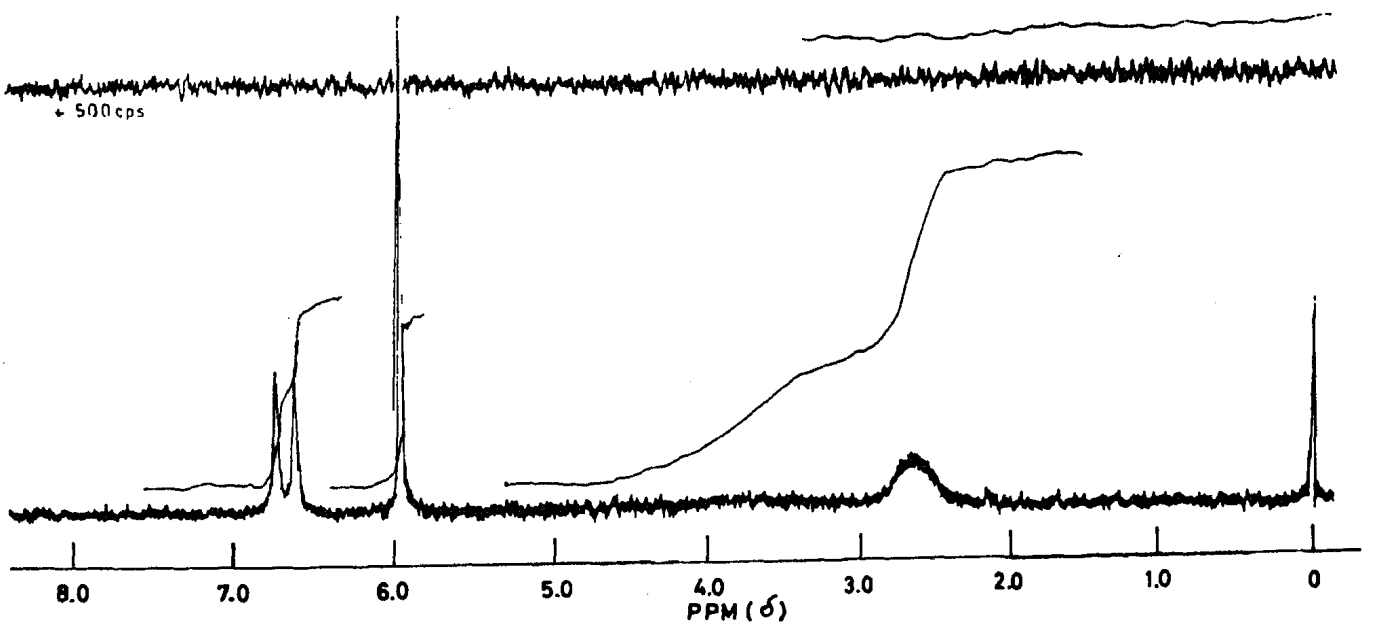

Figure 1. NMR spectrum of 1 in $CDCl_3$.

Table 1. ^{1}H NMR spectral data for 3,4-dihydroisoquinolines and related compounds.

d	Solvent(s)	δ (ppm) and shape of signals of protons at					
		C-1	C-5	C-8	C-3	C-4	Other C
	$CDCl_3$[a,a+d]	—	6·60 (s)	6·73 (s)	—	2·20–3·00 (vbh)	5·95 (s, CH_2O_2)
	$CDCl_3$[a] (−40°)	8·14 (bs)	6·61 (s)	6·72 (s)	3·67 (bt, J 8Hz)	2·62 (t, J 8Hz)	5·98 (s, CH_2O_2)
	$CDCl_3$[a] + D_2O	—	6·60 (s)	6·73 (s)	—	2·20–3·00 (vbh)	5·95 (s, CH_2O_2)
	$CDCl_3$[a] + HCl	8·35 (bs)	6·65 (s)	6·80 (s)	3·75 (bt, J 8Hz)	2·70 (at, J 8Hz)	5·95 (s, CH_2O_2)
	$CDCl_3$[a] + D_2O + CF_3COOH	—	6·65 (s)	6·85 (bs)	—	2·40–3·30 (vbh)	6·00 (s, CH_2O_2)
	$CDCl_3$[a] + D_2O + CF_3COOH	8·55 (bs)	6·85 (s)	7·20 (s)	3·95 (tf, J 8Hz)	3·10 (at, J 8Hz)	6·15 (s, CH_2O_2)
	$CDCl_3$[b,c,d,e]	8·10 (bt)	6·60 (s)	6·70 (s)	3·70 (tf, J 8Hz)	2·60 (at, J 8Hz)	5·93 (s, CH_2O_2)
	$CDCl_3$[e] + NiAcetate (25°)	—	6·46 (s)	6·66 (s)	—	2·62 (bh)	5·82 (s, CH_2O_2)
	$CDCl_3$[e] + NiAcetate (−60°)	8·11 (bs)	6·60 (s)	6·72 (s)	3·63 (at, J 8Hz)	2·62 (t, J 8Hz)	6·06 (s, CH_2O_2)
	CCl_4[f]	8·03 (bs)	6·55 (s)	6·67 (s)	3·65 (tf, J 8Hz)	2·55 (at, J 8Hz)	5·92 (s, CH_2O_2)
	CCl_4[g]	—	6·55 (s)	6·65 (s)	3·20–4·10 (vbh)	2·58 (at, J 8Hz)	5·92 (s, CH_2O_2)
	DMSO-d_6[a]	—	6·75 (s)	6·92 (s)	3·20–4·10 (vbh)	2·55 (at, J 8Hz)	6·03 (s, CH_2O_2)
	Acetone-d_6[a]	—	6·70 (s)	6·87 (s)	3·20–4·10 (vbh)	2·60 (at, J 8Hz)	6·00 (s, CH_2O_2)
	Benzene	8·10 (t, J, 2Hz)	6·30 (s)	6·42 (s)	3·62 (tf, J 8Hz)	2·25 (at, J 8Hz)	5·70 (s, CH_2O_2)
	$CDCl_3$[a]	7·00–8·00 (vbh)	6·83 (s)	6·85 (s)	3·70–4·30 (vbh)	2·65 (bt, J 8Hz)	3·87, 3·88 (2s, OCH_3)
	$CDCl_3$[a] + CF_3COOH	8·97 (bs)	6·95 (s)	7·35 (s)	3·98 (bt)	3·15 (t, J 8Hz)	3·92, 4·02 (2s, OCH_3)
	$CDCl_3$[a]	—	6·70 (s)	6·83 (vbs)	—	2·00–3·50 (vbh)	3·87 (s, OCH_3) 5·15 (s, $C_6H_5C\underline{H}_2$) 7·20–7·70 (m, C_6H_5)
	CCl_4[g]	—	6·58 (s)	6·75 (vbs)	—	2·00–3·50 (vbh)	3·80 (s, OCH_3) 5·05 (s, $C_6H_5C\underline{H}_2$) 7·20–7·50 (m, $\underline{C_6H_5}$)
	$CDCl_3$[a]	—	6·67 (s)	6·83 (bs)	—	2·40–3·00 (bh)	3·87 (s, OCH_3) 5·12 (s, $C_6H_5CH_2$) 7.20–7·60 (m, $\underline{C_6H_5}$)
	$CDCl_3$[a] + DMSO-d_6	—	6·67 (s)	6·83 (bs)	—	2·00–3·00 (vbh)	3·85 (s, OCH_3)

$CDCl_3$[a]	9·20 (s)	—	—	8·52 (J 6Hz)	—	7·10–7·80 (m, C-4, C-7, C-8H)
$CDCl_3$[a] + NH_3	9·20 (s)	—	—	8·52 (d, J 6Hz)	—	7·10–7·80 (m, C-4, C-7, C-8H)
$CDCl_3$[a]	—	7·00 (s)	7·13 (s)	8·20–8·70 (vbh)	7·45 (vbd)	6·10 (s, CH_2O_2)
CCl_4[g]	8·88 (bs)	6·95 (s)	7·08 (s)	8·28 (bd, J, 6Hz)	7·33 (d, J 6Hz)	6·03 (s, CH_2O_2)
$CDCl_3$[a]	9·30 (vbs)	7·30 (s)	—	8·37 (vbd, J 6Hz)	7·50 (bd, J 6Hz)	6·17 (s, CH_2O_2) 7.30 (s, C-6H)
CF_3COOH	9·60 (bd)	7·95 (s)	—	8·37 (bs)	8·37 (bs)	6·53 (s, CH_2O_2) 7·95 (s, C-6H)
$CDCl_3$[a]	7·80–8·50 (vbh)	6·58 (s)	6·72 (s)	3·20–4·00 (vbh)	2·30–2·90 (m)	1·38 (d, CH_3) 5·92 (s, CH_2O_2)
D_2O	8·67 (bs)	6·90 (s)	7·15 (s)	3·95 (at, J 8Hz)	3·13 (at, J 8Hz)	3·68 (s, NCH_3) 6·07 (s, CH_2O_2)
$CDCl_3$[a]	7·95 (bs)	6·72 (d, J 8Hz)	7·32 (d, J 1·5Hz)	3·80 (at, J 8Hz)	2·95 (t, J 8Hz)	5·83 (s, CH_2O_2) 7·17 (s, C_6H_5) 7·00 (dd, J8, 1.5Hz

Source of solvent:
a—Switzerland *b*—Poona *c,d*—USA *e*—England *f*—India-commercial reagent *g*—India-redistilled
Abbreviations for signal shapes:
s—singlet; d—doublet; t—triplet; m—multiplet; h—hump; b—broad; v—very; f—fine structure; a—approximate.

ample of $CDCl_3$ and obtained strange and wholly unexpected results (figure 1). While he signals due to the aromatic and methylenedioxy protons were seen as sharp singlets t 6·73, 6·60 and 5·95 ppm respectively, there was no visible signal below 7·5 ppm as vould have been expected for the azomethine proton, nor between 3 and 5 ppm for the protons on C-3, although integration revealed the presence of less than 25% of one proton in the former and about one proton in the latter regions. The benzylic protons on C-4) were seen as a very broad hump between 2·2 and 3 ppm and integrated nearly correctly. Intrigued by these observations, we extended the study to some other dihydroisoquinolines and related compounds and our findings are reported in this paper.

2. NMR spectra of 3,4-dihydroisoquinolines

^{1}H NMR spectra of 1 and its 6,7-dimethoxy (2), 6-benzyloxy-7-methoxy (3), 6-methoxy-7-benzyloxy (4) and 6-methoxy-7-hydroxy (5) analogues were run in the same sample of $CDCl_3$ and the results are presented in table 1. They are all obviously anomalous to varying degrees, 3 (figure 2) perhaps being conspicuously so. In the spectrum of the 3-methyl-3,4-dihydroisoquinoline 9, the signals due to the methine protons at C-1 and C-3 were again found to be very broad humps. But the spectrum of an acyclic analogue, the schiff base 11, in this sample of $CDCl_3$, was perfectly normal (figure 3), with all protons displaying sharp signals with expected multiplicity. The spectrum of 1 was studied in $CDCl_3$ from the same batch on several occasions over a period of two years and remained consistently mysterious. However, normal spectra were obtained in $CDCl_3$ received from four other sources; abnormality was restored on addition of the first sample of $CDCl_3$ to these solutions.

The NMR spectrum of 1 in a commercial reagent grade of CCl_4 was again normal (figure 4) but became fairly 'abnormal', when the solvent was used after further purification. Similar spectra were obtained in DMSO-d_6 and acetone-d_6. In the last three

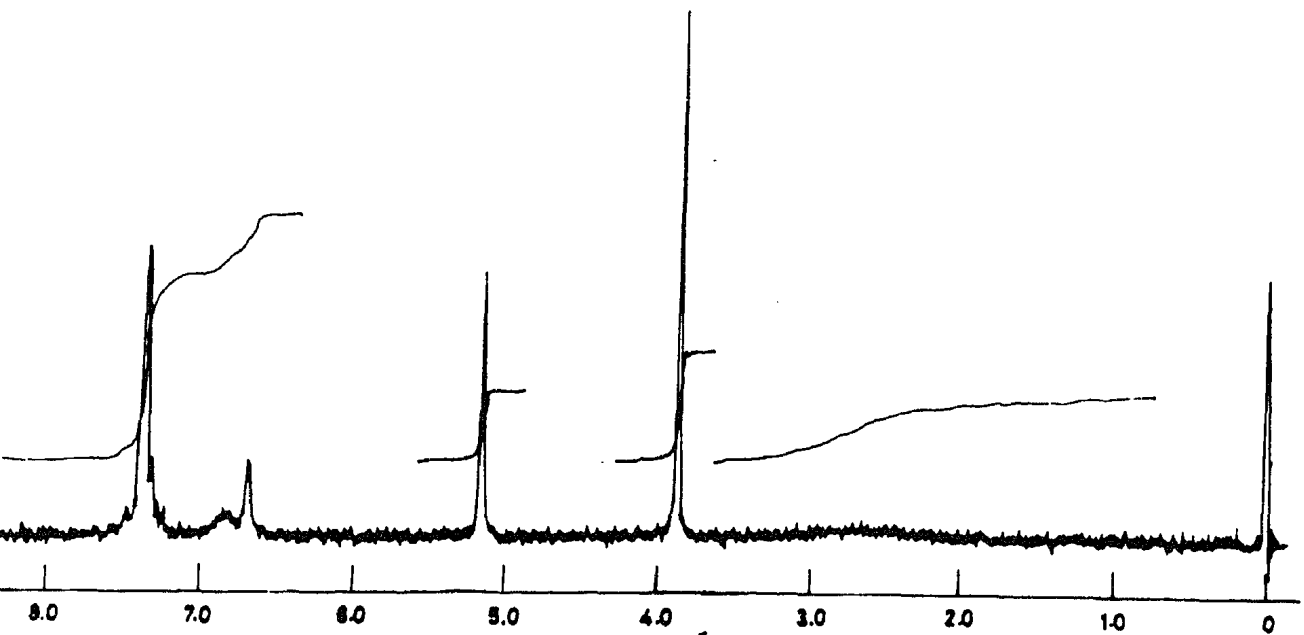

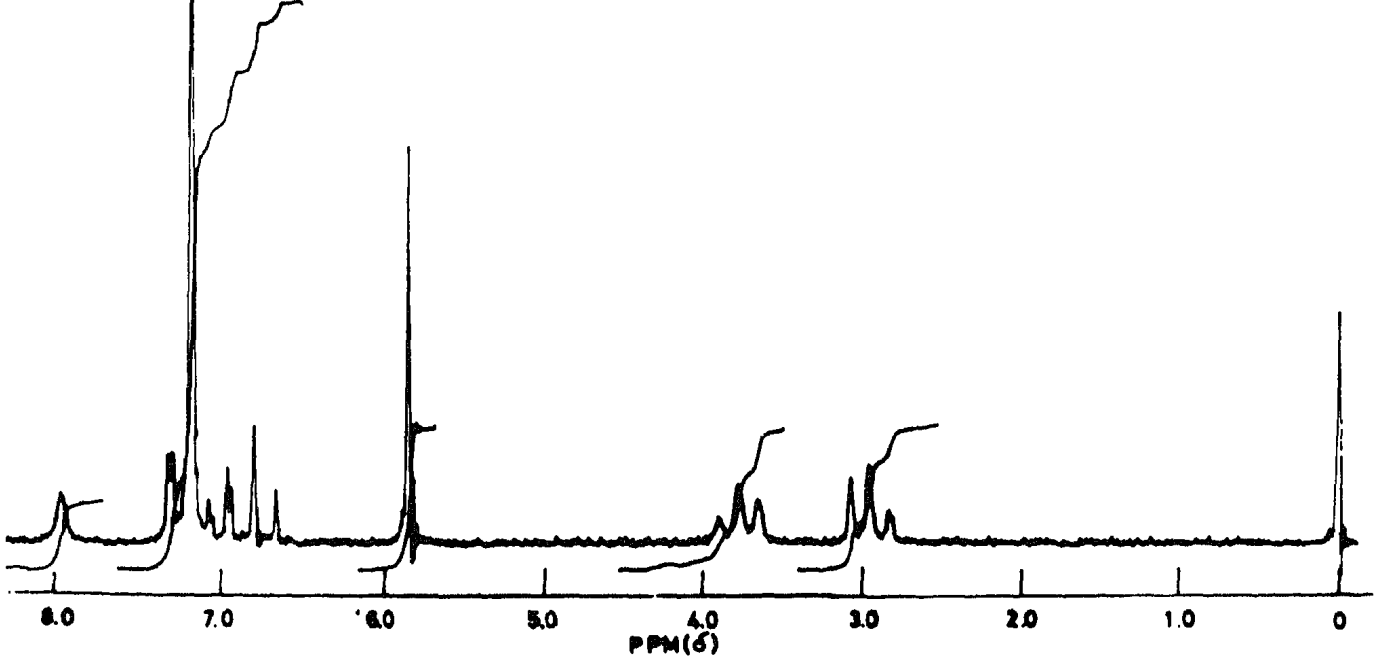

Figure 3. NMR spectrum of 11 in $CDCl_3$.

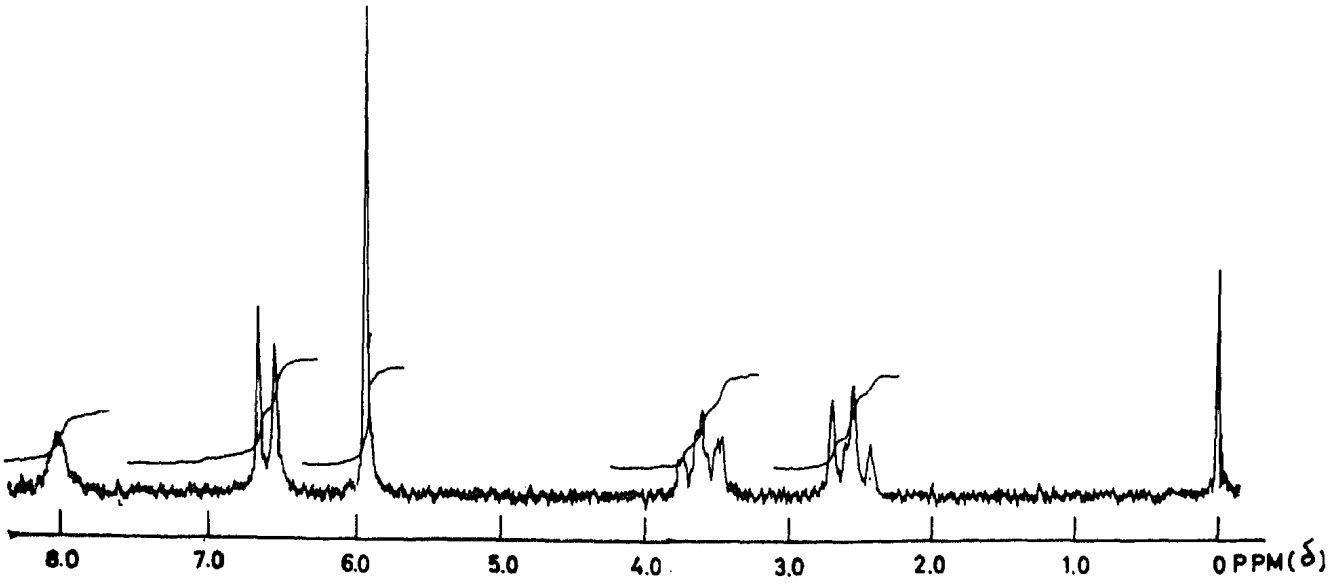

Figure 4. NMR spectrum of 1 in CCl_4.

cases, the signal due to the azomethine proton was still invisible, but the signal of the NCH_2 group was picked up as a broad hump between 3·2 and 4·1 ppm, while the $ArCH_2$ signal sharpened up to an approximate triplet. The spectrum of 1 in ordinary benzene displayed signals due to all the protons, but protons at C-4, C-5 and C-8 had suffered upfield shifts of 0·3–0·4 ppm, due perhaps to the complexation of 1 with the solvent in an appropriate orientation. The spectrum clearly revealed the signals at C-1 and C-3 and their mutual coupling.

The NMR spectrum of 3 in CCl_4 was as abnormal (figure 5) as in $CDCl_3$ with total

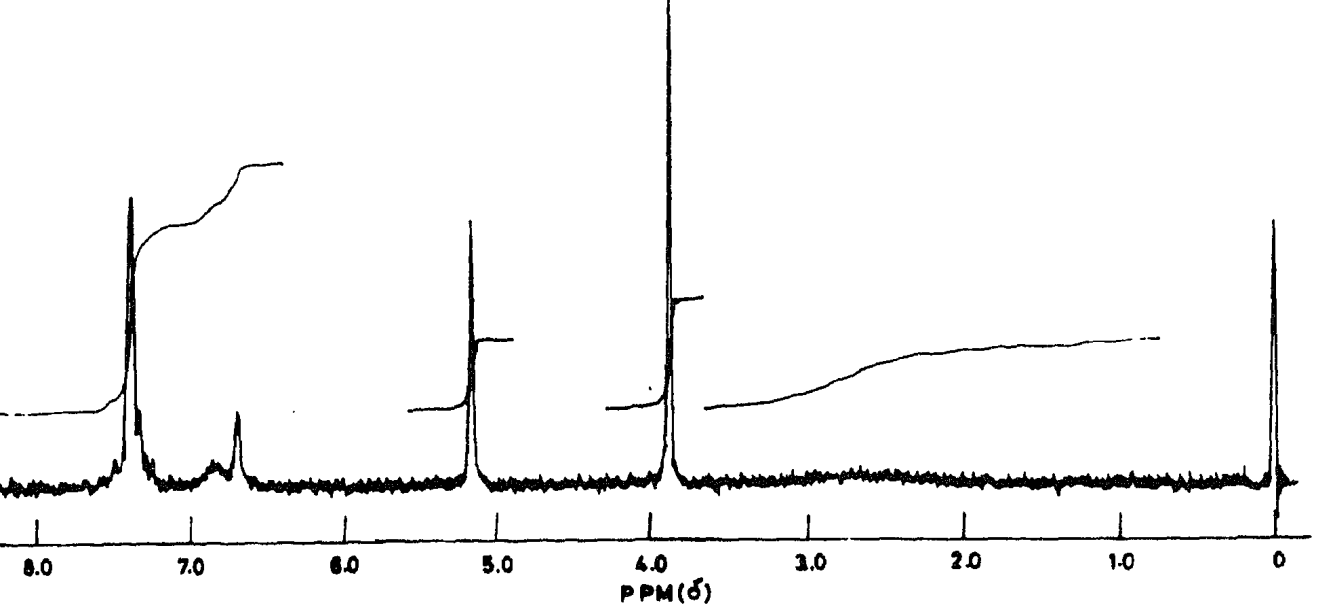

Figure 5. NMR spectrum of 3 in CCl_4.

and further a little trifluoroacetic acid, but normality could be attained by the addition of more trifluoroacetic acid, or hydrogen chloride to the original solution, as evidenced by the appearance of signals with appropriate shape for protons at C-1 and C-3, with some acid-induced shifts. As a logical corollary, the spectrum of the quaternary salt 10 of 1 was run in D_2O and found to possess the appropriate features, with some signals displaced to low field, consistent with the presence of a full charge on the nitrogen atom.

3. NMR spectra of isoquinolines

The spectrum of the parent 3,4-dihydroisoquinoline could not be run due to the difficulty in the synthesis, but we could study isoquinoline 6 itself in the original sample of $CDCl_3$ alone or in the presence of ammonia (to remove traces of acid if present). Both spectra displayed sharp signals for all the protons. However, abnormality appeared to some extent in the spectrum of the 7,8-methylenedioxy derivative (8), and to a greater extent in that of 6,7-methylenedioxyisoquinoline (7). Thus the signal due to the proton at C-1 in 7 was not visible (figure 6) and that of the proton at C-3 was a very broad hump. Even the doublet of the proton at C-4 was visibly broadened. However, normalcy appeared in the spectrum of 7 in CCl_4 and 8 in TFA.

4. Discussion of results

The anomalous nature of spectra of 3,4-dihydroisoquinolines which was apparently a case of extreme line broadening was observed for quite a few 6,7-dialkoxy derivatives, but not for the schiff base 11, in one sample of $CDCl_3$. This was true for 1 and 3 in CCl_4 and for 1 in DMSO-d_6 and acetone-d_6 solution. It was present, perhaps to a lesser extent, for the isoquinolines 7 and 8. These observations prompted us in the first instance to

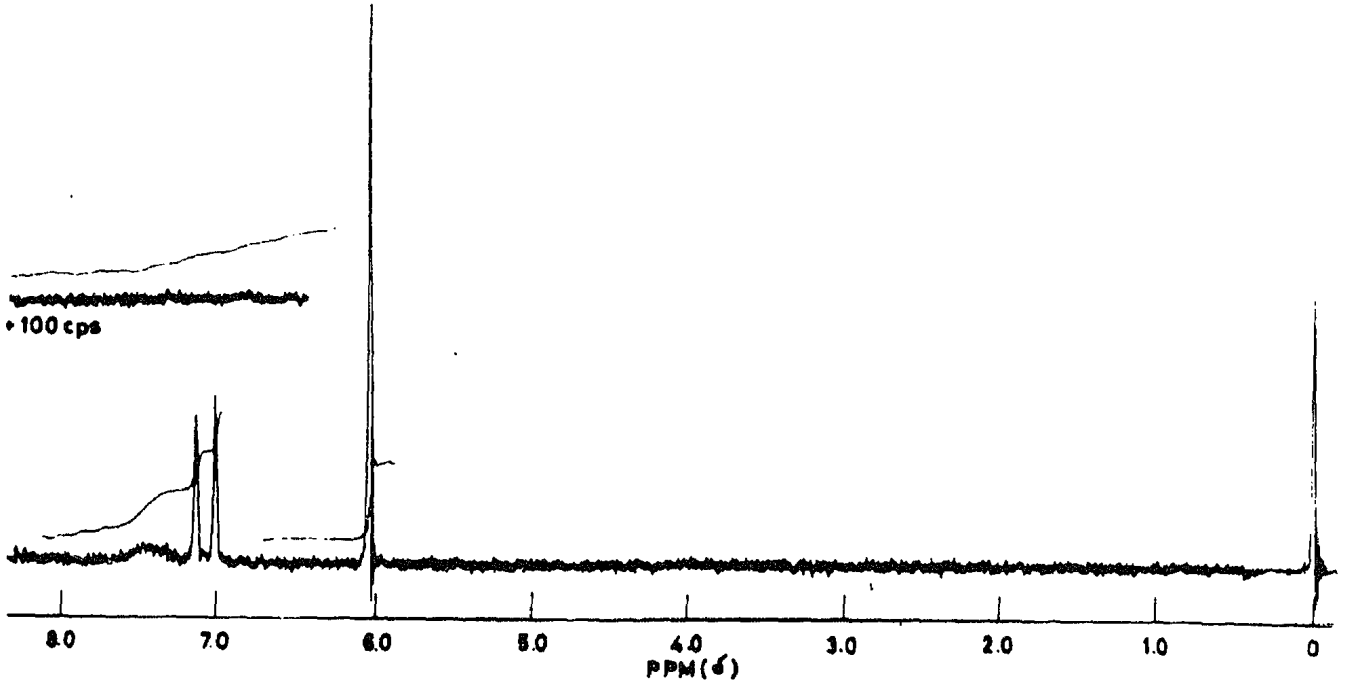

Figure 6. NMR spectrum of 7 in $CDCl_3$.

spectrum of the azomethine 12, the –CF=N absorption has been reported (Cavalli and Piccandi 1969) to be a broad band. It has been speculated that this could be due to such an effect. However, the spectrum of 1 in $CDCl_3$ with simultaneous irradiation at ^{14}N frequency did not revert to normalcy.

We considered the possibility that dissolved oxygen could be responsible for line broadening, but bubbling oxygen into a solution of 1 in a sample of $CDCl_3$ that had given a 'normal' spectrum did not lead to any line broadening. However, addition of crystals of nickel acetate to this solution caused a dramatic effect and produced the 'familiar' 'anomalous' spectrum. When solutions giving rise to anomalous spectra of 1 at usual probe temperatures, were cooled to $-40°$ to $-60°$, the expected signals of *all* the protons in 1 appeared with appropriate line shapes. Thus it seemed possible that the 'anomalous' spectra were caused by a slow equilibrium of 1 as a ligand with some complexing agent, which need not of course necessarily be paramagnetic. However, the low temperature spectrum showed *only one* species, 1 to be present—and hence it would have to be argued that at these temperatures the equilibrium was very much in favour of 1 with the complex present in undetectable proportions. Raising the temperatures should increase the rate of exchange and produce sharp signals, but in $CDCl_3$ upto 50° (the maximum temperature obtainable) this did not happen.

The complexing extraneous impurity could be present in the solvent, (*e.g.* traces of acid). This was considered unlikely since anomaly had occurred in $CDCl_3$, CCl_4, DMSO-d_6 and acetone-d_6. Further, this persisted even in $CDCl_3$ that had been distilled over norhydrastinine (1). It could be present in the solute, but this hypothesis had to be ruled out because similar phenomena were realized with dihydroisoquinolines 1–5 and 9 and isoquinolines 7 and 8. Again a carefully recrystallised sample of 1 behaved

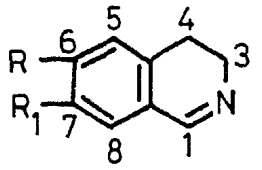

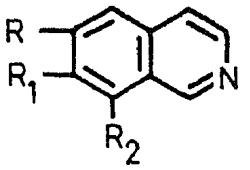

1 $RR_1 = CH_2O_2$
2 $R = R_1 = OMe$
3 $R = PhCH_2O$; $R_1 = OMe$
4 $R = OMe$, $R_1 = PhCH_2O$
5 $R = OMe$; $R_1 = OH$

6 $R = R_1 = R_2 = H$
7 $RR_1 = CH_2O_2$; $R_2 = H$
8 $R = H$; $R_1R_2 = CH_2O_2$

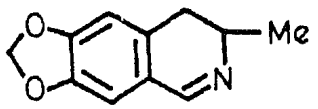

9

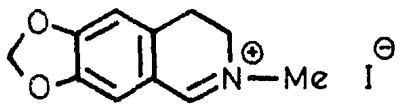

10

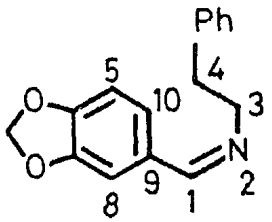

11

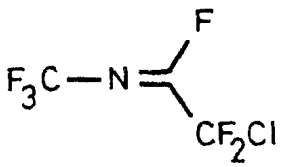

12

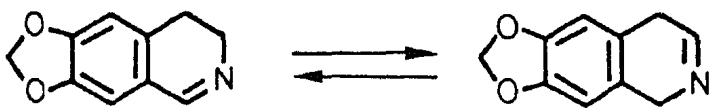

1 13

xamine the unlikely possibility of an 'internal' 'slow' equilibrium*, 1 ⇄ 13. This was onsidered extremely unlikely. But we could rule it out firmly also since exposure of a olution of 1 in a sample of $CDCl_3$ giving a 'normal' spectrum to D_2O for 5 days did not how any change in the signals due to protons at C-1, C-3 and C-4. Further spectra of 1 nd 2 in acids showed separate signals for *protons at both C-1 and C-3*.

We considered one last possibility that dihydroisoquinolines of type 1 and 2 could xist in a slow equilibrium* with dimers 14 and 15 respectively. The concentration of 4 and 15 may be so small at low temperatures that the insensitive NMR technique may ot pick up their signals. Such a speculation has supportive precedent in the literature Goldman *et al* 1969) in the case of the benzazepine 20 which has been shown to go over o 21 on prolonged storage. We failed in our efforts to detect the presence of 14 and 15 n the NMR spectra of 1 and 2 respectively and turned our attention to using mass

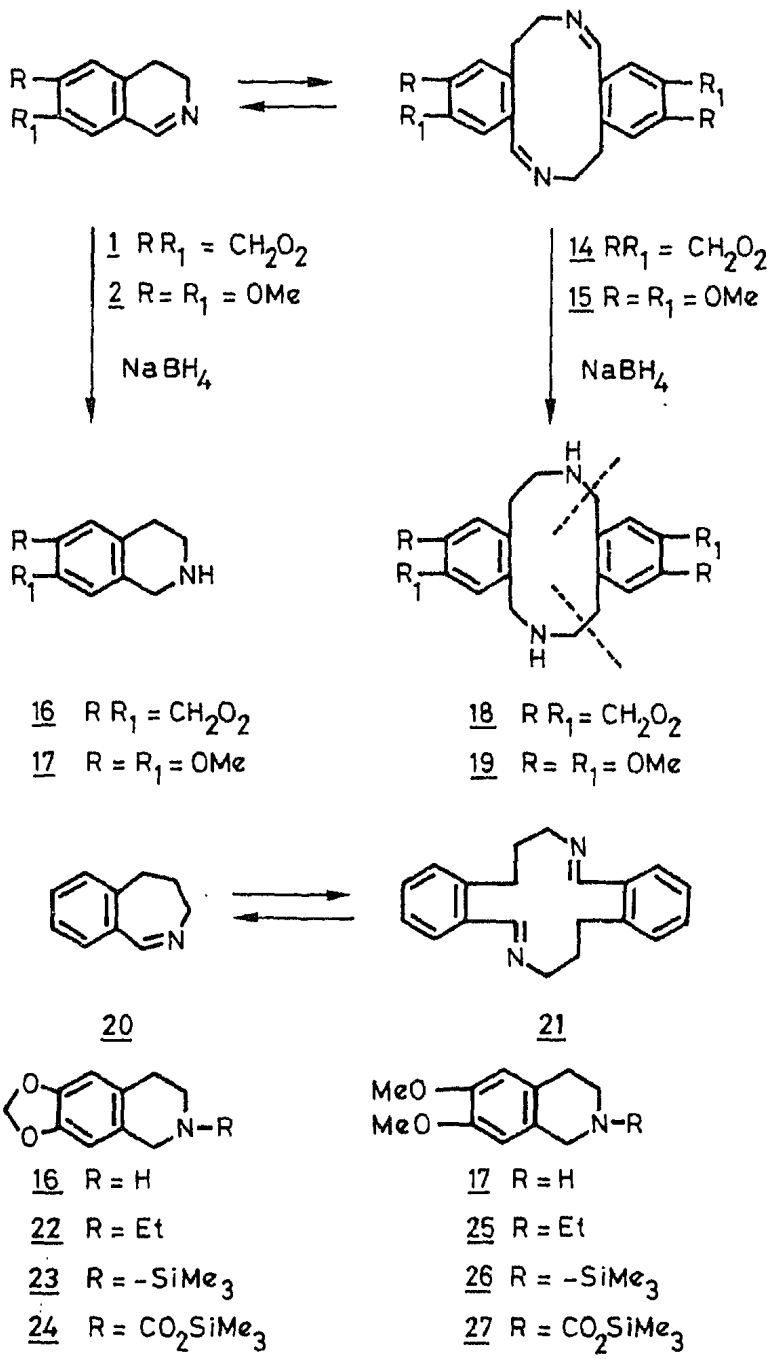

5. Mass spectral studies

Carefully run high resolution mass spectra of 1 showed no mass peaks above $M^{+\bullet}$ at m/z 175 ($C_{10}H_9NO_2$), as the most abundant peak, followed by important fragments at m/z 174, 149, 116 and 89. The dimeric species 14 was not detectable in the sample vaporized from the probe of the mass spectrometer at 50°. It was still possible that traces of 14 and 15 were formed in solution. We considered that reduction would be a sure method of trapping such fugitive species irreversibly. Accordingly 1 was reduced with $NaBH_4$ in ethanol and the product worked up by dilution with water, extraction with ether and evaporation of the dried extract. Low resolution mass spectrum of the

indicated the major impurity to be the ethyl derivative, 22. Thus the spectrum still showed the peak at m/z 205 ($M^{+\bullet}$ of 22), besides a major one at m/z 249 ($M^{+\bullet}$) of 23, the TMS derivative of 16. A small peak at m/z 293 should be due to $M^{+\bullet}$ of 24, the TMS derivative of the N-carboxylic acid of 16 formed by the exposure of 16 to aerial CO_2. The presence of the ethyl species 22 was confirmed by the 360 MHz ^1H NMR spectrum of crude 16. Characteristic signals due to the N-ethyl species were seen at 1.15 (triplet) and 2.6 (quartet) ppm, integration revealing that 22 was present to the extent of about 10%.

The crude reduction product 17 of 2 in EtOH (work-up by dilution with water and extraction with ether) was examined in greater detail. The 360 MHz spectrum in $CDCl_3$ of crude 17 showed the presence of the N-ethyl derivative 25-triplet at 1·15 and quartet at 2 ppm. High resolution electron impact (EI) mass spectrum showed $M^{+\bullet}$ for 17 at m/z 193 ($C_{11}H_{15}NO_2$), $M^{+\bullet}$ for 25 at m/z 221 ($C_{13}H_{19}NO_2$), and its $(M-CH_3)^{+\bullet}$ fragment at m/z 206 ($C_{12}H_{16}NO_2$). After deuterium exchange, peaks at m/z 221 and 206 remained unshifted but the one at m/z 193 moved up to 194. Thus fragmentation of 19 as shown would not be the source of the ion at m/z 221. Field desorption (FD) mass spectrum of crude 17 showed mass peaks only at 193 and 221 and none in the higher mass region. The TMS derivative of crude 17 displayed in its EI spectrum, peaks at m/z 265 ($M^{+\bullet}$ of 26), 309 ($M^{+\bullet}$ of 27) and 221 ($M^{+\bullet}$ of 25). High resolution accurate mass measurements indicated, in addition, the presence of boron complexes as minor constituents.

Interestingly the same ethylated species 22 and 25 were respectively formed when the reduction of 1 and 2 with $NaBH_4$ was performed in *methanol* solution, further work-up constituting dilution with water and extraction with ether. The products were identified by resort to both mass and NMR spectrometry. At the moment, we are obliged to postulate that N-ethylation occurred by reaction of 16 or 17 with ether (or its peroxide) during extraction in the presence of unused excess sodium borohydride. The same ethylated species 25 was formed when the reduction of 2 with sodium borohydride was conducted in water and the product extracted with ether. The involvement of ether in the formation of 25 was confirmed when benzene was used to extract the reduction product from the aqueous solution. The mass spectrum of crude 17 was devoid of any peaks above the one at m/z 193. On the other hand, the products obtained by reducing 2 in methanol, ethanol or water and extracting with methylene chloride again showed peaks at m/z 221. High resolution mass spectra revealed this species to be due to $C_{12}H_{15}NO_3$ ions, corresponding probably to the molecular ion of the N-formyl derivative of 17. Additionally peaks were also seen at m/z 207 and 206, corresponding to $C_{12}H_{17}NO_2$ and $C_{12}H_{16}NO_2$ respectively, arising probably from the N-methyl derivative of 17. We speculate that the reaction of 17 with methylene chloride would lead to a N-chloromethyl derivative which as such (or as the hydroxy methyl compound) can lead to the two products by oxidation-reduction mechanisms. These were however present in trace amounts and not detectable in the NMR spectra. We next studied the reaction of 1-phenyl-3,4-dihydro-6,7-dimethoxyisoquinoline with sodium borohydride under various conditions, especially using ether for extraction. There was again no evidence for the formation of dimeric reduction products, nor was there any

and 2 with 14 and 15 respectively, as the cause for the observed line broadening in the NMR spectra of 3,4-dihydroisoquinolines in certain solvents.

6. Experimental

Dihydroisoquinolines and related compounds studied in this work were prepared by known procedures. ^{1}H NMR spectra were run mostly on a Varian A 60 NMR spectrometer with TMS as internal reference. Probe temperature was generally around 40° unless otherwise stated. Chemical shifts are quoted in ppm downfield from TMS.

Acknowledgements

We are grateful to Dr P Hampson, Imperial Chemical Industries Limited, London, for studies involving ^{14}N decoupling, addition of nickel acetate and variable temperatures.

References

Cavalli L and Piccandi P 1969 *Chem. Commun.* 1132

Goldman I M, Larson J K, Trettor J R and Andrews E G 1969 *J. Am. Chem. Soc.* **91** 4941

Pai B R, Natarajan S, Suguna H, Rajeswari S, Chandrasekharan S and Nagarajan K 1982 *Indian J. Chem.* **B21** 607

Suguna H and Pai B R 1977 *Indian J. Chem.* **B15** 416

Separation of electronic and steric effects: Oxidation of *ortho*-substituted phenyl methyl sulphides by peroxoanions, chromium(VI) and picolinic acid catalysed chromium(VI)

C SRINIVASAN, P KUTHALINGAM, A CHELLAMANI, S RAJAGOPAL and N ARUMUGAM*

School of Chemistry, Madurai Kamaraj University, Madurai 625021, India

MS received 6 July 1983; revised 27 August 1983

Abstract. The kinetics of oxidation of *ortho*-substituted phenyl methyl sulphides by peroxoanions, Cr(VI) and picolinic acid catalysed Cr(VI) have been investigated. Regression analyses of the rate data by using Taft and Charton equations to separate steric effect from electronic effects have been carried out. In peroxoanion oxidations, the localized electronic effect plays a major role. In the uncatalysed and picolinic acid catalysed Cr(VI) oxidations, both localized and delocalized effects are significant. Steric effect plays a minor role in all the oxidations.

Keywords. *ortho*-substituted phenyl methyl sulphides; *ortho*-effect; regression analysis.

1. Introduction

The kinetics of oxidation of alkyl aryl sulphides with peroxodisulphate (PS) (Arumugam *et al* 1978; Srinivasan *et al* 1978), peroxodiphosphate (PP) (Srinivasan *et al* 1980) and uncatalysed and picolinic acid (PA) catalysed Cr(VI) (Srinivasan *et al* 1982) have been extensively investigated in this laboratory. The mechanisms of these oxidations have been established based on the kinetic results obtained with several *para*- and *meta*-substituted phenyl methyl sulphides and from a comprehensive analysis of the rate constants employing linear free-energy relationships. A polar mechanism has been proposed for the oxidation of alkyl aryl sulphides by peroxoanions. On the other hand a mechanism involving one-electron transfer process is envisaged in the uncatalysed and PA catalysed Cr(VI) oxidations. Rates of oxidation of several alkyl phenyl sulphides with the above oxidants also reveal that the reaction centre *viz* the sulphide sulphur is quite sensitive to steric congestion. These studies prompted us to investigate the influence of *ortho*-substituents in the oxidation of aryl methyl sulphides. *Ortho*-substituted benzene derivates often behave differently from the corresponding *meta*- or *para*-substituted compounds. This peculiarity of *ortho*-substituted compounds is sometimes named *ortho*-effect. Numerous attempts (Taft 1956; Charton 1971, 1975; Fujita and Nishioka 1976) have been made to understand quantitatively the nature and composition of the *ortho*-effect, by separating the component effects from each other. The present work is part of an effort to develop a better understanding of the *ortho*-effect in these oxidations. The kinetic data are analysed by employing Taft

2. Experimental

All the *ortho*-substituted phenyl methyl sulphides were obtained by the methylation of the corresponding thiols which were obtained from the *ortho*-substituted anilines by the xanthogenic ester method (Horning 1955). The kinetic measurements were carried out under pseudo first-order conditions by estimating the unreacted oxidant using iodometric procedure. The reaction conditions were identical with those employed in the kinetic studies of *meta*- and *para*-substituted phenyl methyl sulphides (Arumugam *et al* 1978; Srinivasan *et al* 1980, 1982). Statistical calculations were performed with a Micro 2200 diskette recorder (Hindustan Computers). The rate constants were measured at three temperatures. The rate data at 40°C are considered for the analysis of the *ortho*-effect. The substituent parameters are taken from literature (Taft 1956; Shorter 1972; Aslam *et al* 1981).

3. Results and discussion

3.1 *Oxidation of ortho-substituted phenyl methyl sulphides by peroxoanions*

The oxidation of *ortho*-substituted phenyl methyl sulphides by PS was carried out in 50% (v/v) aqueous ethanol while that by PP in 50% (v/v) aqueous acetic acid. The rate data and the activation parameters are set forth in tables 1 and 2. The data reveal that the reactivity is in the order H > Me > OMe > F > Cl > Br > NO_2. Regression analyses have been carried out with Taft's linear free-energy—polar energy relationship [equation (1)] and linear free energy—steric energy relationship [equation (2)] (Taft 1956).

$$\log k_{ortho} = \rho^* \sigma_0^* + h \tag{1}$$

$$\log k_{ortho} = \delta E_s + h \tag{2}$$

In the above equations, σ_0^* (polar) and E_s (steric) are the substituent constants, ρ^* is a

Table 1. Second-order rate constants, enthalpies and entropies of activation for the oxidation of *ortho*-substituted phenyl methyl sulphides by PS[a].

Substituent	$10^3 k_2$ M^{-1} sec^{-1}[b] 35°	40°	45°	$\Delta H^{\neq}$[c] (k J mol^{-1})	$-\Delta S^{\neq}$[c] (J K^{-1} mol^{-1})
H	4·41±0·18	5·90±0·15	7·87±0·39	44·8±6·3	146±21
Me	3·65±0·13	5·07±0·25	6·64±0·11	46·5±5·4	141±18
MeO	2·03±0·06	2·85±0·05	3·77±0·13	47·7±4·6	142±15
F	0·821±0·01	1·15±0·03	1·57±0·03	50·2±3·4	142±11
Cl	0·620±0·03	0·860±0·02	1·25±0·05	54·4±6·3	130±21
Br	0·493±0·01	0·611±0·02	0·856±0·04	61·1±5·9	113±19
NO_2	—	0·324±0·04	0·447±0·02	50·7±28	150±88

[a]General conditions: [Sulphide] ≃ 0·02 M; $[S_2O_8^{2-}]$ = 0·001 M in 50% (v/v) aqueous ethanol at

Table 2. Second-order rate constants, enthalpies and entropies of activation for the oxidation of *ortho*-substituted phenyl methyl sulphides by PP[a].

Substituent	$10^3 k_2$ M^{-1} s^{-1} 35°	40°	45°	$\Delta H^{\neq}$ (kJ mol^{-1})	$-\Delta S^{\neq}$ (J K^{-1} mol^{-1})
H	6·67 ± 0·32	9·90 ± 0·44	14·2 ± 0·67	59·9 ± 7·5	92·9 ± 25
Me	4·96 ± 0·44	7·59 ± 0·37	11·2 ± 0·09	63·6 ± 8·0	82·5 ± 26
MeO	4·32 ± 0·59	5·81 ± 0·42	8·16 ± 0·52	49·4 ± 15	131 ± 46
F	1·32 ± 0·09	2·03 ± 0·14	3·25 ± 0·16	70·7 ± 10	70·7 ± 34
Cl	0·918 ± 0·10	1·51 ± 0·13	2·58 ± 0·14	81·6 ± 14	38·9 ± 42
Br	0·813 ± 0·04	1·31 ± 0·08	2·15 ± 0·11	75·3 ± 8·8	59·9 ± 29
NO_2	0·453 ± 0·03	0·764 ± 0·05	1·26 ± 0·11	80·8 ± 12	46·9 ± 39

[a]General conditions: [Sulphide] ≃ 0·02 M; [PP] = 0·001 M in 50% (v/v) aqueous acetic acid at I = 0·2 M and $[H^+]_T$ = 0·0138 M.

reaction constant analogous to ρ and δ is a steric susceptibility constant. The results of the regression analyses with the Taft's relationships are expressed by the following equations

PS oxidation

$$\log k_{ortho} = -0{\cdot}962\,\sigma_0^* - 2{\cdot}618$$

$$r = 0{\cdot}893;\ s = 0{\cdot}22;\ n = 6$$

(r = correlation coefficient; s = standard deviation; n = number of data points)

$$\log k_{ortho} = 0{\cdot}457\,E_s - 2{\cdot}994$$

$$r = 0{\cdot}604;\ s = 0{\cdot}39;\ n = 6$$

PP oxidation

$$\log k_{ortho} = -0{\cdot}871\,\sigma_0^* - 2{\cdot}368$$

$$r = 0{\cdot}913;\ s = 0{\cdot}18;\ n = 6$$

$$\log k_{ortho} = 0{\cdot}419\,E_s - 2{\cdot}709$$

$$r = 0{\cdot}625;\ s = 0{\cdot}34;\ n = 6$$

For these oxidations a fair correlation with (1) and a poor correlation with (2) indicate the minor role of the 'primary steric effect' or the 'bulk effect'.

To understand the composition of localized (L), delocalized (D) and steric components (S) operating in these reactions, the rate data are analysed with LD (Taft and Lewis 1958) and LDS (Charton *et al* 1979) equations ((3) and (4)).

$$\log k_{ortho} = L\sigma_I + D\sigma_R + h \tag{3}$$

$$\log k_{ortho} = L\sigma_I + D\sigma_R + S\upsilon + h \tag{4}$$

where σ_I, σ_R and υ are inductive, resonance and steric substituent constants respectively.

$(\pm 0{\cdot}194) \quad (\pm 0{\cdot}210)$

$R = 0{\cdot}977$; SE $= 0{\cdot}126$; $n = 7$ (unsubstituted compound included); CL $= 97{\cdot}5\,\%$

(R = multiple correlation coefficient; SE = standard error of the estimate; n = number of data points; CL = confidence level of F test significance)

$$\log k_{\text{ortho}} = -1{\cdot}59\,\sigma_I - 0{\cdot}576\,\sigma_R - 2{\cdot}434$$

$(\pm 0{\cdot}243) \quad (\pm 0{\cdot}228)$

$R = 0{\cdot}977$; SE $= 0{\cdot}121$; $n = 6$ (unsubstituted compound excluded); CL $= 97{\cdot}5\,\%$

$$\log k_{\text{ortho}} = -1{\cdot}58\,\sigma_I - 0{\cdot}318\,\sigma_R - 0{\cdot}156\upsilon - 2{\cdot}267$$

$(\pm 0{\cdot}317) \quad (\pm 0{\cdot}296) \quad (\pm 0{\cdot}216)$

$R = 0{\cdot}980$; SE $= 0{\cdot}134$; $n = 7$; CL $= 99\,\%$

PP oxidation

$$\log k_{\text{ortho}} = -1{\cdot}56\,\sigma_I - 0{\cdot}419\,\sigma_R - 2{\cdot}108$$

$(\pm 0{\cdot}199) \quad (\pm 0{\cdot}215)$

$R = 0{\cdot}970$; SE $= 0{\cdot}129$; $n = 7$; CL $= 97{\cdot}5\,\%$

$$\log k_{\text{ortho}} = -1{\cdot}38\,\sigma_I - 0{\cdot}550\,\sigma_R - 2{\cdot}234$$

$(\pm 0{\cdot}230) \quad (\pm 0{\cdot}223)$

$R = 0{\cdot}972$; SE $= 0{\cdot}119$; $n = 6$; CL $= 95\,\%$

$$\log k_{\text{ortho}} = -1{\cdot}45\,\sigma_I - 0{\cdot}330\,\sigma_R - 0{\cdot}097\upsilon - 2{\cdot}073$$

$(\pm 0{\cdot}342) \quad (\pm 0{\cdot}320) \quad (\pm 0{\cdot}233)$

$R = 0{\cdot}971$; SE $= 0{\cdot}144$; $n = 7$; CL $= 97{\cdot}5\,\%$

Correlations obtained with LD and LDS equations are justified by F-test significance ($> 95\,\%$ CL). For oxidations with peroxoanions the L and D terms in LD equations are significant to $> 99{\cdot}8\,\%$ and $90\,\%$ CL (t-test) respectively when the unsubstituted compound is included in the regression analyses. On excluding the unsubstituted compound the L term is significant to $99{\cdot}5\,\%$ and $99\,\%$ CL of the t-test in PS and PP oxidations respectively; the D term is significant to $90\,\%$ CL in both oxidations. These analyses undoubtedly indicate that the localised effect plays a major role in these oxidations. A better description of the composition of the electrical effect is given by the 'percent delocalized factor', P_D, where $P_D = D \times 100/L + D$ (Charton 1975). The P_D values are 26·6 and 20·8 for excluding and including the unsubstituted compound for the PS oxidation and the corresponding values are 28·5 and 21·2 for the PP oxidation. The h_{obs} value ($-3{\cdot}229$) is not very close to the h_{cal} ($-2{\cdot}434$, unsubstituted excluded; $-2{\cdot}322$, unsubstituted included) for PS oxidation. Similar behaviour is also noted with PP oxidation ($h_{\text{obs}} = -3{\cdot}002$; $h_{\text{cal}} = -2{\cdot}234$ (unsubstituted excluded) and $-2{\cdot}108$

of t-test respectively in both oxidations and the S term is significant to 50% and < 50% CL in PS and PP oxidations respectively. These results also clearly demonstrate the operation of significant localised effect and insignificant delocalised and steric effects in the peroxoanion oxidations. These results indicate that these reaction series may be taken as examples of case 3 of Charton's classification ($\log k_{ortho} = L\sigma_I + D\sigma_R + h'$; $h' \neq h$; Charton 1975).

3.2 *Oxidation of ortho-substituted phenyl methyl sulphides by Cr(VI) and PA catalysed Cr(VI)*

PA is a specific catalyst for the Cr(VI) oxidation of alcohols (Rocek and Peng 1977). Recently we have observed that PA accelerates the Cr(VI) oxidation of alkyl aryl and diphenyl sulphides and the rate acceleration has been attributed to the fast attack of PA complexed Cr(VI) on the sulphide (Srinivasan *et al* 1982). Hence we have measured the rates of both uncatalysed and PA catalysed Cr(VI) oxidations of *ortho*-substituted phenyl methyl sulphides in 50% (v/v) aqueous acetic acid. The kinetic data presented in tables 3 and 4 show that the order of reactivity is H > OMe > Me > F > Br > Cl > NO_2. Correlation analyses have been carried out with equations (1) and (2). The

Table 3. Second-order rate constants, enthalpies and entropies of activation for the oxidation of *ortho*-substituted phenyl methyl sulphides by Cr(VI)[a].

Substituent	$10^3 k_2$ $M^{-1} s^{-1}$ 30°	40°	50°	$\Delta H^{\neq}$ (kJ mol^{-1})	$-\Delta S^{\neq}$ (J K^{-1} mol^{-1})
H	20·9 ± 0·81	31·1 ± 0·74	42·3 ± 1·8	25·9 ± 2·8	192 ± 9·6
MeO	17·4 ± 0·68	25·9 ± 0·42	37·3 ± 1·0	28·5 ± 2·2	185 ± 7·6
Me	17·2 ± 0·48	25·1 ± 0·97	25·6 ± 0·73	27·1 ± 2·4	190 ± 8·2
F	2·10 ± 0·04	2·98 ± 0·19	4·45 ± 0·20	27·9 ± 3·5	204 ± 12
Br	1·61 ± 0·07	2·44 ± 0·05	3·49 ± 0·22	28·9 ± 3·5	203 ± 12
Cl	0·875 ± 0·09	1·28 ± 0·12	2·00 ± 0·06	31·3 ± 6·0	201 ± 21
NO_2	0·114 ± 0·02	0·173 ± 0·04	0·228 ± 0·02	25·9 ± 13	235 ± 44

[a]General conditions: [Sulphide] ≃ 0·01 M; [Cr(VI)] = 0·0005 M in 50% (v/v) aqueous acetic acid at I = 0·02 M and [$HClO_4$] = 0·001 M.

Table 4. Second-order rate constants, enthalpies and entropies of activation for the PA catalysed Cr (VI) oxidation of *ortho*-substituted phenyl methyl sulphides[a].

Substituent	$10^2 k_2$ $M^{-1} s^{-1}$ 30°	40°	50°	$\Delta H^{\neq}$ (kJ mol^{-1})	$-\Delta S^{\neq}$ (J K^{-1} mol^{-1})
H	19·4 ± 1·4	27·1 ± 1·0	30·1 ± 3·5	15·4 ± 6·3	208 ± 21
MeO	18·4 ± 3·1	23·2 ± 4·2	27·4 ± 3·8	13·6 ± 13	214 ± 45
Me	17·2 ± 1·8	21·2 ± 3·4	26·1 ± 3·4	14·4 ± 11	212 ± 36
F	2·54 ± 0·43	3·98 ± 0·49	5·23 ± 0·62	26·9 ± 11	186 ± 38
Br	2·07 ± 0·29	3·43 ± 0·69	4·99 ± 0·76	33·3 ± 13	168 ± 46

$$\log k_{ortho} = -1{\cdot}96\sigma_0^* - 1{\cdot}872$$

$$r = 0{\cdot}969;\ s = 0{\cdot}23;\ n = 6$$

$$\log k_{ortho} = 1{\cdot}05\,E_s - 2{\cdot}656$$

$$r = 0{\cdot}738;\ s = 0{\cdot}62;\ n = 6$$

Catalysed oxidation

$$\log k_{ortho} = -1{\cdot}60\,\sigma_0^* - 0{\cdot}8790$$

$$r = 0{\cdot}967;\ s = 0{\cdot}19;\ n = 6$$

$$\log k_{ortho} = 0{\cdot}867\,E_s - 1{\cdot}520$$

$$r = 0{\cdot}743;\ s = 0{\cdot}51;\ n = 6$$

The operation of significant polar effect with a very minor role of primary st
becomes evident from the observed satisfactory correlations with (1)
correlations with (2) in both uncatalysed and catalysed oxidations. The data
further analysed by LD and LDS equations and the results are given below:
Uncatalysed oxidation

$$\log k_{ortho} = -2{\cdot}93\,\sigma_I - 1{\cdot}49\,\sigma_R - 1{\cdot}681$$
$$(\pm 0{\cdot}271)\quad (\pm 0{\cdot}294)$$

$$R = 0{\cdot}985;\ \text{SE} = 0{\cdot}175;\ n = 7;\ \text{CL} = 97{\cdot}5\,\%$$

$$\log k_{ortho} = -2{\cdot}63\,\sigma_I - 1{\cdot}71\,\sigma_R - 1{\cdot}890$$
$$(\pm 0{\cdot}266)\quad (\pm 0{\cdot}259)$$

$$R = 0{\cdot}992;\ \text{SE} = 0{\cdot}138;\ n = 6;\ \text{CL} = 99\,\%$$

$$\log k_{ortho} = -2{\cdot}69\,\sigma_I - 1{\cdot}30\,\sigma_R - 0{\cdot}210\upsilon - 1{\cdot}616$$
$$(\pm 0{\cdot}446)\quad (\pm 0{\cdot}416)\quad (\pm 0{\cdot}303)$$

$$R = 0{\cdot}987;\ \text{SE} = 0{\cdot}188;\ n = 7;\ \text{CL} = 99{\cdot}5\,\%$$

Catalysed oxidation

$$\log k_{ortho} = -2{\cdot}39\,\sigma_I - 1{\cdot}23\,\sigma_R - 0{\cdot}7257$$
$$(\pm 0{\cdot}257)\quad (\pm 0{\cdot}279)$$

$$R = 0{\cdot}980;\ \text{SE} = 0{\cdot}167;\ n = 7;\ \text{CL} = 97{\cdot}5\,\%$$

$$\log k_{ortho} = -2{\cdot}12\,\sigma_I - 1{\cdot}43\,\sigma_R - 0{\cdot}9180$$
$$(\pm 0{\cdot}262)\quad (\pm 0{\cdot}255)$$

$$R = 0{\cdot}988;\ \text{SE} = 0{\cdot}136;\ n = 6;\ \text{CL} = 97{\cdot}5\,\%$$

$$\log k_{ortho} = -2{\cdot}18\,\sigma_I - 1{\cdot}06\,\sigma_R - 0{\cdot}192\upsilon - 0{\cdot}6577$$
$$(\pm 0{\cdot}427)\quad (\pm 0{\cdot}400)\quad (\pm 0{\cdot}290)$$

Though a satisfactory correlation is obtained with LDS equation (F-test significance is $> 99\%$ in both oxidations), the steric term is significant to only $< 50\%$ CL of the t-test. Successful correlation is obtained with LD equation (F-test significance $> 97{\cdot}5\%$ CL in both oxidations). The L and D terms are significant to $> 99{\cdot}5\%$ and $> 99\%$ CL of the t-test in both oxidations respectively. The P_D values are 39·4 and 33·7 for excluding and including the unsubstituted compound for the uncatalysed oxidation and the corresponding values are 40·3 and 34·0 for the catalysed oxidation. The value of h_{obs} ($-1{\cdot}508$) is not very close to the h_{cal} ($-1{\cdot}890$, unsubstituted excluded; $-1{\cdot}681$, unsubstituted included for uncatalysed oxidation). Similar behaviour is also noted with catalysed oxidation ($h_{obs} = -0{\cdot}576$; $h_{cal} = -0{\cdot}918$ (unsubstituted excluded) and $-0{\cdot}726$ (unsubstituted included). These results indicate that the reaction series may also belong to case 3 of Charton's classification.

3.3 *Isokinetic relationships*

The Petersen's error criterion (Petersen *et al* 1961) *i.e.* the observed range of $\Delta H^{\neq}$ value should be greater than 2δ (where δ is the calculated maximum possible error) must be satisfied for the validity of $\Delta H^{\neq} - \Delta S^{\neq}$ isokinetic relationship. Except in PP oxidation, in all the other reaction series this condition is not satisfied. However, Exner plots (plots of $\log k_{45°}$ *vs* $\log k_{35°}$ in peroxoanions and plots of $\log k_{50°}$ *vs* $\log k_{30°}$ in uncatalysed and PA catalysed Cr(VI) oxidations) are excellent ($r \geqslant 0{\cdot}995$). The existence of such isokinetic relationships is an indication of the operation of the same mechanism (Leffler 1955) in all sulphides in each oxidation.

4. Conclusion

The following conclusions emerge from the foregoing analyses: (i) The localized effect is a major component in all oxidations. (ii) the steric effect plays a minor role and appears to be constant. (iii) With the LDS equations the regression coefficients of σ_I, σ_R and υ terms are all negative. The negative sign of electronic-effect terms, *viz* σ_I and σ_R, is readily explicable in terms of the reaction mechanism (Srinivasan *et al* 1978, 1980, 1982). The negative regression coefficient for the υ (steric) term corresponds to the reaction being subject to steric retardation by *ortho*-substituents. (iv) The intercept h obtained in each of the reaction series by the application of LD and LDS equation does not correspond closely to the $\log k$ value for the parent system. (v) All these four reaction series may hence be considered as examples of case 3 of Charton's classification (Charton 1975).

Acknowledgement

The authors thank the University Services and Instrumentation Centre for providing facilities for calculations. One of the authors (PK) thanks Madurai Kamaraj University, Madurai and UGC, New Delhi, for the award of the Teacher Fellowship and AC thanks CSIR, New Delhi, for the award of a Senior Research Fellowship.

Charton M 1971 *Prog. Phys. Org. Chem.* **8** 235
Charton M 1975 *J. Org. Chem.* **40** 407
Charton M and Charton B I 1978 *J. Org. Chem.* **43** 1161
Charton M, Gawinecki R, Rasala D, Lenard Z and Tomasik P 1979 Abstracts-Euchem Conferenc
Italy p. 0–3
Fujita T and Nishioka T 1976 *Prog. Phys. Org. Chem.* **12** 49
Horning E C 1955 *Organic syntheses* (New York: John Wiley and Sons Inc.) Coll. Vol. **3**, p. 80
Leffler J E 1955 *J. Org. Chem.* **20** 1205
Petersen R C, Markgraf J H and Ross S D 1961 *J. Am. Chem. Soc.* **83** 3819
Rocek J and Peng T Y 1977 *J. Am. Chem. Soc.* **99** 7622
Shorter J 1972 Correlation analysis in organic chemistry: an introduction to linear free-energy r
(Oxford: Clarendon Press) p. 18
Srinivasan C, Kuthalingam P and Arumugam N 1978 *Can. J. Chem.* **56** 3043
Srinivasan C, Kuthalingam P and Arumugam N 1980 *J. Chem. Soc. Perkin II* 170
Srinivasan C, Chellamani A and Rajagopal S 1982 Abstracts—Sixth IUPAC Conference on Phys
Chemistry, Belgium: *Bull. Chim. Soc. Belg.* **91** 449
Taft R W 1956 Steric effects in organic chemistry (ed) M S Newman (New York: John Wile
Chap. 13
Taft R W and Lewis I C 1958 *J. Am. Chem. Soc.* **80** 2436

Synthesis, infrared and mass spectral studies of substituted 2-cyclohexyl-2,3-dihydro-1H-1,3,2-benzodiazaphosphole 2-oxides

M S R NAIDU* and C DEVENDRANATH REDDY
Department of Chemistry, Sri Venkateswara University, Tirupati 517 502, India

MS received 5 July 1983; revised 13 October 1983

Abstract. A series of the title compounds have been prepared and the structures assigned to them were confirmed by IR and mass spectra. The existence of hydrogen bonding between the amidic hydrogens and the phosphoryl oxygen in these compounds is indicated by the IR spectra. The benzodiazaphosphole ring system appears to be quite stable under electron impact. An interesting type of McLafferty rearrangement occurred in many of these molecules resulting in the formation of ions of benzodiazaphosphinous acid along with the ejection of cyclo-hexane moiety from the molecular ion. Cleavage of P-N bonds of the molecular ions leading to the formation of the *o*-phenylene diamine cations is observed.

Keywords. Benzodiazaphosphole 2-oxides; infrared; mass spectral study.

1. Introduction

Organophosphorus compounds structurally relating to purine and 8-azaguanine have been synthesized and shown to possess promising antitumour activity (Arnold *et al* 1958; Takamizawa *et al* 1970). The nitrogen mustard derivative of the benzodiazaphosphole ring was first prepared by Friedman (1963) which was found to possess antitumour activity (Hsu *et al* 1964). Zimmer and Sill (1964) prepared a pyridine analogue of this compound which is an effective anticancer agent giving complete regression in walker 256 tumours in rats. Even the phosphoric acid derivatives not containing the nitrogen mustard group have been shown to be effective anti-cancer agents (Perroneous *et al* 1952; Crossley *et al* 1953). Several organophosphate esters like malathion and ekatin are dreadful organophosphorus poisons finding widespread use as agrochemicals particularly as powerful insecticides (Heath 1961; Khorana 1961). The present paper describes the synthesis, IR and mass spectral studies of a series of 2-cyclohexyl benzo-diazaphosphole 2-oxides, (**2–8**) naphthodiazaphosphorine 2-oxide (**9**) and diazaphospholopyridine 2-oxide (**10**).

2. Results and discussion

The title compounds (**2–10**, table 1) are prepared by reacting equimolar quantities of cyclohexyl phosphonicdichloride (1) with different substituted *o*-diamines in refluxing inert solvent like bromobenzene or *o*-dichlorobenzene in nitrogen atmosphere. The progress of the condensation was followed by collecting the evolved hydrogen chloride

* To whom all correspondence should be addressed.

Table 1. Synthesis of benzodiazaphosphole 2-oxides

Compound	Diamine	Yield (%)[a]	Reaction time in min.[b]	M.P. (°C)	Molecular formula	IR spectra (cm^{-1}) P=O	P–NH	P–N–C_{aro} P–N_{phenyl}
2	3,4-Diaminotoluene	70[d]	180	273–75[e]	$C_{13}H_{19}N_2OP$	1178	3150	1280
3	4,5-Dimethyl-*o*-phenylenediamine	77[d]	150	195–98[f]	$C_{14}H_{21}N_2OP \cdot H_2O$	1140	3160	1300
4	4-Chloro-*o*-phenylenediamine	71[d]	160	176–78[g]	$C_{12}H_{16}N_2OClP \cdot H_2O$	1140	3150	1285
5	4-Nitro-*o*-phenylenediamine	34[c]	130	213–14[h]	$C_{12}H_{16}N_3O_3P \cdot 2H_2O$	1125	3245	1280
6	N-phenyl-*o*-phenylenediamine	73[c]	140	209–11[i]	$C_{18}H_{21}N_2OP$	1200	3150	1278
7	N-cyclohexyl-o-phenylenediamine	76[d]	190	210–12[j]	$C_{18}H_{27}N_2OP$	1210	3150	1278
8	N,N'-dimethyl-*o*-phenylenediamine	39[c]	180	110–12[k]	$C_{14}H_{21}N_2OP$	1250	—	1290
9	1,8-diamino-naphthalene	95[c]	110	325–28[l]	$C_{16}H_{19}N_2OP$	1175	3145	1268
10	2,3-Diamino-pyridine	88[c]	1440	233–35[m]	$C_{16}H_{19}N_2OP$	1160	3125	1300

All products gave satisfactory microanalyses: C, ± 0.3; H, ± 0.1; N, ± 0.7.

(*a*) Product isolated after one crystallization, (*b*) The times recorded were only approximate as the reagents were mixed at 50–100° and then heated to reflux. Co were carried out in refluxing. (*c*) Bromobenzene and (*d*) *o*-Dichlorobenzene. Compounds recrystallised from (*e*) methanol (*f*) 2-propanol-methanol (*g*) 2-propan methanol-chlorobenzene (*i*) benzene-ether (*j*) dilute methanol (*k*) cyclohexane-petroleum ether (60–80°) (*l*) 2-propanol-cyclohexane and (*m*) methanol-aceto

in water and titrating it with standard sodium hydroxide solution. The refluxion of the reaction mixture was stopped when evolution of hydrogen chloride ceased. The solvent was removed under reduced pressure and the residual viscous semisolids were purified by recrystallization.

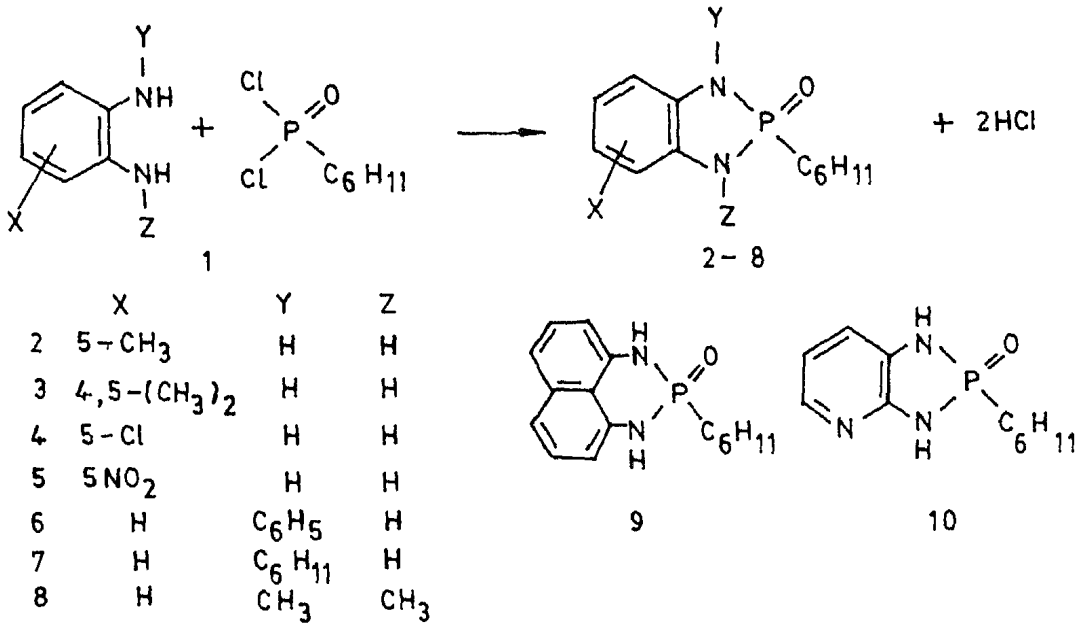

1

2–8

+ 2HCl

	X	Y	Z
2	5-CH_3	H	H
3	4,5-$(CH_3)_2$	H	H
4	5-Cl	H	H
5	5NO_2	H	H
6	H	C_6H_5	H
7	H	C_6H_{11}	H
8	H	CH_3	CH_3

9

10

The cyclization of 2,3-diaminopyridine with **1** was not successful with this procedure. However, it was accomplished by refluxing 2,3-diaminopyridine with **1** in the presence of triethyl amine in bromobenzene. All these compounds are crystalline solids possessing high melting points and are readily soluble in polar solvents.

The condensation of cyclohexyl phosphonicdichloride (1) with *o*-diamine forming benzodiazaphosphole is presumed to be a nucleophilic displacement reaction by the amino groups of *o*-diamine on the phosphorus atom of the phosphonicdichloride. The influence of a substituent either in the benzene ring or on the nitrogens of the *o*-diamines cannot be given in a quantitative relationship without further studies but some general observations may be made regarding the effect of a substituent in the condensation reaction. Basing on yields and reaction time, the presence of substituents like methyl, dimethyl at 4-position of *o*-diamine has little effect on the rate of condensation. Thermal instability in refluxing solvents and poor yields of **5** is due to the strong electron withdrawing effect of the nitro group. But N- and N,N'-disubstitution in *o*-diamine enhances the rate of cyclization and improves the yields indicating that N-substitution facilitates the formation of benzodiazaphosphole. This also suggests that steric factors are less important than polar effects in this nucleophilic substitution reaction.

Cyclization of 1,8-diaminonaphthalene with phosphonic-dichloride (**1**) is almost quantitative showing that the formation of six-membered naphthodiazaphosphorine is more favourable than the analogous five-membered benzodiazaphosphole. Reaction of **1** with *o*-diamines requires high boiling solvent and longer reflux time than 4-chloro-3-methyl phenyl and 4-nitrophenyl phosphorodichloridates (Naidu and Reddy 1973). This may be due to the presence of electronegative atom like oxygen between

2.1 *IR spectra*

The characteristic infrared absorption bands associated with the major functional groups of these compounds are presented in table 1. All the compounds have shown P=O and P–NH stretching vibrations in the regions 1140–1200 and 3125–3245 cm^{-1} showing that the oxygen atom of the phosphoryl group is involved in the hydrogen bonding with the amidic hydrogen atom (Bellamy 1958; Colthup *et al* 1964). Two characteristic bands for $P–N–C_{(aromatic)}$ group, one at 1318–1268 cm^{-1} for phenyl–N and another at 900–966 cm^{-1} for P–N appeared for all the compounds (Colthup *et al* 1964).

2.2 *Mass spectra*

The mass spectra of these compounds (table 2) are studied to confirm their structures and to understand their behaviour under electron impact. As a typical example, the fragmentation pattern of 2 is presented in scheme 1.

The molecular ion (I) appears with very high intensity (97 %) at m/z 250. Cleavage of the P–C bond with simultaneous migration of the β-hydrogen of the cyclohexane moiety to the phosphoryl oxygen results in the formation of the benzodiazaphosphinous acid ion (II) at m/z 168 with the elimination of cyclohexane (Goff *et al* 1977). This ion which forms the base peak of the spectrum subsequently loses hydrogen radical forming the benzodiazaphosphole 2-oxide ion (III) at m/z 167 (35 %).

The ion at m/z 195 (23 %) is presumed to be derived from the M^+ ion by the McLafferty rearrangement (McLafferty 1959) of the γ-hydrogen in the cyclohexane moiety to the phosphoryl oxygen atom.

Decomposition of the molecular ion with the cleavage of P–N bonds leads to the formation of the ions at m/z 132 (9 %), 122 (6 %) and 121 (17 %). These protonated species of 2-diamines might have formed by the double hydrogen rearrangement during the fission of P–N bonds. The ions at m/z 105, 104 and 94 are derived from 4-methyl *o*-phenelenediamine moiety by the step wise loss of H, $–NH_2$ and HCN which are characteristic of *o*-diamines (Henrick *et al* 1974).

Table 2. Mass spectral data

Compound	m/z (% relative abundance)
2	250 (M^+, 97), 195 (23), 182 (11), 181 (11), 168 (100), 167 (35), 151 (22), 150 (20), 149 (15), 121 (17), 119 (16), 94 (11), 83 (5), 55 (26)
3	264 (M^+, 50), 209 (8), 182 (37), 181 (14), 164 (10), 137 (10), 136 (100), 135 (53), 121 (63), 120 (11), 119 (12), 118 (13), 108 (22), 93 (15), 91 (10), 83 (5)
4	270 (M^+, 18·9), 215 (5), 202 (3), 188 (9), 187 (5), 177 (10), 144 (32), 143 (12), 142 (100), 141 (19), 97 (13), 83 (5), 80 (18), 78 (10)
5	154 (3), 110 (17), 97 (33), 84 (59), 83 (38), 82 (21), 81 (10), 80 (15), 68 (100), 66 (11)
6	312 (M^+, 31), 258 (7), 230 (53), 229 (13), 213 (15), 183 (13), 182 (31), 181 (36), 119 (11), 111 (13), 109 (11), 105 (15), 99 (11), 97 (22), 95 (16), 85 (31), 83 (27), 81 (24), 77 (33), 71 (56), 69 (38), 57 (100)
7	318 (M^+, 60), 294 (24), 241 (15), 240 (100), 239 (14), 181 (23), 168 (15), 154 (75), 153 (46), 137 (18), 83 (6), 81 (30), 67 (12)
8	264 (M^+, 100), 209 (5), 182 (8), 181 (87), 180 (41), 164 (28), 134 (10), 133 (12), 132 (30), 118 (17)

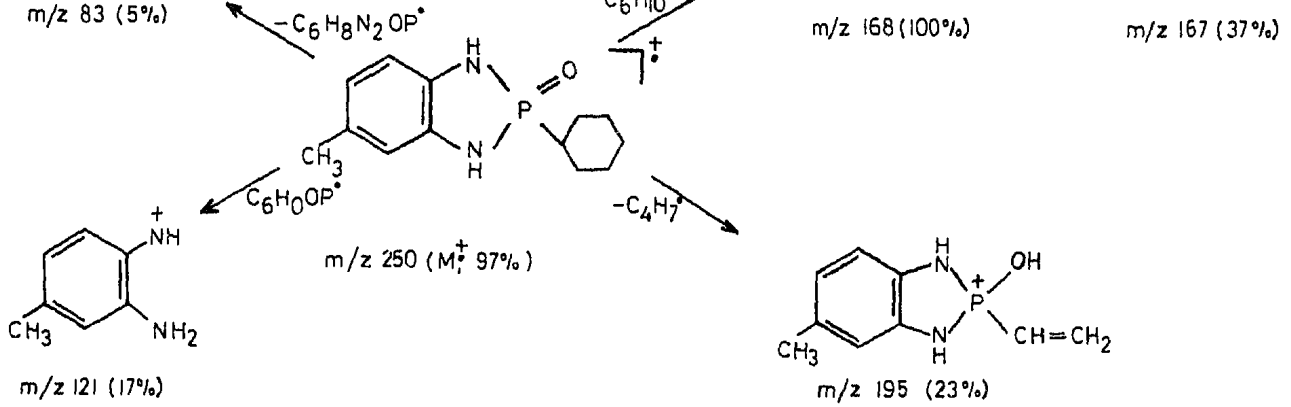

Scheme 1

All the compounds show molecular ion with varying intensity except 5. The molecular ions in **8** and **10** themselves appear as base peaks. The nitrosubstituent in **5** has completely deactivated the diazaphosphole ring leading to the extensive decomposition of the molecule. Presence of methyl groups on both the nitrogens in **8** has stabilized the benzodiazaphosphole ring system. Stability of **10** may be attributed to the presence of six membered naphthodiazaphosphorine ring system.

For **3**, **4** and **9** the diamino radical cations derived from their molecular ions appear as base peaks while the ions at m/z 68 ($C_5H_6^+$) and 57 $(CH_3-(CH_2)_3)^+$ obtained by the cleavage of cyclohexane moiety in the molecules form the base peaks for **5** and **6**.

The spectra of all the compounds, except **5** showed the ions for $(M-C_6H_{11})^+$ and $(M-C_6H_{10})^+$. Peaks corresponding to the ion species derived from substituted *o*-diamine and cyclohexane moieties appeared in all these molecules.

3. Experimental

All melting points are uncorrected and were determined on a Mel-Temp apparatus. The infrared spectra were recorded on a Perkin-Elmer model 700 infrared spectrophotometer, mass spectra were determined by using a Varian Mat CH7 spectrometer with electron energy 70 eV and trap current 100 μA. The elemental analysis was performed by Dr R D McDonald of the Australian Microanalytical Service.

3.1 *Starting materials*

Substituted *o*-diamines were obtained either commercially or synthesized by conventional methods.

3.2 *Cyclohexyl phosphonicdichloride* (1)

Oxygen was bubbled through the stirred solution of phosphorus trichloride (410 g, 3 mole) in dry cyclohexane (63 g, 0·75 mole) at room temperature until the exothermic reaction was complete (15 hr). The solution was fractionally distilled and the major fraction (56 g, 36%) distilling at 160–165°C/56 mm was collected. The material solidified on standing in a vacuum desicator (Clayton and Jensen 1948), m.p. 36–37°C.

A solution of cyclohexyl phosphonicdichloride in *o*-dichlorobenzene (5.03 g, 0.025 mol in 25 ml) was added dropwise to a stirred solution of 3,4-diaminotoluene (3.05 g, 0.025 mole in 25 ml). The mixture was refluxed with stirring under a slow stream of nitrogen until the evolution of hydrogen chloride was complete (180 min). *o*-Dichlorobenzene was recovered under reduced pressure and the residue on treatment with methanol gave 4·4 g (70 %) of the compound, m.p. 260–68°. On recrystallization of this material four times in methanol an analytical sample of 2 as white crystalline plates, m.p. 273–275°, was obtained.

All the compounds reported (3–8) were prepared with this general procedure.

3.4 2-*Cyclohexyl*-2,3-*dihydro*-1*H*-1,3,2-*diazaphospholo* (4,5-*b*)*pyridine* 2-*oxide* (**9**)

A solution of cyclohexyl phosphonic dichloride in bromobenzene (5·03 g, 0·025 mole in 25 ml) was added dropwise to a hot solution of 2,3-diaminopyridine (2·7 g, 0·025 mole) and triethylamine (5·5 g, 0·05 mole) in bromobenzene (50 ml). The mixture was refluxed with stirring for 24 hr under nitrogen atmosphere. The solvent was removed on a flash evaporator and the residue on washing with water and trituration with methanol and acetone mixture (4:1) afforded an analytical sample as yellow granules, 5.2 g (88 %) m.p. 233–35°C.

Acknowledgements

The authors thank Dr K L Loening, Nomenclature Director, Chemical Abstract Service, for his advice in naming the compounds and C V Nageswara Rao for his help in preparing the paper. One of the authors (CDR) is thankful to UGC for the award of a fellowship.

References

Arnold H, Bourseaux F and Brock N 1958 *Nature* (*London*) **181** 931

Bellamy L J 1958 *The infrared spectra of complex molecules* (London: Methuen) p. 311

Clayton J O and Jensen W L 1948 *J. Am. Chem. Soc.* **70** 3880

Colthup N B, Daly L H and Wiberley S B 1964 Introduction to infrared and Raman spectroscopy (New York: Academic Press) p. 189 305

Crossley M, Allison J, Parker R, Kuh E and Seeger D 1953 *Proc. Soc. Exptl. Biol. Med.* **83** 438

Friedman O M, Papanastassiou Z B and Levi R S 1963 *J. Med. Chem.* **6** 82

Goff S D, Jelus B L and Schwiezer E E 1977 *Org. Mass Spectrom.* **12** 33

Heath D F 1961 *Organophosphorus poisons* (Oxford: Pergamon)

Henrick H, Kepert D L, Shewehuk R, Trigwell K R and Wild S B 1974 *Aust. J. Chem.* **27** 727

Hsu P, Kao I S, Tsai J S, Chou C H, Liv M C, Scheu M L, Meng T Y, Jeu Y F, Pan R F and Li S W 1964 *Sci. Sinica* (*Peking*) **13** 789

Khorana H G 1961 *Some recent developments in the chemistry of phosphate esters of biological interest* (New York: Wiley)

McLafferty F W 1959 *Anal. Chem.* **31** 82

Naidu M S R and Reddy C D 1973 *Indian J. Chem.* **12** 349

Perroneous G, Halliday S, Mekenzie D and Williams J 1952 *Proc. Soc. Exptl. Biol. Med.* **81** 614

Reddy C D 1975 *The condensation of phosphonicdichlorides and phosphorodichloridates with o-diamines*, Ph.D.

Oxidation of benzaldehyde semicarbazone by Tl(III) acetate—a structure reactivity correlation

R BALAKRISHNAN and VANGALUR S SRINIVASAN*
Department of Chemistry, Vivekananda College, Mylapore, Madras 600 004, India

MS received 4 October 1982; revised 1 August 1983

Abstract. The kinetics of Tl(III) acetate oxidation of semicarbazones of benzaldehyde and substituted benzaldehydes have been investigated in aqueous (90%) acetic acid. Electron-releasing substituents in the phenyl ring enhance the rate of the reaction, whereas electron-withdrawing substituents retard the rate. The rho value of -1 favours electron-deficient transition state. To account for the major product of the reaction, *viz* respective benzaldehyde, a suitable scheme involving N-thallated intermediate has been proposed.

Keywords. Tl(III) acetate; oxidation of aryl semicarbazones; carbonyl product; N-thallated intermediate.

1. Introduction

The present work has been undertaken to study the structure-activity relationship in the Tl(III) acetate oxidation of benzaldehyde semicarbazone and for this purpose a large number of substituted semicarbazones of benzaldehyde have been prepared following the procedure available in literature (Vogel 1978).

2. Results and discussion

The kinetics of Tl(III) acetate oxidation of semicarbazones of benzaldehyde have been studied in binary solvent mixtures of acetic acid–water in the temperature range 40 to 60°C.

2.1. *Dependence of rate on the concentration of reactants*

The reaction exhibits total second order kinetics—first order with respect to oxidant and reductant used. The rate expression for the reaction is,

$$\frac{-\mathrm{d}[\mathrm{Tl(III)}]}{\mathrm{d}t} = k_2[\mathrm{Tl(III)}][\mathrm{semicarbazone}] \qquad (1)$$

2.2 *Dependence of rate on ionic strength*

Table 1 summarises the influence of added neutral salt, Na_2SO_4, on the oxidation rate in the range 0·1–0·5 M. The small but positive salt effect may be attributed to the ionic strength effect on dipole–dipole reaction.

* To whom all correspondence should be addressed.

The oxidation rate has been retarded to a larger extent by the initial addition of NaCl in small quantities (table 2) which cannot, therefore, be attributed entirely to the ionic strength effect alone. This can be traced to the formation of species like $[Tl(OAc)_2Cl]$ or $[Tl(OAc)_3Cl]^-$ which are less powerful oxidant compared to the reactive species like $Tl(OAc)_3$ or the ion-pair $[Tl(OAc)_2^+ OAc^-]$. A similar behaviour has also been observed with OAc^- (table 2) and the retardation observed in this case may be due to the formation of $[Tl(OAc)_4]^-$.

2.4 *Effect of initially added* Tl(OAc)

There is approximately 8% reduction in rate due to the addition of Tl(OAc) of concentration 2×10^{-2} M but in any kinetic run, a second order kinetics has been observed over three half-lives.

2.5 *Structural influence*

Introduction of a strongly electron withdrawing substituent such as *m*-nitro produces a five-fold decrease in rate while an electron-releasing substituent like *p*-methoxy increases the rate. Figure 1 gives the Hammett plots for this reaction at different temperatures and the respective rho values.

Table 1. Rate dependence on ionic strength*.
{[semicarbazone] = 2×10^{-3} M: [Tl(III)] = 2×10^{-3} M: Solvent = 90% aq. HOAc: Temp. = 50°C}

$[Na_2SO_4]$ M	$k_2 \times 10^2$ $M^{-1} s^{-1}$
—	0·89
0·1	0·99
0·2	1·2
0·4	1·7
0·5	1·9

*at 0·02 M NaCl

Table 2. Effect of added Cl^- and OAc^- on the rate of oxidation.
{[Semicarbazone] = 2×10^{-3} M: [Tl(III)] = 2×10^{-3} M: solvent = 90% aq. HOAc: Temp. = 60°C}

	10^2[Salt] M	$k_2 \times 10^2$ $M^{-1} s^{-1}$
(a) NaCl	—	68
	1	4·5
	2	2·0
	4	0·94
(b) NaOAc	10	18
	30	5·2

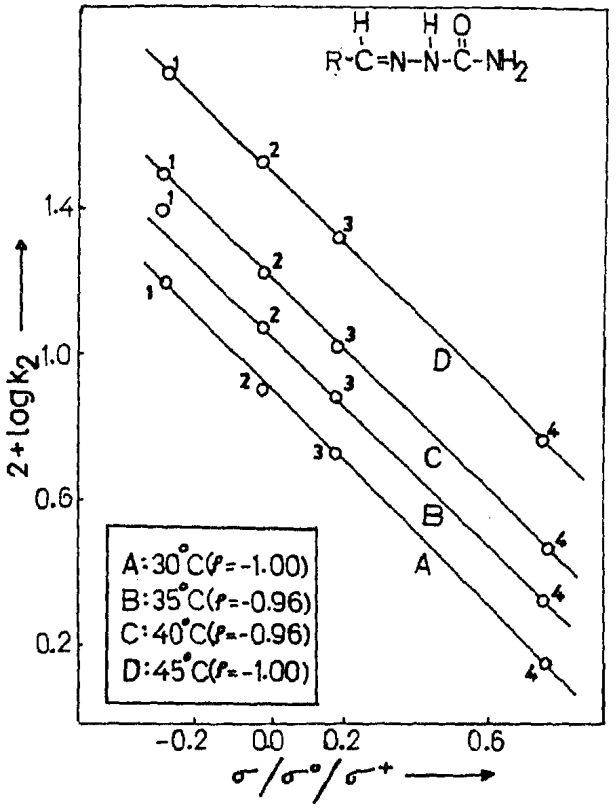

Figure 1. Hammett plot for Tl(III) acetate oxidation of aryl semicarbazones.
R = (i) *p*–OCH_3; (ii) –H; (iii) *o*-Cl (iv) *m*–NO_2.

2.6 *Dependence of rate on solvent dielectric constant*

The specific rates for the Tl(III) acetate oxidation of semicarbazone increases with increasing water content in the system (table 3). The experimental data give linear plots of $\log k_2$ versus $(D-1)/(2D+1)$, indicating that the reaction is dipole–dipole. Also $\log k_D$ versus $1/D$ graph is linear in keeping with Amis equation,

$$\ln k_D = \ln k_\infty - \frac{2\mu_1\mu_2}{kTDr^3} \tag{2}$$

Table 3. Influence of solvent dielectric constant on rate
{[Semicarbazone] = 2×10^{-3} M: [Tl(III)] = 2×10^{-3} M: Temp. = 35°C}

Substituent	Solvent composition %HOAc–%H_2O	$k_2 \times 10^1$ $M^{-1}s^{-1}$
H	90–10	1·2
	80–20	4·0
	70–30	6·4
o-Chloro	90–10	0·79
	80–20	2·4
	70–30	3·9
m-Nitro	90–10	0·22
	80–20	0·81

compounds, the evaluation of r values from the slopes was hampered.

2.7 *Temperature influence*

The reaction exhibits Arrhenius dependence and from the plots of log k_2 versus $1/T$, activation energies have been evaluated. From these values, enthalpies, entropies and free energies of activation have been derived and summarised in table 4. These are in the right order of magnitude observed for a bimolecular reaction.

3. Mechanism of Tl(III) acetate oxidation of aryl semicarbazones

The reduction of Tl(III) to Tl(I) can occur by two one-electron processes, producing an organic radical which can reduce mercuric chloride to mercurous chloride. Hence the mechanism proposed for the Tl(III) acetate oxidation of benzaldehyde semicarbazones involves a radical intermediate which in subsequent step can form the product, benzaldehyde, according to scheme 1:

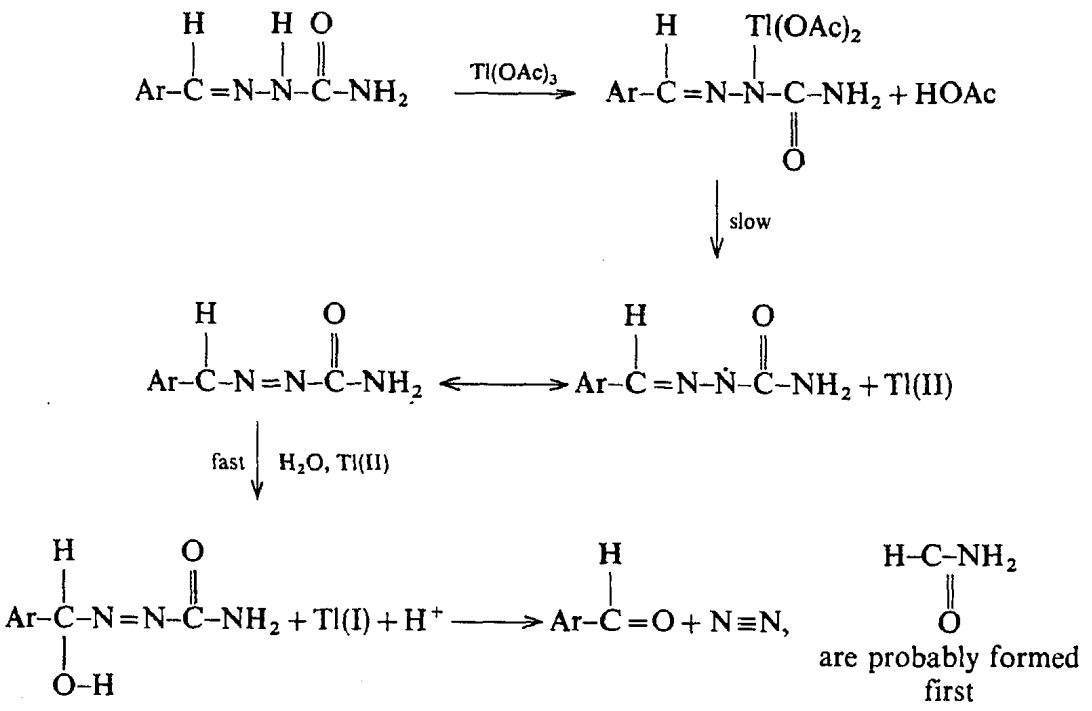

Table 4. Arrhenius parameters

Substituents	E_a (i)	ΔH^* (ii)	ΔS^* (iii)	ΔG^* (iv)
H	13·1	12·5	−22	19·5
o-Chloro	13·0	12·5	−23	19·7
m-Nitro	13·2	12·6	−24	20
p-Methoxy	13·5	12·9	−20	19·1

This scheme is similar to the one proposed for the Ce(IV) oxidation of semicarbazones (Anand Rao *et al* 1981).

According to the above scheme the N-thallated intermediate formed decomposes in a slow step to form a nitrogen radical which in subsequent steps form benzaldehyde as one of the products. The decomposition of N-thallated intermediate is aided by electron-releasing substituents like *p*-methoxy group and the observed Hammett correlation for the substituent influences seems to agree with the above mechanism. The intermediate may then get decomposed to yield benzaldehyde.

By analogy with $Pb(OAc)_4$ (Gladstone *et al* 1969; Butler and King 1977) and $Hg(OAc)_2$ (Butler *et al* 1981), $Tl(OAc)_3$ reactions probably involve an N-metallo intermediate. In all cases a carbonyl product is regenerated.

It is interesting to note that specific rates of Tl(III) acetate oxidation of benzaldehyde semicarbazone is comparable to the rate of benzophenone semicarbazone (table 5) which does not possess a C–H bond adjacent to the phenyl ring. This favours the C–H bond remaining in tact in the Tl(III) acetate oxidation of benzaldehyde semicarbazone. Probably in the case of the former, the C-thallation is sterically hindered and N-thallation predominates. The comparable rate of $Tl(OAc)_3$ oxidation of benzophenone semicarbazone and benzaldehyde semicarbazone, therefore, seems to favour scheme 1.

4. Materials and methods

The aromatic aldehydes used for preparing semicarbazones were of extra pure variety (Fluka AG/Koch light/K and K/Aldrich) and the physical constants of semicarbazones agreed with literature values. Tl(III) acetate was prepared from thallic oxide (BDH) by dissolving a known quantity of it in 100% acetic acid at 60°C in 4 hr. The resultant solution is filtered off and standardised by an iodometric procedure to a starch end point (Henry 1966, 1967). Thallous acetate was prepared by dissolving calculated quantity of thallous carbonate (BDH) in acetic acid. The other compounds such as sodium acetate, sodium chloride, potassium nitrate, sodium sulphate etc (BDH) were used as such. The velocity of the reaction has been measured by estimating the concentration of unreacted Tl(III) iodometrically (Henry 1966, 1967). The specific rates are reproducible to within $\pm 7\%$ and these are the average of atleast two runs. The specific rates, calculated either by using integrated rate equations or from the plot of

Table 5. Specific rates of Tl(III) acetate oxidation of aryl semicarbazones

Compound	$k_2(M^{-1}s^{-1})$
$H_5C_6-C(H)=N-N(H)-C(=O)-NH_2$	0.16
$H_5C_6-C(H)=N-N(H)-C(=O)-NH_2$*	0.18

Table 6. Stoichiometry.

[Tl(III)] initial mM	[Semicarbazone] mM	[Oxidant] consumed mM	[Reductant] taken mM
6·2	3	2·9	3
6·2	2	1·8	2

$x/a-x$ or $\log(b-x/a-x)$ versus time, closely agree with each other. The velocity for all these substrates was measured over a temperature range of 40 to 60°C and the activation energies were obtained graphically by plotting $\log k_2$ against $1/T$.

4.1 *Product analysis*

The semicarbazone (10 mmol) was dissolved in acetic acid–water mixture 90% HOAc–10% H_2O (V/V). The oxidant, Tl(III) acetate, dissolved in the same solvent mixture, was then added to the semicarbazone solution (30 mmol, in excess) and maintained at 30°C for 4 hr. The mixture was then diluted with equal volume of ice water and extracted with $CHCl_3$ in three portions. Extracts were dried over anhydrous $MgSO_4$, filtered and the acetic acid was neutralised by adding saturated $NaHCO_3$ solution. The organic product is then extracted with ether and from the UV and IR spectra, it has been identified as the corresponding aldehyde. The inorganic product has not been identified.

4.2 *Stoichiometry*

Table 6 summarises the stoichiometric results obtained in the Tl(III) acetate oxidation of aryl semicarbazones and it has been found that for nearly 1 mole of Tl(III) acetate consumed 1 mole of semicarbazone is oxidised.

4.3 *Mercuric chloride test*

The product solution gives a white precipitate with mercuric chloride solution whereas the blank solutions containing either Tl(III) or semicarbazone do not give any precipitate with $HgCl_2$.

References

Anand Rao M, Sethuram B and Navaneeth Rao T 1981 *Indian J. Chem.* **A20** 575
Butler R N and King W B 1977 *J. Chem. Soc. Perkin. Trans. I* 282
Butler R N, Morris G J and O Donohue A M 1981 *J. Chem. Res. (S)* 61
Butler R N, Morris G J and O Donohue A M 1981 *J. Chem. Soc. Perkin Trans. I* 61
Gladstone W A F, Aylward J B and Norman R O C 1969 *J. Chem. Soc. (C)* 2589
Henry P M 1966 *J. Am. Chem. Soc.* **88** 1597
Henry P M 1967 *J. Am. Chem. Soc.* **89** 4423

© Printed in India.

Synthesis, reactions and characterisation of some new β-ketoester boroacetates

YASHPAL SINGH and A K RAI*

Chemical Laboratories, University of Rajasthan, Jaipur 302 004, India

MS received 21 July 1983; revised 13 October 1983

Abstract. The reactions of methyl esters of aroyl pyruvic acids (aroyl = benzoyl, *p*-chlorobenzoyl, *p*-bromobenzoyl and *p*-methylbenzoyl) with boric acid in acetic anhydride solution yield derivatives of the general formula $(OAc)_2B[OC(R)CHCOCOOMe]$ (R = C_6H_5, *p*-ClC_6H_4, *p*-BrC_6H_4 and *p*-$CH_3C_6H_4$). The reactions of these derivatives with protic ligands such as glycols, *o*-aminophenol and *o*-aminothiophenol have also been carried out. These derivatives have been characterised by elemental analysis and molecular weight measurements. The tetra-coordination around central boron atom has been established by IR, ^1H NMR and ^{11}B NMR spectral evidence.

Keywords. β-ketoester boroacetates; spectral data; tetra-coordinate boron.

1. Introduction

β-Diketone derivatives of boron have been studied (Barabas *et al* 1968; Simpson and Porter 1972; Dey *et al* 1975; Cotton and Ilsey 1982; Shapel'KO *et al* 1970; Kopteva *et al* 1978) extensively but no attempt appears to have been made to study their β-ketoester analogues. Methyl ester of aroyl pyruvic acids which behave as β-ketoesters form corresponding metal and metalloid derivatives (Hugos and O'Conner 1974; Podolov *et al* 1974; Singh *et al* 1982). In the present paper the synthesis and characterisation of some β-ketoester boroacetate complexes are described and an attempt has been made to establish their probable structures on the basis of physico-chemical and spectral studies.

2. Experimental

Due to the hydrolysable nature of the β-ketoester boroacetate derivatives, care was taken to exclude moisture from the apparatus during the experiments. Toluene (BDH) was sodium-dried, acetic anhydride (BDH) was distilled before use (b.p. 153°C). Boric acid (BDH, AR) was used without further purification. Methyl esters of aroyl pyruvic acids were prepared by the method reported in literature (Lehninger and Witzemann 1942).

Boron was estimated as methyl borate (Thomas 1949). Acetoxy group/acetic acid was estimated by titrating against standard N/10 NaOH solution. Infrared spectra were recorded in nujol-mull using a Perkin-Elmer model 577 grating infrared spectrophotometer. The ^1H NMR spectra were obtained from a Perkin-Elmer R-12B spectrometer. Molecular weights were determined ebullioscopically with Gallenkamp ebullio-

Table 1. Synthetic, physical and analytical data of β-ketoester boroacetate

H_3BO_3/boroacetate (g)	Ligand (g)	Product (% yield)	Physical state m.p. (°C)	% Analysis	
				%OAc or (g) Acetic acid	%B
H_3BO_3 0·68	$PhCOCH_2COCOOMe$ 2·27	$(OAc)_2B[OC(Ph)CHCOCOOMe]$ 80	Brown crystalline solid 176	35·02 (35·33)	3.21 (3·23)
H_3BO_3 0·43	$ClPhCOCH_2COCOOMe$ 1·67	$(OAc)_2B[OC(ClPh)CHCOCOOMe]$ 79	Light brown crystalline solid 182	32·02 (31·82)	3.05 (2·92)
H_3BO_3 0·37	$BrPhCOCH_2COCOOMe$ 1·71	$(OAc)_2B[OC(BrPh)CHCOCOOMe]$ 82	Light brown crystalline solid 134	28·31 (28·57)	2·75 (2·61)
H_3BO_3 1·19	$CH_3PhCOCH_2COCOOMe$ 4·24	$(OAc)_2B[OC(CH_3Ph)CHCOCOOMe]$ 79	Crimson crystalline solid 197	33·64 (33·91)	2·98 (3·10)
$OB_2(OAc)_4$ 0·66	$ClPhCOCH_2COCOOMe$ 1·15	$(OAc)_2B[OC(ClPh)CHCOCOOMe]$ 81	Light brown crystalline solid 182	31·98 (31·82)	3·09 (2·92)
$HSC_6H_4NH_2$ 0·49	$(OAc)_2B[OC(CH_3Ph)CHCOCOOMe]$ 1·36	$\overline{SC_6H_4NHB}[OC(CH_3Ph)CHCOCOOMe]$ 85	Red viscous solid	0·38 (0·38)	3·26 (3·20)
$HOC_6H_4NH_2$ 0·46	-do- 1·48	$\overline{OC_6H_4NHB}[OC(CH_3Ph)CHCOCOOMe]$ 80	Red powder 220	0·41 (0·43)	3·30 (3·35)
$HOCH_2C(CH_3)_2CH_2OH$ 0·28	-do- 1·62	$\overline{OGOB}[OC(CH_3Ph)CHCOCOOMe]$ 76	-do- 238	0·54 (0·55)	3·22 (3·24)

$G = -CH_2C(CH_3)_2CH_2-$

2.1 *Synthesis of bis(acetato)boron (methyl 4-methyl α,γ-dioxabenzene butanoato O^{α} O^{γ})*

A calculated amount of methyl ester of *p*-methylbenzoyl pyruvic acid (4·24 g, 19·57 mM) was mixed with acetic anhydride solution of boric acid (1·19 g, 19·53 mM). The reaction mixture was refluxed till a distinct colour change (light yellow to dark brown) took place. The mixture was allowed to stand overnight and the pink coloured crystals separated out. The crystals were washed with ether and vacuum dried (yield 79%). Found B, 2·98; OAc, 32·64; Calcd. for $C_{16}H_{17}O_8B$, B, 3·10, OAc, 33·91%.

2.2 *Reaction of bis(acetato)boron (methyl-4-methyl α, γ-dioxabenzene butanoato O^{α} O^{γ}) with 2-aminothio phenol in 1 : 1 molar ratio*

A toluene solution (~ 20 ml) of 2-aminothiophenol (0·49 g, 3·98 mM) was mixed with a toluene solution (~ 30 ml) of *bis*(acetato)boron pyruvate (1·33 g, 3·82 mM). The reaction mixture was heated under reflux using a fractionating column. The acetic acid liberated during the course of the reaction was fractionated out azeotropically with toluene and estimated periodically (Found 0·41 : Calcd, 0·43 g). After the completion of the reaction, the excess solvent was distilled off and the compound was dried under reduced pressure and the compound was recrystallised with benzene/*n*-hexane mixture (70:30) (yield, 85%). Found B, 3·26 Calcd. for $C_{18}H_{16}$ NSB, B, 3·20%.

3. Results and discussion

Boric acid reacts with methyl esters of aroyl pyruvic acids (aroyl = benzoyl, *p*-chlorobenzoyl, *p*-bromobenzoyl and *p*-methylbenzoyl) in 1 : 1 molar ratios in acetic anhydride solution to give *bis*(acetato)boron pyruvates, which crystallises out from the reaction mixtures on allowing them to stand overnight at room temperature.

These reactions appear to take place through the formation of oxy-*bis*(diacetato borane) which further interact in the presence of acetic anhydride with ligands to give *bis*(acetato)boron pyruvates. The second step of the above reaction was confirmed by studying the reaction of one of the ligands with oxy-*bis*(diacetato borane) in acetic anhydride solution. The resulting product was found to have the similar composition and physico-chemical characteristics.

These derivatives are non-volatile coloured crystalline solids having sharp melting points. They are soluble in common organic solvents, hydrolytically unstable and monomeric in refluxing benzene. Their important physical properties have been summarised in table 1.

The acetoxy groups in *bis*(acetato)boron pyruvate derivatives are quite reactive and can easily be replaced by protic organic ligands like glycols, *o*-aminophenol and *o*-aminothiophenol. The reactivity of these derivatives is in contrast to the earlier observations of Singh and Tandon (1979, 1980) who reported the inert nature of the acetoxy groups in *bis*(acetato)boron Schiffs base derivatives.

The reactivity of the acetate groups in *bis*(acetato)boron-pyruvates is enhanced due to the presence of free carbonyl group (acetate) which attracts the bonding electrons of

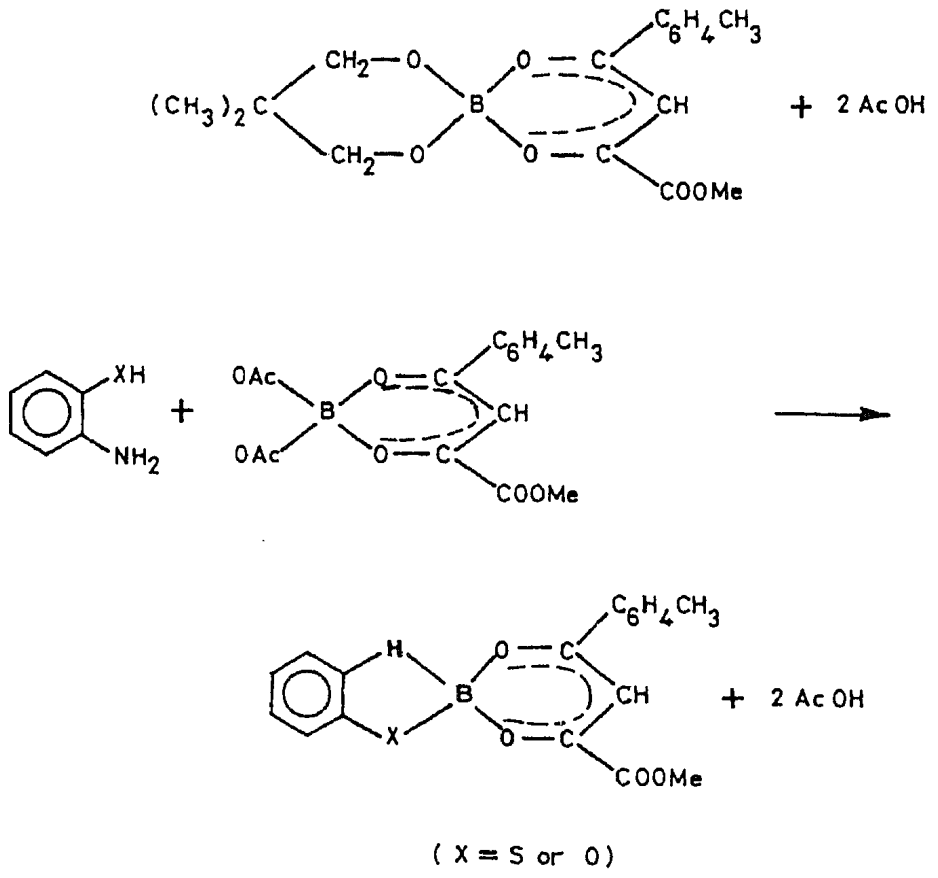

the B–O bond (acetoxy group); as a result the bond is weakened and ruptured under the influence of the protic reagents.

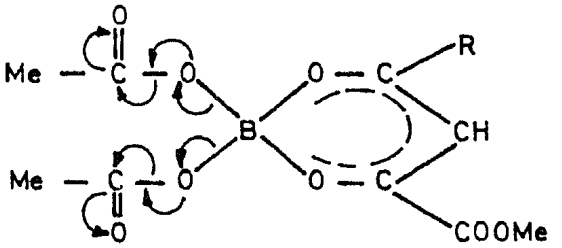

3.1 *IR spectra*

On the basis of their comparative study with corresponding ligands, an attempt has been made to draw some conclusions regarding the mode of bonding in these derivatives. The IR spectra of *bis*(acetato)boron pyruvates exhibit a broad band at 1720–1740 cm^{-1} and is assigned to C=O stretching frequency (Niedenzu and Fritz 1965; Alcock *et al* 1976). In the spectra of the ligand a sharp band is observed at $\sim 1720\,cm^{-1}$ and the broadening of this band indicates that the two carbonyl frequencies (one of the acetate group and another of the ester group of the ligand)

of C=O bond (due to ligand) indicates that the ester group of the ligand does not take part in the complex formation.

Another medium intensity band at $\sim 1260\,cm^{-1}$ may be assigned to the ν_{C-O} frequencies (acetate group) (Alcock *et al* 1976). A strong band observed in the range $1580–1590\,cm^{-1}$ in the spectra of *bis*(acetato)boron pyruvates may be assigned to C=O ligand. This band occurs at $1600–1535\,cm^{-1}$ in the free ligands. The shift $\sim 50\,cm^{-1}$ in (C=O stretching frequency) towards lower wave number may be due to the coordination of the carbonyl oxygen to the central boron atom. A strong band at $1510–1520\,cm^{-1}$ observed in the spectra of these derivatives may be assigned to C=C + C=O.

A medium intensity band observed in the region $710–720\,cm^{-1}$ may be assigned to B ← O stretching (Gates and Mooney 1968).

3.2 *^1H NMR spectra*

The ^1H NMR spectra of these complexes have been recorded in $CDCl_3$ using TMS as internal reference and are summarised in table 2. The absence of any signal for –OH proton in the spectra of the complexes (δ10·6 ppm in the ligand) shows the deprotonation of the –OH proton during complex formation.

A singlet observed at δ3·98 ppm which was earlier assigned to the methyl protons does not show any appreciable shift in its position (δ4 ppm) on complexation. This shows that C=O group does not take part in bonding between ligand and the central boron atom.

A down-field shift has been observed in the signal due to –CH proton. This signal appeared at δ7·1 ppm in the ligand and observed at δ7·3 ppm in the corresponding boron complexes. This shift of 0·2 ppm may be attributed to the delocalization of electrons in the complex which induces additional stability to the complexes.

A singlet due to CH_3 protons of the acetate group has been observed at δ2·10 ppm in the spectra of these boron derivatives (Singh *et al* 1983).

3.3 *^{11}B NMR spectra*

The ^{11}B NMR spectrum of one of the representative compound $(OAc)_2B[OC(ClC_6H_4)$-$CHCOCOOMe]$ has been recorded in $CDCl_3$. The spectrum shows a sharp singlet at δ1·82 ppm with reference to $BF_3 \cdot O(C_2H_5)_2$. The appearance of only one sharp signal

Table 2. ^1H NMR spectra data for β-ketoester boroacetates

Compound	COOMe (s)	–CH (s)	CH_3 (acetate) (s)	Phenyl (m)
$(OAc)_2B[OC(C_6H_5)CHCOCOOMe]$	3·90	7·30	2·00	7·4–8·0
$(OAc)_2B[OC(ClC_6H_4)CHCOCOOMe]$	4·00	7·30	2·10	7·4–7·6
$(OAc)_2B[OC(BrC_6H_4)CHCOCOOMe]$	3·90	7·30	2·15	7·4–8·1
$(OAc)_2B[OC(CH_3C_6H_4)CHCOCOOMe]$	3·90	7·30	2·05	7·4–7·5 8·0–8·15

compound. A comparison of ^{11}B chemical shift with the values reported in the literature confirm that the boron atom in this complex has a coordination number of four (Onak *et al* 1959; Brown and Bladon 1969; Hohaus and Riepe 1973, 1976).

Acknowledgement

One of the authors (YPS) is thankful to CSIR, New Delhi for financial assistance.

References

Alcock N W, Tracy V M and Waddinton T C 1976 *J. Chem. Soc. Dalton Trans* 2243

Barabas A, Isfan E, Roman M, Paraschir M, Romas H and Balabon A T 1968 *Tetrahedron* **24** 1133

Brown N M D and Bladon P 1969 *J. Chem. Soc.* A526

Cotton F A and Ilsey W H 1982 *Inorg. Chem.* **21** 300

Dey K, Bhar J K, Ray K C and Sen S K 1975 *J. Indian Chem. Soc.* **52** 999

Gates P N and Mooney E F 1968 *J. Inorg. Nucl. Chem.* **30** 839

Hohaus E and Riepe W 1973 *Z. Naturforsch* **288** 440

Hohaus E and Riepe W 1976 *Z. Naturforsch* **318** 324

Hugos J G and O'Conner M J 1974 *Aust. J. Chem.* **27** 1161

Kopteva T S, Medvedeva V G, Radionov A N, Rucheva N I, Skoldinov A P and Shigorin D N 1978 *Zh. Obshch. Khim.* **48** 1587

Lehninger A L and Witzemann E J 1942 *J. Am. Chem. Soc.* **64** 874

Niedenzu K and Fritz P 1965 *Z. Anorg. Allgem. Chem.* **340** 329

Onak T P, Landesman H, William R E and Shapiro I 1959 *J. Phys. Chem.* **63** 1533

Podolov B D, Jordanovako V B, Kurunosk M R and Tosev D N 1974 *J. Inorg. Nucl. Chem.* **36** 1495

Shapel'KO N N, Kurkovskaya L N, Medvodeva V G, Skoldinov A P and Vasyanina L K 1970 *Zh. Strukt. Khim* **10** 936 (*Chem. Abst.* 1972 **72** 37549)

Simpson J and Porter G B 1972 *J. Chem. Soc. Perkin Trans* **2** 1796

Singh H B and Tandon J P 1979 *Indian J. Chem.* **A17** 620

Singh H B and Tandon J P 1980 *J. Inorg. Nucl. Chem.* **42** 768

Singh Y P, Saxena S and Rai A K 1982 *Synth. React. Inorg. Met. Org. Chem.* **12** 867

Singh Y P, Saxena S and Rai A K 1983 *Indian J. Chem.* **A22** 298

Thomas I H 1946 *J. Chem. Soc.* 820

Crystal structure of 6-[(1-methyl-4-nitroimidazol-5-yl)thio] purine*

K R ACHARYA

Physical Chemistry Division, National Chemical Laboratory, Pune 411 008, India

MS received 11 July 1983; revised 26 October 1983

Abstract. 6-[(1-methyl-4-nitroimidazol-5-yl)thio] purine, is an immunosuppressant derivative of the antitumour drug, 6-mercaptopurine. Crystals are monoclinic with $a = 4{\cdot}488(2)$, $b = 31{\cdot}886(4)$, $c = 8{\cdot}067(2)$Å and $\beta = 105{\cdot}99(2)°$ in the space group $P2_1/c$. The crystal structure was solved by direct methods using diffractometer data and refined by least squares to an R-index of 0·065 for 502 observed reflections. The molecule crystallizes in the N(9)-H tautomer form, in contrast to the N(7)-H tautomer form found in crystals of 6-mercaptopurine and assume a conformation in which the substituents on the sulphur atom are directed away from imidazole moiety of the purine.

Keywords. Mercaptopurine; crystal structure; direct methods; immunosuppressor.

1. Introduction

6-[(1-methyl-4-nitroimidazol-5-yl)thio] purine, azathioprine (AZTP) which is also known as imuran, is a purine analogue (figure 1). After its administration, it is converted to 6-mercaptopurine (6-MP) (which is effective in cancer chemotherapy). It is an immunosuppressant agent and has been employed for the treatment of '*rheumatoid arthritis*' (Wang 1979) and it has a significant anti-inflammatory action. AZTP can be converted *in vivo* to 6-MP by non-enzymic thiolysis and thereafter its mechanism of action is the same as that of 6-MP (Gale *et al* 1972). With the improved understanding of the drug action in view, the crystal structure of AZTP was analysed.

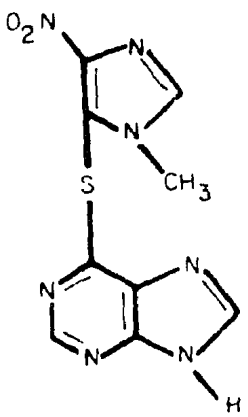

2. Experimental

Azathioprine (AZTP) (Sigma Chemical Company, Missouri, USA); $C_9H_7N_7O_2S$; M_r 277·3; small yellow flakes (from acetone solution); crystal dimension: 0·7 × 0·1 × 0·7 mm.; Enraf-Nonius CAD4-11M diffractometer; lattice parameters from 20 reflections ($12° < 2\theta < 26°$); monoclinic; $a = 4·488(2)$, $b = 31·886(4)$, $c = 8·067(2)$ Å, $\beta = 105·99(2)°$, $V = 1149·5$Å^3; $Z = 4$; D_m: benzene-carbontetrachloride mixture: 1·59; D_c: 1·60 Mgm^{-3}; m.p. = 413 K. Data collection: h, k, ± 1 with $2\theta \leqslant 48°$, MoK_α radiation ($\lambda = 0·7107$Å); graphite monochromator; $\omega - 2\theta$ scan mode, three standard reflections every 2000 seconds of x-ray exposure; 1912 independent, 502 with $F > 3\sigma(F)$, Lp correction, absorption and decay not applied; $P2_1/c$, general positions: $\pm(x, y, z; x, 1/2 - y, 1/2 + z)$ from systematic absences OkO, $k \neq 2n$ and hOl, $l \neq 2n$; direct methods (MULTAN-78; Main *et al* 1978; $176E > 1.62$), anisotropic full matrix for non-hydrogen atoms (LALS: Gantzel *et al* 1961); H from stereochemical considerations

Table 1. Positional coordinates with standard deviations for non-hydrogen atoms.

Atom	x	y	z	Beq (Å)^2
S	0·540 (1)	0·3863 (1)	0·4318 (6)	3·3 (5)
N (1)	0·353 (3)	0·3885 (4)	0·723 (2)	2·1 (5)
C (2)	0·315 (4)	0·4101 (4)	0·856 (2)	2·1 (5)
N(3)	0·422 (3)	0·4466 (4)	0·915 (1)	2·0 (6)
C(4)	0·575 (3)	0·4655 (5)	0·810 (2)	2·4 (5)
C(5)	0·636 (3)	0·4462 (5)	0·667 (1)	2·4 (5)
C(6)	0·510 (3)	0·4086 (5)	0·628 (2)	2·5 (4)
N(7)	0·796 (3)	0·4711 (3)	0·587 (2)	2·2 (3)
C(8)	0·837 (3)	0·5039 (5)	0·684 (2)	2·6 (3)
N(9)	0·711 (3)	0·5005 (3)	0·822 (1)	3·0 (3)
C(10)	0·382 (4)	0·3377 (5)	0·442 (2)	3·3 (5)
C(11)	0·144 (5)	0·3168 (6)	0·334 (2)	2·5 (4)
N(12)	0·118 (5)	0·2780 (5)	0·373 (3)	2·7 (5)
C(13)	0·351 (7)	0·2754 (7)	0·512 (3)	3·6 (5)
N(14)	0·530 (4)	0·3086 (4)	0·559 (2)	2·9 (6)
C(15)	0·797 (5)	0·3125 (5)	0·710 (2)	3·4 (5)
N(16)	−0·082 (4)	0·3350 (5)	0·185 (2)	3·2 (6)
O(17)	−0.036 (3)	0·3696 (4)	0·136 (2)	3·7 (3)
O(18)	−0·316 (4)	0·3156 (5)	0·119 (2)	3·5 (3)

Table 2. Positional coordinates with standard deviations for hydrogen atoms

	x	y	z	Biso
H (C2)	0·25 (3)	0·385 (4)	0·96 (2)	2·8
H (C8)	0·97 (3)	0·537 (4)	0·66 (2)	3·2
H (N9)	0·64 (3)	0·515 (4)	0·87 (2)	3·7
H (C13)	0·44 (3)	0·246 (4)	0·59 (2)	4·6

and verified from ΔF synthesis, only positions refined. $R = \Sigma[||F_o| - |F_c||]/\Sigma[|F_o|] = 0{\cdot}065$. $\Sigma w[|F_o| - |F_c|]^2$ minimised, where $w = [3{\cdot}5 + 1{\cdot}0|F_o| + 0{\cdot}02|F_o|^2]^{-1}$; final ΔF map featureless, $F(000) = 428{\cdot}0$. The atomic scattering factors were taken from the International Tables for X-ray Crystallography (1974). The final fractional coordinates for the non-H atoms and H atoms are listed in tables 1 and 2 respectively. Final anisotropic thermal parameters for all the non-H atoms and the values of observed and calculated structure factors can be supplied by the author on request.

3. Discussion

A perspective view of the molecule is shown in figure 2 (Johnson 1965). Mercaptopurine derivatives with a substituent bonded to the sulphur atom would be expected to have one of two conformations that are related to each other by a rotation of 180° around the C(6)–S bond. To maintain partial double bond character in the C(6)–S bond, the mercapto group must be coplanar with the purine moiety; therefore, the substituent must point either toward or away from the imidazole ring of the base. Careful examination of N^6-monosubstituted adenine derivatives (Sternglanz and Bugg 1973; Bugg and Thewalt 1972; Thewalt and Bugg 1972a) indicates that even relatively small aliphatic groups at the N(6) position tend to point away from the imidazole ring [*trans* to the C(5)–C(6) bond]. However, molecular orbital calculations indicate that this *trans*-conformation is the stable one (Berthod and Pullman 1973). Further, an examination of the space-filling molecular model suggests that the alternative conformation where the substituent is *cis* to the imidazole moiety is unstable on account of the steric interactions between the substituent and the atom N(7). The same is true about the structure of AZTP reported here. The S–C(10) bond is *trans* to the C(5)–C(6) bond [C(5)–C(6)–S–C(10) = 175°] as the substituent bonded to the sulphur atom is directed away from the imidazole moiety of the base. Bond distances and angles of AZTP are listed in table 3. The two purine rings are almost planar. The significant difference between S–C(6) (1·77Å) and S–C(10) (1·72Å) bond lengths may be due to the effect of substituents.

The crystal structure of AZTP viewed down the *a* axis is shown in figure 3. The molecules are joined by pairs of N(9)–H . . . . N(3) hydrogen bonds [N(9)–H(N9)

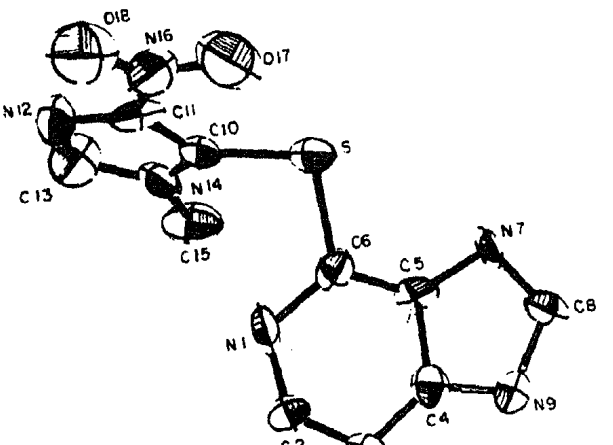

Table 3. Molecular dimensions with esd's in parentheses.

Bond distances (Å):			
S–C (6)	1·77 (2)	S–C (10)	1·72 (2)
C (5)–C (6)	1·32 (2)	C (5)–C (4)	1·39 (2)
C (5)–C (7)	1·35 (2)	N (7)–C (8)	1·29 (2)
C (8)–N (9)	1·38 (2)	N (9)–C (4)	1·26 (2)
C (4)–N (3)	1·37 (2)	N (3)–C (2)	1·29 (2)
C (2)–N (1)	1·33 (2)	N (1)–C (6)	1·34 (2)
C (10)–C (11)	1·35 (2)	C (11)–N (16)	1·46 (3)
N (16)–O (17)	1·21 (3)	N (16)–O (18)	1·21 (2)
C(11)–N(12)	1·29 (2)	N (12)–C (13)	1·30 (3)
C (13)–N (14)	1·32 (3)	N (14)–C (15)	1·46 (2)
N (14)–C (10)	1·35 (2)		
Bond angles (deg):			
C (6)–S–C (10)	100·5 (8)	C (6)–N (1)–C (2)	115 (1)
C (5)–N (7)–C (8)	101 (1)	N (7)–C (5)–C (4)	113 (1)
N (7)–C (5)–C (6)	132 (1)	C (4)–C (5)–C (6)	115 (1)
N (7)–C (8)–N (9)	114 (1)	C (5)–C (4)–N (3)	124 (1)
N (9)–C (4)–N (3)	131 (1)	C (4)–N (3)–C (2)	112 (1)
S–C (6)–N (1)	120 (1)	S–C (6)–C (5)	116 (1)
N (1)–C (6)–C (5)	123 (1)	N (1)–C (2)–N (3)	130 (1)
C (10)–C (11)–N (12)	115 (2)	C (10)–C (11)–N (16)	126 (2)
N (12)–C (11)–N (16)	119 (2)	S–C (10)–C (11)	132 (1)
S–C (10)–N (14)	121 (1)	C (11)–C (10)–N (14)	105 (1)
N (14)–C (13)–N (12)	118 (2)	C (13)–N (12)–C (11)	100 (2)
C (10)–N (14)–C (13)	102 (2)	C (10)–N (14)–C (15)	131 (1)
C (13)–N (14)–C (15)	127 (2)	O (17)–N (16)–C (11)	119 (2)
O (17)–N (16)–O (18)	122 (2)	C (11)–N (16)–O (18)	119 (2)
C (5)–C(4)–N (9)	105 (1)	C (8)–N (9)–C (4)	108 (1)

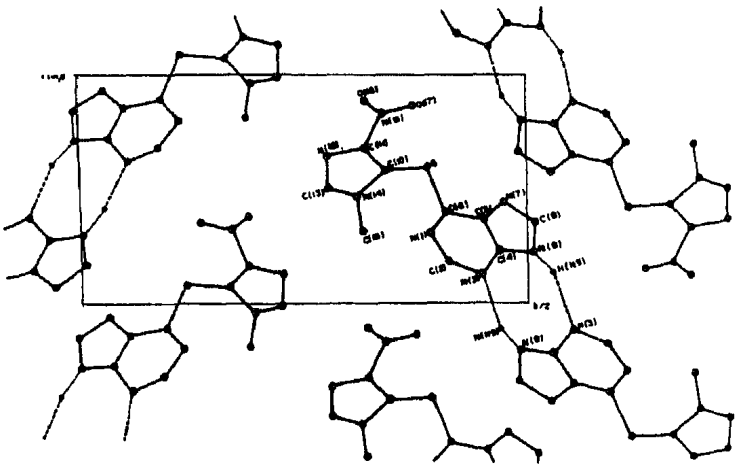

Figure 3. Molecular packing of AZTP along *a*.

= 0·85, N(9) . . . N(3) = 2·90, N(3) . . . H(N9) = 2·18Å and N(9)–H(N9) . . . N(3) = 162·2°] across a crystallographic inversion centre to yield hydrogen bonded dimers.

mercaptopurine (Sletten *et al* 1969; Brown 1969) which possess unsubstituted thio groups, crystallize as N(7)–H tautomers. However, no general straightforward correlation is known between the intrinsic stabilities of the isolated tautomeric forms and their presence in the crystals of the substances (Pullman and Pullman 1971). The sulphur atom in AZTP is a poor hydrogen bond acceptor. A similar observation was made in the crystal structure of N^6-(Δ^2-isopentenyl)-2-methyl-mercaptoadenine (Mc Mullan and Sundaralingam 1971). In contrast, the unsubstituted thio groups are hydrogen bond acceptors in the crystal structures of 6-thioguanosine (Thewalt and Bugg 1972b), 6-thioguanine (Bugg and Thewalt 1970) and 2-thio-6-methyl purine (Srinivasan and Chandrasekharan 1968; Donohue 1969) thus suggesting that the addition of substituents to the sulphur atom of 6-mercaptopurine may have an important effect on the hydrogen bonding properties of the base.

Acknowledgement

The author thanks Drs A P B Sinha, K Venkatesan, L M Pant, S S Tavale, N N Dhaneshwar and T N Guru Row for constant encouragement and stimulating discussions.

References

Berthod H and Pullman B 1973 *C. R. Acad. Sci. (Paris)* **D276** 1767

Brown G M 1969 *Acta Crystallogr.* **B25** 1338

Bugg C E and Thewalt U 1970 *J. Am. Chem. Soc.* **92** 7441

Bugg C E and Thewalt U 1972 *Biochem. Biophys. Res. Commun.* **46** 779

Donohue J 1969 *Acta Crystallogr.* **B25** 2418

Gale E F, Cundliffe E, Reynolds P E, Richmond M H and Waring M J 1972 *The molecular basis of antibiotic action* (London: John Wiley) p. 183

Gantzel P K, Sparks R A and Trueblood K N—LALS 1961 A program for the full matrix least squares refinement of positional, thermal parameters and scale factors

International tables for x-ray crystallography 1974 (Birmingham: Kynoch Press) Vol. **4**

Johnson C K—ORTEP 1965 A Fortran Thermal ellipsoid plot program for crystal structure illustrations—Report ORNL-3794 Oak Ridge National Laboratory, Tennessee

Main P, Hull S E, Lessinger L, Germain G, Declercq J P and Woolfson M M—MULTAN 1978 A system of computer programs for the automatic solution of crystal structures from x-ray diffraction data (Univ. of York, England and Louvain, Belgium)

Mc Mullan R K and Sundaralingam M 1971 *J. Am. Chem. Soc.* **93** 7050

Pullman B and Pullman A 1971 *Advances in heterocyclic chemistry* (Academic Press: London) Vol. **13** p. 155

Sletten E, Sletten J and Jensen L H 1969 *Acta Crystallogr.* **B25** 1330

Srinivasan R and Chandrasekharan R 1968 *Acta Crystallogr.* **B24** 1698

Sternglanz H and Bugg C E 1973 *Biochem. Biophys. Acta* **308** 1

Thewalt U and Bugg C E 1972a *Acta Crystallogr.* **B28** 1767

Thewalt U and Bugg C E 1972b *J. Am. Chem. Soc.* **94** 8892

Wang R I H 1979 *Practical drug therapy* (Philadelphia: Lippincott Co.) p. 544

A microcomputer system for mass spectrometer control and data acquisition

P G OZA, H S MAZUMDAR, A K CHOUDHARY and K GOPALAN*
Physical Research Laboratory, Ahmedabad 380009, India

MS received 11 July 1983

Abstract. A microcomputer system has been designed for semi-automatic operation of a solid source mass spectrometer used for geochronological studies. It sequentially steps the magnetic field through pre-selected values, reads the digitized ion currents for a given time and temporarily stores the data which can be transferred to a paper tape or directly to a desk top calculator for further analysis. The unit is relatively inexpensive, made of readily available components and can be adapted to many laboratory automation tasks.

Keywords. Mass spectrometer; data acquisition; microprocessor.

1. Introduction

A microprocessor based unit has been designed to control the magnetic field of a mass spectrometer for sequential peak jumping and to digitally store peak heights and baseline data for subsequent processing with an off-line computer. Besides being simple and relatively inexpensive it enables a single minicomputer to service many mass spectrometers. A similar unit using TTL-MSI logic was described by Dick (1975). The microprocessor used in the present design reduces the hardware complexities of a TTL-based circuit, and in addition provides for temporary data storage and if required, some simple data manipulation. Though designed for a semi-automatic operation of a solid source mass spectrometer for geochronological studies, it can be readily adapted or modified for many laboratory automation tasks.

2. Description of the system

The unit can step the magnetic field of a mass spectrometer sequentially through a maximum of 250 pre-selected values corresponding to peak and baseline positions. Since the isotopic analysis of most of the elements for geochronological studies requires not more than a dozen field values, the total number of channels can be grouped into independent blocks each storing the field patterns corresponding to commonly used mass spectra. It outputs a 16 bit binary word equivalent to 4 digit number in 1248 BCD format for each field value to the electromagnet supply *via* a high precision D/A converter. The output of the D/A converter in conjunction with base reference voltage selectable in the magnet supply serves to control the magnetic field either in the current

memory capacity) with 7-digit precision, execute a chosen number of cyclic scans (up to 99) and at the end, transfer the stored peak height and baseline data in block format either to a teletype or directly to a desk top calculator through an IEEE 488 interface. A bank of 4 BCD thumbwheel switches in conjunction with a set of push-button switches enable front panel entry of the foregoing parameter for a given experiment (figure 2). A bank of 13 pairs of seven-segment LED's on the front panel display the pre-selected parameters and, in addition, the number of cyclic scans completed, the four-digit incremental field currently being supplied, to the magnet supply and the integrated V/F output except for the least significant digit, when the unit is in the RUN mode.

3. Hardware description

The system shown schematically in figure 1 consists of an Intel 8080 microprocessor with 2 kbytes RAM and 2 kbytes PROM. The other important hardware components are two Intel 8255 chips, one 8251 and one 8253, the choice being mainly to alleviate software complexity. Out of the total of six individually programmable 8 bit parallel I/O ports in the two 8255's, two ports (PAo-7, PBo-7) are used to supply the 4-digit field value in 1248 BCD format to the magnet control unit *via* a D/A converter. Two other parallel I/O ports (PC 1-7, PBo-7) are used for the 15 bit IEEE 488 interface with one bit from one of these ports (PCo) serving to open the gate for the two cascaded counters (Intel 8253) of 16 bit each for the preset 'read time'. Another I/O port (PAo-7) drives the cathodes of 13 pairs of LED display through a chain of decoders (2 × 7447) and display driver circuit. The last I/O port is divided into two parts of four lines each, one part (PC_{4-7}) being programmed in the input mode and connected to the horizontal rows of the thumbwheel and push-button switches. The other part (PCo-3) is programmed in the output mode and connected to a 4 to 16-line linear decoder (74154). Thirteen of the 16 decoded outputs drive the common anodes of the 13 LED pairs through an inverter chain (7404 × 3) and display driver circuit. Eight, out of the 13 lines, are common to these vertical columns of the push-button and thumbwheel switch array. Intel 8251 UART serves as a serial I/O port with 110 baud rate to communicate with the teletype ASR 33. This teletype was initially used in software development and later for data print out and loading any auxiliary programme separate from the permanent resident programme either by key entry or through paper tape. Two of the three individually programmable 16-bit counters in Intel 8253 have been cascaded to count the V/F converter output pulse train during the 'read time'. The third counter is programmed to divide the ϕ_2 clock signal at 2·04 MHz from the CPU clock generator (8224) to derive a signal at 1 msec interval to serve both as an external interrupt for the processor and as a clock signal for generating the preset delay time and read time. The oscillator signal at 18·432 MHz from 8224 clock generator is scaled down to 7·04 kHz through a divider chain (74161 × 3) and supplied to 8251 serial I/O port to generate the required baud rate of 110.

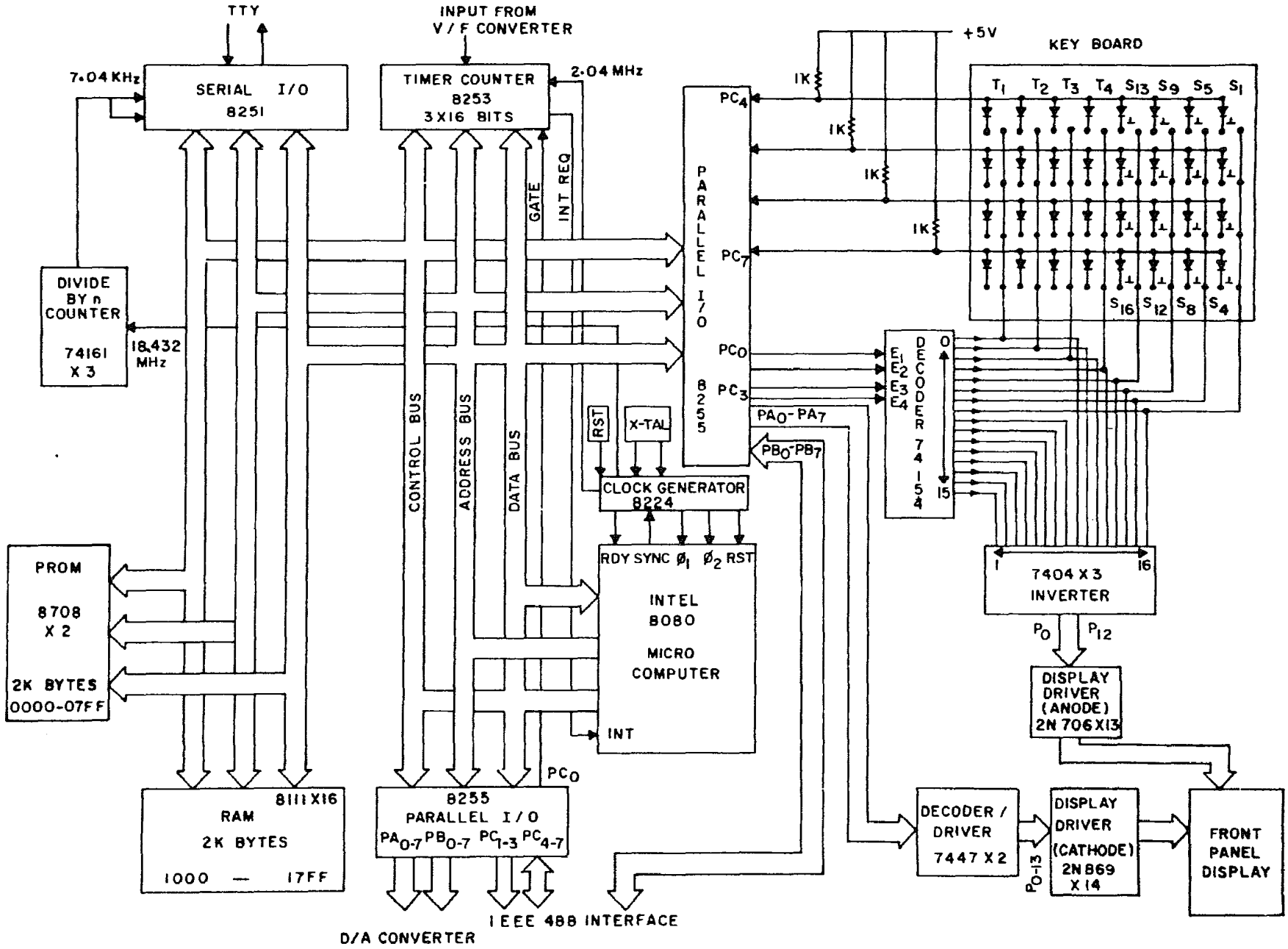

Figure 1. Schematic diagram of the microcomputer system implemented around Intel 8080 microprocessor with peripherals and communication interface.

The software has been developed in two independent packages, the background and foreground. The former supports the display and the switch array routines while the latter serves as the mother or the main programme. The switch and display array used in this unit require the microprocessor to be interrupted at regular intervals to scan the switch array to recognise any new entry and to update the display accordingly. The Intel 8080 microprocessor has been provided with a single interrupt vector. On every interrupt the CPU executes a RST 7 (restart) instruction causing the monitor to execute an unconditional CALL to RAM location (13 FD Hex) and initiate the programme called interrupt service sub-routine stored at that location. The CPU then returns to the operations it was performing before the interrupt had occurred. Thus the CPU is time-shared between the interrupt service sub-routine and the main programme. The background package keeps an image of switch array and display in memory and scans one column of the switch array at every interrupt to compare with the resident image to recognise any new entry. One complete scan of the switch and display arrays takes 16 msec to give a flickerless display. The mother programme has been written to incorporate the following features.

When the LOAD switch is activated, the LOAD sub-routine is executed which calls for the entry of an identification number for the block of channels to be used for a given element. The operator then enters the number of channels to be included in that block and then proceeds to enter the digital field values for each channel of the selected block. The programme stops at this point and the operator can recall the sequence for checking and editing, if necessary. Blocks of field patterns for other elements can be stored in a similar manner. The parameter entries are sequence-independent and protected against false entry.

On the first activation of the RUN switch, the RUN sub-routine is executed which calls for the entry of delay time, read time and the number of cyclic scans for the particular experiment for which the field pattern has already been stored. With the activation of the RUN switch again, the unit starts with the 4-digit field value in the first channel of the selected block, allows the delay time to elapse, reads the V/F output corresponding to

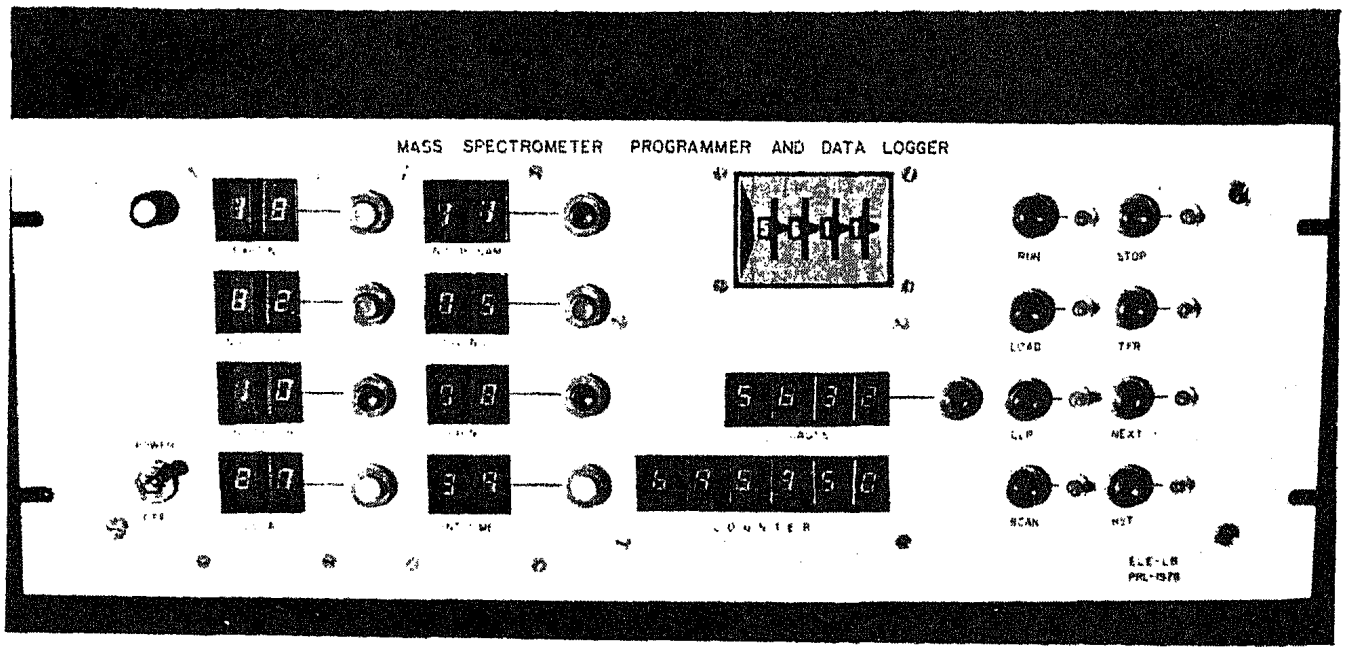

the ion current intensity at the selected field position for the durations of the read time stores the accumulated value and then jumps to the next channel in the sequence. The repetition of the sequence stops at the end of the desired cycle.

The SCAN switch, initiates the SCAN sub-routine which calls for the entry of two 4-digit field values, delay time and read time. On activating the RUN switch now, the unit advances the field from lower value to higher value in unit steps, holding each field value for the duration of the selected delay time and read time. This scan feature allows the user to observe the profile of a mass peak in great detail.

All the subroutines branch off to ERROR subroutine whenever a wrong sequence of switches are used or a wrong entry is provided thereby terminating the erroneous operation. The ERROR subroutine brings about immediate lock out of the switch array and blinking of the display corresponding to the erroneous parameter for a delay time provided in the subroutine, after which the unit automatically recovers from the error hang up without losing the pre-stored parameters or data.

The TRANSFER switch enables the transfer of the stored data either to a teletypewriter or directly to a desk top calculator through an IEEE 488 interface, which at present is not included in the unit.

Any programme under execution can be temporarily halted for intermediate inspection and could be resumed by means of the respective function switch.

Acknowledgements

Technical assistance from Mr A K Jain, Mr A M Puthawala and Mrs Vasanthi is gratefully acknowledged.

Reference

Dick A 1975 *Int. J. Mass. Spectrom. Ion Phys.* **18** 193

..... *S Narayanaswami, S Rajeswari, B R Pai, K Nagarajan, W J Richter and S J Shenoy* 145

Separation of electronic and steric effects: Oxidation of *ortho*-substituted phenyl methyl sulphides by peroxoanions, chromium(VI) and picolinic acid catalysed chromium(VI) ..... *C Srinivasan, P Kuthalingam, A Chellamani, S Rajagopal and N Arumugam* 157

Synthesis, infrared and mass spectral studies of substituted 2-cyclohexyl-2,3-dihydro-1H-1,3,2-benzodiazaphosphole 2-oxides ..... *M S R Naidu and C Devendranath Reddy* 165

Oxidation of benzaldehyde semicarbazone by Tl(III) acetate—a structure reactivity correlation ..... *R Balakrishnan and Vangalur S Srinivasan* 171

Synthesis, reactions and characterisation of some new β-ketoester boroacetates ..... *Yashpal Singh and A K Rai* 177

Crystallography

Crystal structure of 6-[(1-methyl-4-nitroimidazol-5-yl)thio] purine..... *K R Acharya* 183

Instrumentation

A microcomputer system for mass spectrometer control and data acquisition ..... *P G Oza, H S Mazumdar, A K Choudhary and K Gopalan* 189

Indexed in CURRENT CONTENTS

Edited and published by C N R Rao for the Indian Academy of Sciences, Bangalore 560 080. Typeset by

Proceedings of the
Indian Academy of Sciences

Chemical Sciences

CONTENTS

Physical and Theoretical

Kinetic studies on the homogeneous hydrogenation of fumaric and maleic acids catalysed by bis(dimethylglyoximato) cobalt(II)..... (*Mrs*) *S Vasanthkumar, S Vancheesan, J Rajaram and J C Kuriacose* 73

Excess volumes and isentropic compressibilities of binary mixtures of di-*n*-butylamine with iso-alkanols at 303·15 K..... *G S Sastry, M Ramamurthy and P R Naidu* 83

Electron impact study of $C_6H_5^+$ fragment ion obtained from three molecules ..... *Ezzat T M Selim, A I Helal and N F Zahran* 87

Thermal decomposition studies of catalysed double base propellants ..... *Haridwar Singh and K R K Rao* 93

Compensation effect in the electrical conduction process in a series of pyrenyl polyenes ..... *A Sircar, B Mallik and T N Misra* 99

The infrared and Raman spectra of 2,4- and 2,5-dimethylbenzaldehydes ..... *P Venkoji* 105

Inorganic and Analytical

Preparation and characterization of vanillin thiosemicarbazone complexes with Co(II), Ni(II), Cu(II), Zn(II), Cd(II), and Hg(II)..... *K K Aravindakshan and C G R Nair* 111

An efficient method of preparation of pheophytin *a*—Divalent metal pheophytinates ..... *P R Droupadi and V Krishnan* 117

Transition metal derivatives of 3-4-diphenyl-5-mercapto-1,2,4-triazole..... *J Singh and N K Singh* 125

Characterisation and antimicrobial activity studies of the mixed ligand complexes of Cu(II) with 8-hydroxyquinoline and salicylic acids..... *Y Anjaneyulu, R Y Swamy and R Prabhakara Rao* 131

Reactions of dichloro-bis(cyclopentadienyl) titanium(IV) with bidentate Schiff bases ..... *B Khera and N K Kaushik* 139

(Continued on inside back cover)